



:

,

, 2009



« μ : ,  
μ »

: \_\_\_\_\_, μ

μ . μ μ μ μ

\_\_\_\_\_ μ μ

μ μ μ μ

\_\_\_\_\_ μ μ

. μ μ μ

μ

\_\_\_\_\_ μ μ

. μ μ μ μ

. μ μ μ μ

. μ μ μ μ

. μ μ μ μ

. μ μ μ μ

μ

μ  
μ &

μ μ

μ

( . . . . )

μ μ

μ

μ. 167/06.04.2009

μ

μ

μ

μ μ , μ  
. 3685/2008

μ

12

.5

.2083/92,

.9

.4

μ

μ

μ μ

μ

μ

μ

μ μ

μ

μ

μ

μ μ

μ

/

,

μ

,

μ μ

&

μ

μ μ : « μ

:

,

μ

μ

».

μ

,

μ 26

2009 μ

10:00 μ.μ

«

»

μ

( μ. . 1413/25.06.2009)

μ

μμ

μ

μ

«

μ

,

μ

μ

μ

,

μ

μ

μ

μ μ

,

μ

»

«

μ

».

μ

μ

,




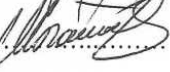

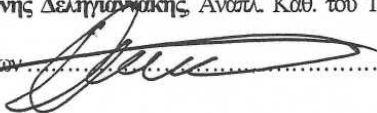
μ μ

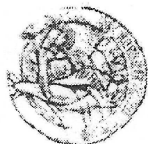
μ

μ

μ , 7μ . 36  
 .1268/82, . 12 13 .2083/92 . 9 . 4 . . 3685/2008  
 . 40 41 μ μ  
 ( 310/10.03.05 . 2°).  
 μ μ 30 μ 2008  
 ( . . 562/15.12.2008)  
 μ μ .  
 μ : « μ : , μ μ  
 μ » μ , μ  
 μ μ μ .  
 μ , μ μ  
 . μ  
 , μ (6)  
 μ (0).  
 , μ (6) μ (0) μ μ  
 . 6 . 40 μ μ  
 ( 310/10.03.05 . 2°).  
 μ  
 , 26 2009

**Η Εξεταστική Επιτροπή**

1. Δημήτριος Γουρλής, Επικ. Καθ. του ΤΜΕΥ του Παν/μίου Ιωαννίνων.....
2. Μιχαήλ Καρακασίδης, Αναπλ. Καθ. του ΤΜΕΥ του Παν/μίου Ιωαννίνων.....
3. Γεώργιος Φρουδάκης, Αναπλ. Καθ. του Τμ. Χημείας του Παν/μίου Κρήτης.....
4. Φίλιππος Πομώνης, Καθ. του Τμ. Χημείας του Παν/μίου Ιωαννίνων.....
5. Θωμάς Μπάκας, Καθ. του Τμ. Φυσικής του Παν/μίου Ιωαννίνων.....
6. Κωνσταντίνος Μπέλτσιος, Αναπλ. Καθ. του ΤΜΕΥ του Παν/μίου Ιωαννίνων.....
7. Ιωάννης Δεληγιάννης, Αναπλ. Καθ. του Τμ. Διαχ/σης Περιβ. & Φυσ. Πόρων του Παν/μίου Ιωαννίνων.....



ΠΑΝΕΠΙΣΤΗΜΙΟ ΚΡΗΤΗΣ  
ΣΧΟΛΗ ΘΕΤΙΚΩΝ ΚΑΙ  
ΤΕΧΝΟΛΟΓΙΚΩΝ ΕΠΙΣΤΗΜΩΝ  
ΤΜΗΜΑ ΧΗΜΕΙΑΣ

Ομάδα  
Θεωρητικής &  
Υπολογιστικής  
Χημείας



Α. Κνωσού, Τ.Θ. 2208, Ηράκλειο 710 03, Τηλ: +30 2810 545055, Fax: +30 2810 545001, Email: [frudakis@chemistry.ucc.gr](mailto:frudakis@chemistry.ucc.gr)

: μ μ μ  
μ &

: « . . »

, 24 2009

μ ,

26

μ  
, μ μ : « μ :  
- μ  
» μ 7μ , μμ μ  
μμ μ μ μ μ  
Randall Q. Snurr Northwestern University, US .

μ

μ μμ '03 (03 548) μ : Μ

-

μ

(7)

μ

μ

μ





Institute of Advanced Materials, Groningen, )  
 XPS, AFM, STM).  
 Mössbauer  
 (VSM),  
 Calabria ( ) . Enrico Maccallini  
 . Raffaele G. Agostino  
 (UPS) (STM, AFM, SEM),  
 XRD,  
 (SEM)  
 Raman  
 &  
 /



μ  
 μ , μ μ μ  
 μ μ μ . μ μ  
 , 2009

- μμ μ μ μμ 2003  
 (03 548), μ :  
 • 75% μ —  
 • 25% μ μ —  
 — μμ  
 • μ  
 8.3 —



ΕΛΛΗΝΙΚΗ ΔΗΜΟΚΡΑΤΙΑ  
 ΥΠΟΥΡΓΕΙΟ ΑΝΑΠΤΥΞΗΣ



ΕΥΡΩΠΑΪΚΗ ΕΠΙΤΡΟΠΗ  
 ΕΥΡΩΠΑΪΚΟ ΚΟΙΝΩΝΙΚΟ ΤΑΜΕΙΟ (ΕΚΤ)

•	.....	1
•		
<b>B1.</b>		
1.1.	.....	5
1.2.	μ - .....	6
1.3.	μ .....	10
1.3.1	.....	10
1.3.2	μ Laser .....	12
1.3.2	μ μ .....	13
1.4.	.....	16
1.4.1.	.....	16
1.4.2.	.....	17
1.4.3.	μ .....	17
1.4.4.	& .....	20
1.5.	μ .....	21
1.6.	μ - μ .....	22
1.6.1	' μ .....	23
1.6.2	μ - .....	31
1.6.2.1.	μ μ μ - , .....	31
1.6.2.2.	μ μ - .....	32
1.6.2.2.1.	- μ .....	33
1.6.2.2.2.	- .....	35
1.6.2.2.3.	.....	36
1.7.	.....	40
<b>2.</b>		
1.8.	- .....	43
1.9.	μ μ .....	46

1.10.	$\mu$	Mössbauer .....	47
1.11.	$\mu$	Raman .....	54
1.12.	$\mu$	.....	55
1.13.	$\mu$	.....	58
.		.....	63
.		-	
<b>1.</b>			
1.1	$\mu$	$\mu$ 1,3-	83
1.1.1.	$\mu$	Raman .....	84
1.1.2.	$\mu$	- .....	86
1.1.3.	$\mu$	$\mu$ &	87
1.1.4.	$\mu$	- .....	89
1.1.5.	$\mu$	$\mu$ .....	93
1.1.6.	$\mu$	$\mu$ - .....	94
1.2	$\mu$	$\mu$	95
1.2.1.	$\mu$	Raman .....	96
1.2.2.	$\mu$	$\mu$ .....	97
1.2.3.	$\mu$	$\mu$ $\mu$ .....	98
1.2.4.	$\mu$	$\mu$ - .....	99
<b>2.</b>			
2.1	$\mu$	$\mu$	100
	$\mu$	FePt .....	100
2.1.1.		.....	101
2.1.2.		- .....	102
2.1.3.	$\mu$	Raman .....	104
2.1.4.	$\mu$	Mössbauer .....	105
2.1.5.		.....	111
2.1.6.	$\mu$	$\mu$ - .....	115

2.2		$\mu$		$\mu$					
									116
2.2.1.	$\mu$					Raman			118
2.2.2						-			124
2.2.3.	$\mu$					össbauer			128
2.2.4.	$\mu$	$\mu$				-			135
2.3		$\mu$		$\mu$		Sn,			
			$\mu$			-Fe <sub>2</sub> O <sub>3</sub>			136
2.3.1.									137
2.3.2.				$\mu$					139
2.3.3.	$\mu$				$\mu$				139
2.3.4.	$\mu$					össbauer			140
2.3.5.						-			141
2.3.6.	$\mu$					-			145
2.3.7.	$\mu$	$\mu$				-			146
2.4		$\mu$					$\mu$	RuPt	147
2.4.1.									148
2.4.2.	$\mu$					Raman			149
2.4.3.						-			150
2.4.4.				$\mu$					152
2.4.5.	$\mu$	$\mu$				-			153
2.5		$\mu$					$\mu$		
									154
2.5.1.									154
2.5.2.	$\mu$					M		-	156
2.5.3.						-			157
2.5.4.	$\mu$	$\mu$				-			159
2.6		$\mu$					-	$\mu$	
	$\mu$					-Fe <sub>2</sub> O <sub>3</sub>			160
2.6.1.						-			161

2.6.2.	$\mu$	Raman .....	165
2.6.3.	$\mu$	M - .....	167
2.6.4.	$\mu$	.....	168
2.6.5.	$\mu$	$\mu$ - .....	169
3.		.....	170
<b>E.</b>	<b>M</b>	- .....	173
.		.....	179
.	<b>ABSTRACT</b>	.....	183
.		.....	185
.		.....	187
<b>I.</b>		.....	191



(Carbon NanoTubes

CNTs)

$\mu$   
 $(\mu \mu - \mu)$ ,  
 $\mu \mu$   
 $\mu$   
 $\mu \mu \mu \mu \mu \mu$   
 $\mu \mu \mu$   
 $\mu /$  CNTs

$\mu \mu \mu \mu \mu \mu$   
 $(\mu \mu \mu \mu \mu \mu)$   $\mu$   
 $\mu \mu \mu$   
 $\mu \mu \mu \mu \mu \mu$   
 $\mu \mu \mu \mu \mu \mu$   
 $\mu \mu \mu \mu \mu \mu$   
 $\mu \mu \mu \mu \mu \mu$

CNTs

$\mu \mu \mu \mu \mu \mu$   
 $(\mu \mu \mu \mu \mu \mu)$   
 $\mu \mu \mu \mu \mu \mu$

Multi-Wall Carbon Nanotubes

i.

( . . . )

ii.

UV-Vis, STS

PR),  $\mu$

(Raman, FT-IR, Mössbauer,

( GA-DTA),  $\mu$

S

( RD)  $\mu$   $\mu$  ( , AFM, STM  
).  $\mu$  ,







**1.**

**1.1.**

(Carbon Nanotubes  $\mu$  CNTs)

1991 Dr. Sumio Iijima<sup>1</sup> ( $\mu$ )

$\mu$   $\mu$  )

$\mu$  ,

$\mu$   $\mu$   $\mu$  4-30  $\mu$ m  $\mu$

1 mm.  $\mu$  ,  $\mu$   $\mu$

, ,  $\mu$

$\mu$  ,  $\mu$   $\mu$

$\mu$  2.2 nm. ,  $\mu$

$\mu$  « »  $\mu$

$\mu$  .

,  $\mu$   $\mu$  ,

$\mu$   $\mu$   $\mu$

$\mu$   $\mu$  ,

$\mu$   $\mu$  .

1.2.

CNTs (fibers) (filaments) . CNTs  $\mu^2$  .

(i) Nanotubes  $\mu$  SWCNTs), (Single Wall Carbon

(ii) Nanotubes  $\mu$  DWCNTs ) (Double Wall Carbon

(iii) Nanotubes  $\mu$  WCNTs). (Multi Wall Carbon

, SWCNTs  $\mu$

MWCNTs<sup>3,4</sup>.  $\mu$  1993,  $\mu$  0.4  $\mu$  2 nm.

H  $\mu$  SWCNT  $\mu$   $\mu$   $\mu$  C)

(  $\mu$  1.2.2).  $\mu$   $\mu$  C,

(n, m)  $\mu$   $\mu$   $\mu$   $a_1$

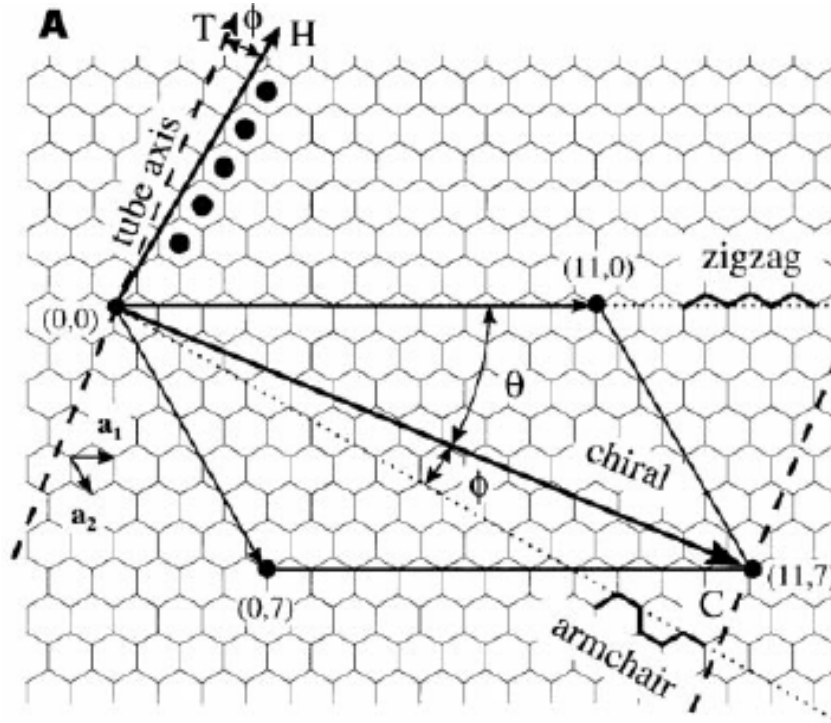
$a_2$   $\mu$  :

$C=na_1 + ma_2$ .

$\mu$   $\mu$  , n m,

$\mu$  d ( n m m 0)

SWCNTs  $\mu$   $d=a \sqrt{m^2+nm+n^2}/\pi$   $=\text{arc tan}[-3m/(2n+m)]$   
 (arc tan:  $\mu$  )<sup>5</sup>.

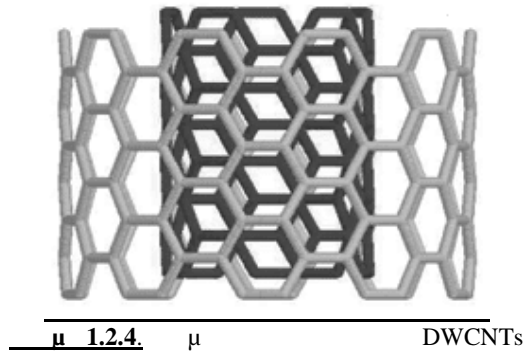


μ 1.2.2. μ μ μ μ μ SWCNTs.

μ μ SWCNTs μ  
 n m. μ , 1 SWCNTs  
 m=0. μ zig-zag ( μ 1.2.3a)  
 μ μ μ μ . 2  
 SWCNTs n=m [ armchair ( μ  
 1.2.3b)]. T SWCNTs chiral ( μ 1.2.3c)  
 n m m 0. chiral, μ  
 μ ( μ  
 SWCNT μ C), μ 0 30 . SWCNTs,  
 o μ ( μ 1.2.3d).  
 μ μ μ  
 μ μ μ μ SWCNTs.

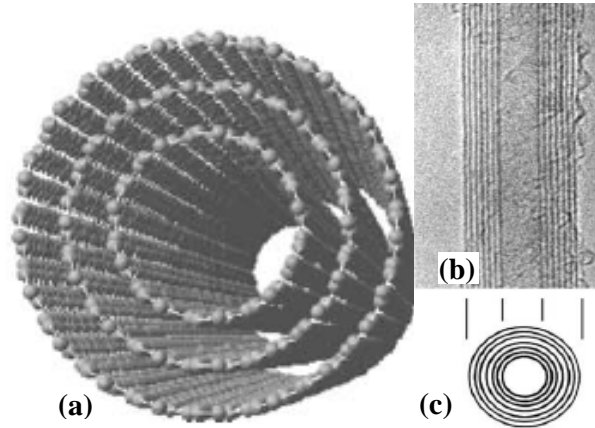


DWCNTs  $\mu$   $\mu$   
 $\mu$   $\mu$  <sup>7</sup>. H  $\mu$   
 $\mu$  (  $\mu$  1.2.4a 1.2.4b).  $\mu$   
 $\mu$  (2–3nm)  $\mu$   $\mu$   $\mu$   
SWCNTs.  $\mu$   
SWCNTs  $\mu$  MWCNTs, DWCNTs  
 $\mu$  CNTs.  $\mu$   $\mu$   
DWCNTs  $\mu$   $\mu$   
 $\mu$   $\mu$  SWCNTs<sup>8</sup>,  $\mu$   
 $\mu$  (field emitters)  $\mu$   
SWCNTs MWCNTs<sup>9</sup>.



DWCNTs o  
SWCNT ,  $\mu$   
 $\mu$  .  
 $\mu$   $\mu$   $\mu$   $\mu$   $\mu$   
 $\mu$  <sup>10</sup>. DWCNTs  $\mu$   
 $\mu$   $\mu$   $\mu$   $\mu$   
 $\mu$  .  
MWCNTs  $\mu$   
 $\mu$  (  $\mu$  1.2.5).  $\mu$   
 $\mu$   $\mu$   $\mu$  0.3-0.4 nm.

$\mu$  MWCNTs  $\mu$  5 100 nm  $\mu$   
 $\mu$   $\mu$   $\mu\text{m}$ .



$\mu$  1.2.5. (a)  $\mu$  (TEM) WCNT  $\mu$  , (b)  $\mu$  MWCNTS  $\mu$  7  $\mu$  (c)  $\mu$  .

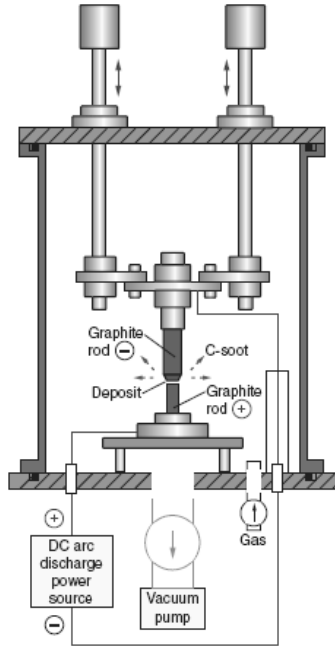
### 1.3.

$\mu$  ,  $\mu$   $\mu$  CNTs  $\mu$  (electric arc discharged),  $\mu$  laser (laser ablation)  $\mu$  (Catalytic Chemical Vapor Deposition CCVD).

#### B1.3.1 (Electric Arc Discharge)

$\mu$  . CNTs  $\mu$   $\mu$  Kratschmer 1990<sup>11</sup>.  $\mu$   $\mu$  1.3.1  $\mu$   $\mu$   $\mu$  (vacuum pump).  $\mu$  (gas)  $\mu$   $\mu$  (DC arc discharge power source)  $\mu$   $\mu$  (graphite rods).  $\mu$   $\mu$

$\mu$   $\mu$  (C-soot)  $\mu^{12}$ .  $\mu$   $\mu$   $\mu$   
 $\mu$  CNTs<sup>1</sup>.



$\mu$  1.3.1.

13

WCNTs  $\mu$  He,  
 SWCNTs  
 (Ni, Co, Fe, Pt, Pd . . )  $\mu$   
 $\mu$  Ni-Co<sup>14</sup>.  
 S  
 $\mu$  15, 16.  $\mu$  SWCNTs  
 MWCNTs  $\mu$ .  
 DWCNTs  $\mu$   $\mu$   $\mu$   $\mu$   
 $\mu$   $\mu$  SWCNTs  $\mu$   
 $\mu$  17-19.  
 $\mu$  CNTs  $\mu$   $\mu$   
 $\mu$   $\mu$   $\mu$ ,  $\mu$   
 $\mu$  CNTs  
 $\mu$   
 $\mu$   $\mu$ .



**B1.3.2  $\mu$  laser (Laser ablation)**

$\mu$  laser,  $\mu$  CNTs Smalley <sup>20, 21</sup>  $\mu$

1.3.2  $\mu$   $\mu$

(furnace),  $\mu$  (pump), (quartz tube), (target rod)  $\mu$ ,  $\mu$

(trap)  $\mu$  (flow controllers)<sup>20, 21</sup>  $\mu$  laser ( YAG CO<sub>2</sub>)  $\mu$  (window)  $\mu$

$\mu$  Ar  $\mu$   $\mu$  CNTs. Ar

1cm<sup>3</sup>/s 500 torr . CNTs  $\mu$

laser  $\mu$

$\mu$   $\mu$   $\mu$

$\mu$   $\mu$   $\mu$

CNTs,  $\mu$   $\mu$   $\mu$

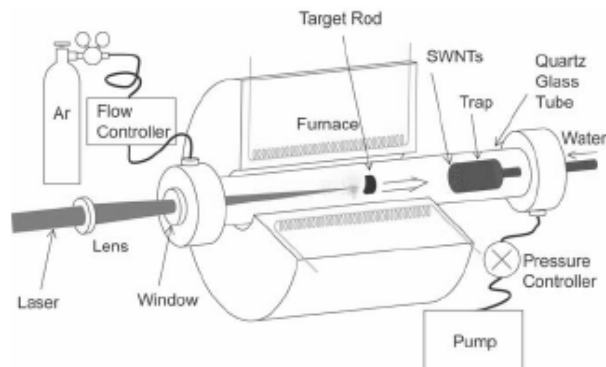
$\mu$  CNTs  $\mu$   $\mu$

$\mu$  ,  $\mu$

<sup>22, 23</sup>  $\mu$   $\mu$   $\mu$

CNTs<sup>24</sup>.  $\mu$  CNTs

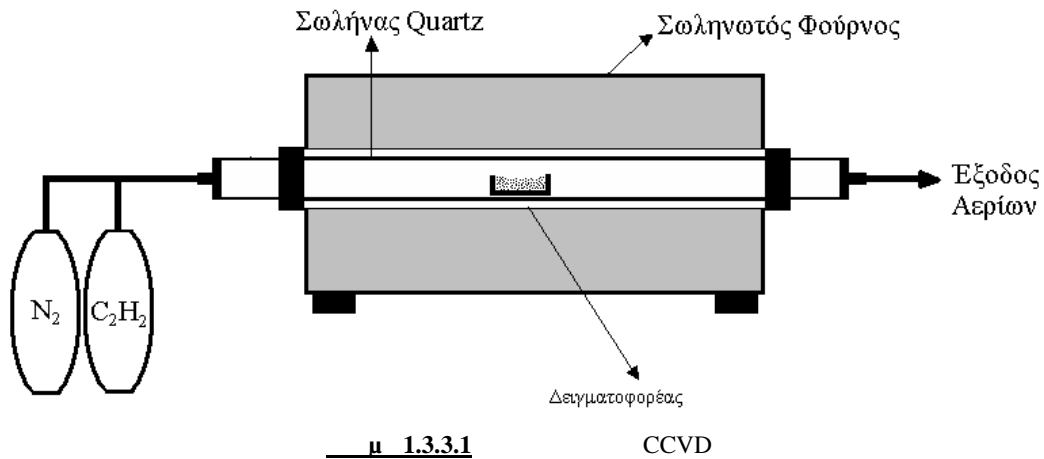
s)  $\mu$   $\mu$   $\mu$  (  $\mu$  (  $\mu$  ns)<sup>22</sup>.



$\mu$  1.3.2.  $\mu$  laser <sup>21</sup>.

### B1.3.3

μ μ (Catalytical Chemical Vapor Deposition  
CCVD) μ μ CNTs,  
μ μ  
μ μ .  
μ μ μ CNTs ( μ  
μ laser) CCVD μ  
μ μ  
μ μ .  
( ,  
) μ , μ  
CNTs μ ( ,  
μ , μ CNTs, μ CNTs, CNTs  
μ μ ). CCVD μ μ  
1959<sup>25-27</sup>. CCVD  
μ μ μ μ CNTs  
μ <sup>28, 29</sup> ( μ <sup>30</sup>), μ <sup>31, 32</sup>  
<sup>13, 33</sup> .  
μ μ μ μ  
CNTs, Endo <sup>34</sup> μ μ CNTs  
1100 °C, o José-Yacamán  
<sup>35</sup> MWCNTs 700 °C μ  
μ Fe μ  
μ μ μ μ o  
<sup>36</sup>, μ <sup>37</sup> . SWCNTs  
Dai <sup>38</sup> μ μ  
, μ μ  
<sup>39</sup> μ <sup>40</sup> .  
CNTs μ  
( 15-60 min) μ  
μ (600-1200 °C),  
( μ 1.3.3.1).



CNTs

μ μ μ . μ

( . . . ) - μ

μ .

( . . . ) μ μ

μ

μ μ

μ *in situ* ( μ floating catalyst).

μ μ μ μ

CNTs. μ μ CNTs

μ μ μ μ

μ μ « » (fullerene dome)

μ μ CNTs

μ ( μ<sup>41, 42</sup>).

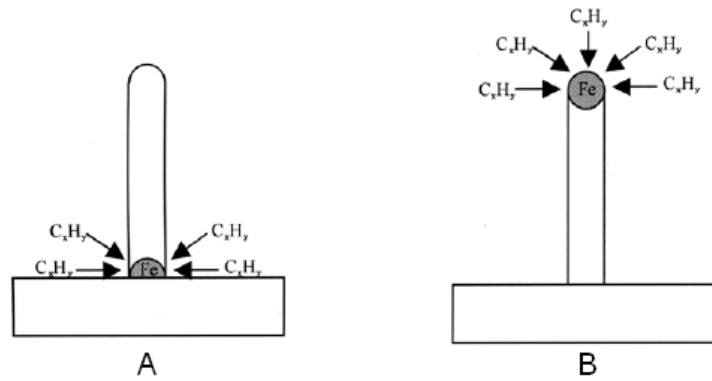
μ μ , CNTs

μ μ μ μ

( 'base growth model', μ 1.3.3.2 ).

μ μ ,

( 'tip growth model', 1.3.3.2 ). H  
 SWCNTs MWCNTs  
 SWCNTs ( nm)  
 WCNTs ( nm).



1.3.3.2 CNTs «base growth model»  
 CNTs «tip growth model»

CNTs  
 CCVD (600-900 °C)  
 MWCNTs (900-1200 °C)  
 SWCNTs  
 CCVD (aligned) CNTs  
 Li  
 Fe  
 CNTs  
 Terrones  
 CCVD  
 Pan

μ CNTs μ  
 μm μ μ μ CCVD 44.  
 μ (Fe, Co, Ni) μ μ  
 CNTs μμ  
 μ  
 μ , μ μ CNTs μ μ  
 μ μ . μ  
 μ μ , μ  
 μ in situ CNTs.  
 μ μ μ μ μ  
 . μ μ  
 μ μ 45. μ  
 μ μ μ  
 μ CNTs<sup>46</sup>. , μ μ  
 μ μ μ μ μ  
 μ CNTs. μ , μ μ  
 , μ  
 CNTs μ μ μ 47.

## B1.4

CNTs μ μ  
 μ μ μ μ  
 μ .

### B1.4.1

μ μ μ μ μ μ  
 .  
 μ μ μ 2s  
 2p . μ μ  
 μ μ (interatom binding energies)  
 μ μ μ  
 μ s n-p μ spn .

$\mu$  (sp, sp<sup>2</sup>, sp<sup>3</sup>)  $\mu$  .  $\mu$   
 $\mu$  sp<sup>3</sup>  $\mu$  , (planar)  $\mu$   $\mu$  -  
 $\mu$  sp<sup>2</sup>  $\mu$  .

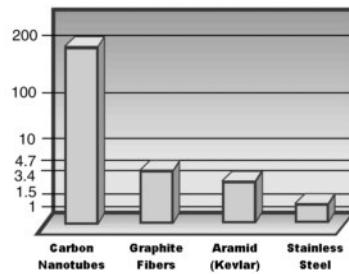
**B1.4.2**

$\mu$   $\mu$   $\mu$   $\mu$   
 $\mu$   $\mu$  C-C,  $\mu$   $\mu$   
 $\mu$   $\mu$  Pa  
 $\mu$   $\mu$  ,  $\mu$   $\mu$  (  $\mu$   
 1.4.2.1).



$\mu$  1.4.2.1.  $\mu$   $\mu$   $\mu$  SWCNT

$\mu$  1.4.2.2  $\mu$   $\mu$   $\mu$   
 $\mu$   $\mu$  ,  $\mu$  , Kevlar  
 $\mu$  100  $\mu$   
 $\mu$  1/6 .

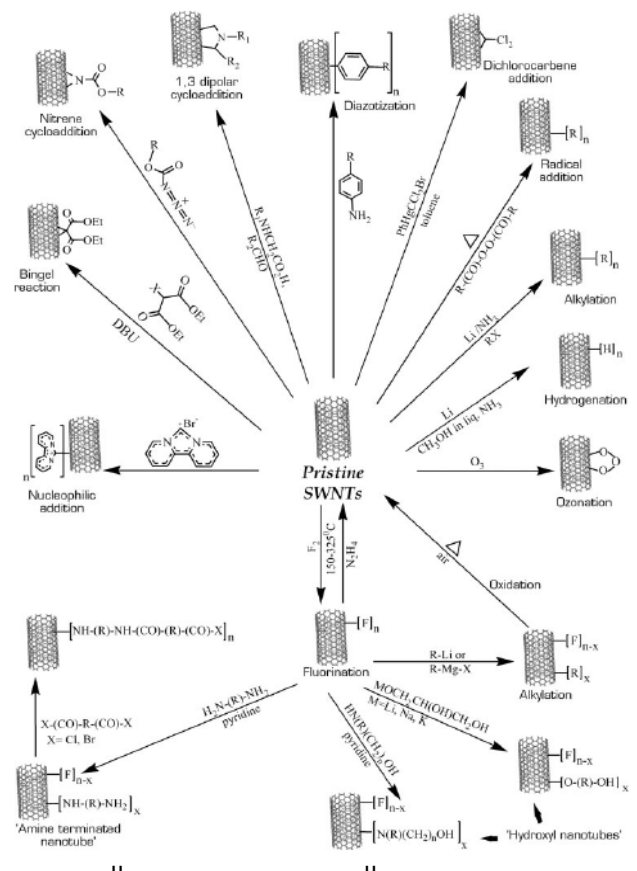
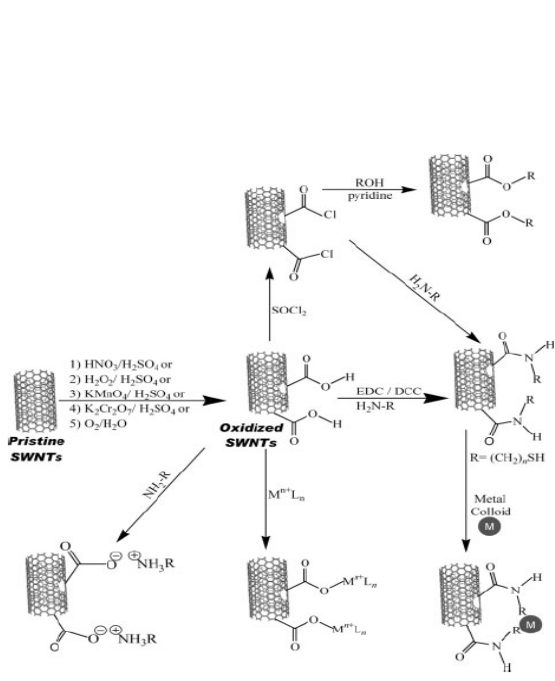


$\mu$  1.4.2.2.  $\mu$  SWCNTs  $\mu$   $\mu$   $\mu$

**B1.4.3**  $\mu$

H  $\mu$  /

μ . μ μ , μ  
 . μ μ μ μ μ μ  
 (supramolecular) μ , CNTs  
 μ μ μ . CNTs μ  
 « » μ μ μ  
 . μ μ μ  
 μ μ μ μ μ  
 μ μ μ μ μ :  
 I. μ μ μ μ -  
 II. μ - μ (adsorption) (wrapping)  
 III. μ μ μ  
 μ :  
 1) A CNTs<sup>50-52</sup>  
 2) CNTs<sup>53-55</sup>  
 3) CNTs<sup>56, 57</sup>  
 4) CNTs<sup>58-60</sup>  
 5) μ CNTs<sup>61</sup>  
 6) μ CNTs<sup>62, 63</sup>  
 7) CNTs<sup>64-66</sup>  
 8) - μ CNTs<sup>67, 68</sup>  
 9) CNTs μ μ<sup>69</sup>  
 10) CNTs<sup>70-72</sup>  
 11) μ (grafting) μ CNTs<sup>73-75</sup>



μ 1.4.3.1.

- μ - μ
- μ μ :
- 1) μ μ :
- 1.1) μ 76, 77
- 1.2) μ 78, 79
- 1.3) μ 80, 81
- 1.4) μ 82, 83
- 1.5) μ ( 84, 85, μ 86, 87,
- μ 88, 89 . .)
- 2) 90-92
- 3) 93, 94
- 4) μ 95, 96



- μ          μ          :
- 1)    97, 98    99, 100
  - 2)          μ          101, 102
  - 3)    103, 104

**B1.4.4          &**

μ          μ          105 .          μ          μ

μ          μ          sp<sup>2</sup>          μ          μ

μ          μ          van der Waals

0.34 nm.

μ μ          (semi-metal)          μ          μ          μ

(0.04 eV), μ          μ

μ          μ

μ          μ          CNTs          μ

μ          (          armchair, chiral SWCNTs          ,          1.2).

μ          μ          μ          (n,m)          μ          μ

μ          μ          μ          m=n,          μ          μ μ

μ          μ          n-m=3j          j

μ          μ          μ          μ .

CNTs μ          μ          (electron localization)

μ          μ          (          ,          )          μ          .

μ          μ          μ          μ          ,

μ          μ          μ          μ          μ          106 .

μ          107 μ          μ          μ          μ          ,          μ

μ          .

**B1.5**      $\mu$

$\mu$                                     $\mu$                                    ,

$\mu$       $\mu$                                     $\mu$

$\mu$       $\mu$                                    :

- -         (nano-probes)         -         (nano-sensors)<sup>108-</sup>  
111.
- -         (nano-fillers)          $\mu$          ,          $\mu$   
 $\mu$           $\mu$          112-115.
- -          $\mu$          (          $\mu$          116,  
117,          $\mu$          118).
- -          $\mu$          119, 120 .
- -          $\mu$          121-
- 123
- -      $\mu$          (nano-templates)<sup>124</sup>  
 $\mu$  .





CNTs  $\mu$   $\mu$  <sup>140</sup>  $\mu$  <sup>141</sup>,  
 $\mu$  <sup>140, 142</sup>

Chen <sup>143</sup>  $\mu$   $\mu$   $\mu$   
 $\mu$   $\mu$  Pt, Ag, Au, Pd Cu  
 $\mu$  <sup>144</sup>

$\mu$   $\mu$   $\mu$  CNTs,  
 $\mu$   $\mu$  NPs.  
 $\mu$   $\mu$   $\mu$

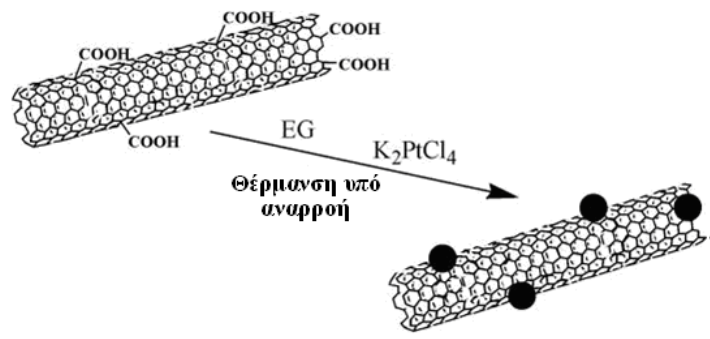
$\mu$   $\mu$   $\mu$   $\mu$   
 $\mu$   $\mu$   $\mu$   $\mu$   $\mu$   $\mu$   
CNTs.

O Lordi <sup>145</sup>  $\mu$   $\mu$   $\mu$   $\mu$   $\mu$   $\mu$   
 $\mu$   $\mu$   $\mu$  “ ”  
 $\mu$   $\mu$   $\mu$  Pt,  $\mu$

(  $\mu$  1.6.1.1). 10% NPs

Pt,  $\mu$   $\mu$  1-2 nm.  $\mu$  Pt-SWNT  
3- $\mu$  -2-  $\mu$

75 °C.



$\mu$  1.6.1.1  $\mu$   $\mu$   $\mu$  Pt

Cells PEFC)  $\mu$   $\mu$  (Polymer electrolyte Fuel  
 (Direct Methanol Fuel Cells DMFC)  
 $\mu$  Pt  $\mu$  Pt  $\mu$   
 $\mu$   $\mu$  Pt  
 $\mu$   $\mu$   $\mu$   $\mu$  Pt  
 $\mu$   $\mu$   $\mu$   $\mu$   
 $\mu$   $\mu$   $\mu$   $\mu$   
 Xin  $\mu$   
 Pt-MWCNTs  $\mu$   $\mu$   
 DMFC<sup>146</sup>.  
 $\mu$   $\mu$   $\mu$  Pt  $\mu$  MWCNTs.  
 $\mu$   $\mu$   $\mu$   $\mu$  Pt  
 $\mu$   $\mu$   $\mu$   $\mu$   $\mu$  Pt  
 $\mu$   $\mu$  10 wt%  $\mu$   $\mu$  NPs Pt  $\mu$   $\mu$   
 $\mu$   $\mu$  . TEM XRD  $\mu$   $\mu$   $\mu$   
 2.5 nm. DMFC,  $\mu$   
 $\mu$   $\mu$   $\mu$   $\mu$   $\mu$   
 $\mu$   $\mu$   $\mu$   $\mu$  XC-72  
 $\mu$  Pt.  
 $\mu$  NPs Pt  $\mu$   
 MWCNTs  $\mu$  XC-72 .  
 $\mu$   $\mu$   $\mu$   $\mu$  Pt  $\mu$   $\mu$   $\mu$  5 nm  
 $\mu$   $\mu$   $\mu$   $\mu$   $\mu$   $\mu$   
<sup>147</sup> . Pt  $\mu$  30%  
 wt,  $\mu$   $\mu$   $\mu$   
 $\mu$   $\mu$  2,  $\mu$   
 $\mu$   $\mu$   $\mu$  Pt.

Liu <sup>148</sup>  $\mu\text{m}$   $\mu\text{m}$   $\mu\text{m}$   
 $\mu\text{m}$  Pt  $\mu\text{m}$   $\mu\text{m}$  CNTs.  
 Pt-CNT  $\mu\text{m}$   
 PEM  $\mu\text{m}$   $\mu\text{m}$   
 $\mu\text{m}$   $\mu\text{m}$   $\mu\text{m}$   $\mu\text{m}$  Pt/Ru/Ir  $\mu\text{m}$   $\mu\text{m}$  (1  
 nm). NPs CNTs  $\mu\text{m}$   
 Pt/Ru/Ir-CNT  $\mu\text{m}$   
<sup>138</sup>  $\mu\text{m}$   
 $\mu\text{m}$  Ni  $\mu\text{m}$   
 CNTs , Ni-CNT  $\mu\text{m}$   
<sup>149, 150</sup> Xu  
 $\mu\text{m}$  Pd Sn NPs Ni Pd  
 CNTs<sup>135</sup>  $\mu\text{m}$   $\mu\text{m}$  CNTs,  $\mu\text{m}$   
 $\mu\text{m}$   $\mu\text{m}$   $\mu\text{m}$   $\mu\text{m}$  ,  
 ,  $\mu\text{m}$  CNTs  
 $\mu\text{m}$   $\mu\text{m}$   $\mu\text{m}$   $\mu\text{m}$   $\mu\text{m}$   
 $\mu\text{m}$   $\mu\text{m}$   $\mu\text{m}$   $\mu\text{m}$  MWCNTs  
 $\mu\text{m}$   $\mu\text{m}$   $\mu\text{m}$   $\mu\text{m}$   $\mu\text{m}$   
 $\mu\text{m}$   $\mu\text{m}$   $\mu\text{m}$   $\mu\text{m}$   $\mu\text{m}$   
 CNT<sup>151</sup>  $\mu\text{m}$   $\mu\text{m}$   
 O Dai  $\mu\text{m}$   $\mu\text{m}$   
 $\mu\text{m}$  CNTs<sup>152</sup>  $\mu\text{m}$   
 $\mu\text{m}$  Pt Au  $\mu\text{m}$   
 $\mu\text{m}$   $\mu\text{m}$   $\mu\text{m}$   $\mu\text{m}$   $\mu\text{m}$   
 $\mu\text{m}$   $\mu\text{m}$   $\mu\text{m}$   $\mu\text{m}$   $\mu\text{m}$   
 $\mu\text{m}$  SWCNTs  $\mu\text{m}$   $\mu\text{m}$   
 $\mu\text{m}$  3  $\mu\text{m}$   $\mu\text{m}$   $\mu\text{m}$   $\mu\text{m}$  HAuCl<sub>4</sub> (Au<sup>3+</sup>)  
 $\mu\text{m}$  Na<sub>2</sub>PtCl<sub>2</sub> (Pt<sup>2+</sup>).  $\mu\text{m}$  SWCNTs  
 $\mu\text{m}$   $\mu\text{m}$   $\mu\text{m}$   $\mu\text{m}$   
 $\mu\text{m}$   $\mu\text{m}$  SWCNTs

μ   μ   μ   μ   .   μ

Ni<sup>2+</sup>   Cu<sup>2+</sup>   Au   Pt.   μ   Ag<sup>+</sup>,

μ   μ   .   μ   μ

μ   μ   Cu   Ag   CNTs   μ   153.

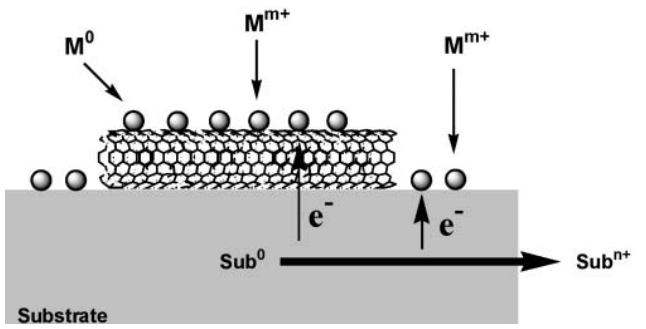
μ   μ   ( . . Au) μ   μ   μ

μ   μ   μ   ( . . Cu)

μ   μ   μ ( μ 1.6.1.2).   μ   μ   μ

μ   μ   μ   μ   μ

μ   μ   μ   μ   μ .



μ 1.6.1.2.   μ   μ -   μ

,   μ   Au, Pt   Rh   SWCNTs,

μ   μ   (   μ   ) μ

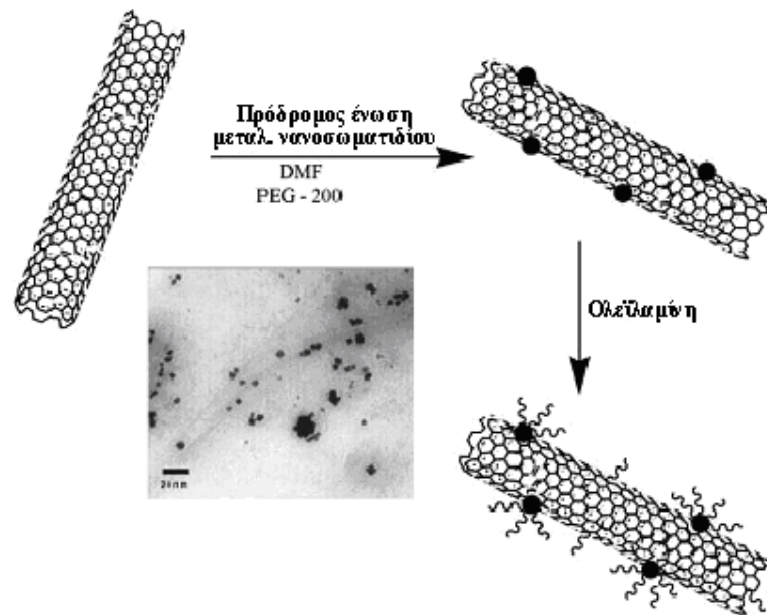
<sup>154</sup> ( μ 1.6.1.3).   μ ,

μ

154

μ   μ   μ   .





μ 1.6.1.3.      μ      μ      μ      μ      μ      μ      μ

SWCNTs      Au, Pt      Rh

(electrodeposition)<sup>136, 155, 156</sup>

μ      CNTs      μ      HAuCl<sub>4</sub>, K<sub>2</sub>PtCl<sub>4</sub>, (NH<sub>4</sub>)<sub>2</sub>PdCl<sub>4</sub>      μ

μ      μ      μ      Au, Pt      Pd      μ

CNTs.      μ      μ      μ      , μ

μ      μ      μ      μ      μ      μ

CNTs μ      μ      μ      μ      μ      μ

μ      μ      NPs-CNT      μ      μ      .

CNTs      μ      μ      μ      μ      μ      μ

μ .      μ      , μ μ      ,      μ

μ      μ      μ      μ      μ      μ      μ

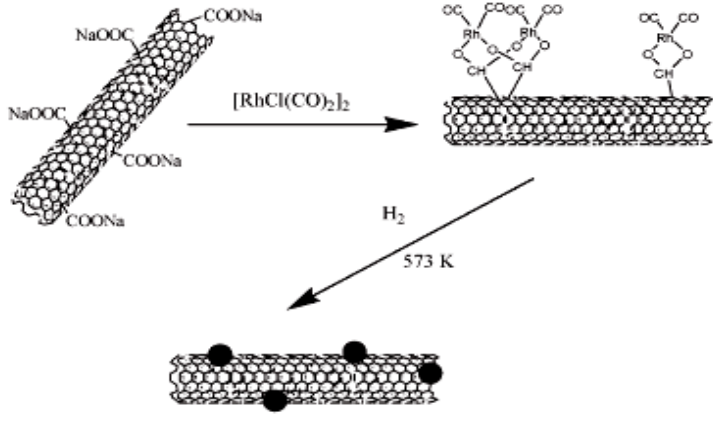
μ      μ      μ      μ      μ      μ      μ

, CNTs μ      μ      μ      μ      μ      μ

μ      μ      μ      μ      μ      μ      μ

NPs  $\mu$   $\mu$   $\mu$   $\mu$   $\mu$   $\mu$   
 CNTs  $\mu$   $\mu$   $\mu$   $\mu$   $\mu$   $\mu$   
 $\mu$   $\mu$   $\mu$  Pd, Rh  $\mu$  Rh/Pd CNTs  
 $\mu$  -  $\mu$  ( - )  $\mu$   $\mu$   $\mu$   
 $\mu$  NPs CNTs.  $\mu$   $\mu$   
 $\mu$   $\mu$  -  $\mu$   $\mu$   
 $\mu$   $\mu$  NPs  $\mu$  CNTs (  $\mu$   
 1.6.1.4).  $\mu$   $\mu$   $\mu$  NPs  
 $\mu$   $\mu$   $\mu$   $\mu$   $\mu$   $\mu$   
 - 13% 17% wt. Pt  
 Rh <sup>157</sup>  $\mu$  Rh  
 $\mu$   $[\text{Rh}_2\text{Cl}_2(\text{CO})_4]$   $\mu$   $\mu$

158



$\mu$  1.6.1.4.  $\mu$   $\mu$   $\mu$   $\mu$   $\mu$  NPs  
 CNTs  $\mu$   $\mu$   $\mu$  -  $\mu$   $\mu$   $\mu$

Hor  $\mu$  Pt CNTs<sup>139</sup>.  
 $\mu$  ,  $\mu$   
 $\mu$   $\mu$  HNO<sub>3</sub>  $\mu$   $\mu$  H<sub>2</sub>SO<sub>4</sub>-HNO<sub>3</sub>,  
 $\mu$   $\mu$  NPs Pt  
CNTs.  $\mu$   
 $\mu$  .  
Pt-CNT  $\mu$   $\mu$   
Pt(II)-  $\mu$  <sup>159</sup> .  $\mu$   
 $\mu$   $\mu$   $\mu$   $\mu$   
. Xu  $\mu$   
 $\mu$   $\mu$  Pt CNTs  $\mu$   $\mu$  <sup>160</sup> .  
 $\mu$   $\mu$   $\mu$   $\mu$   
 $\mu$  NPs.

1.6.2

(a)

(b)

1.6.2.1

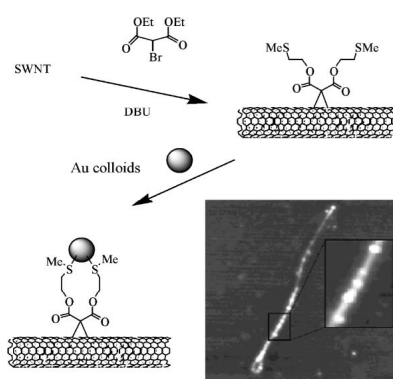
Haddon<sup>161</sup>, SWCNTs

SWCNTs. Au

SWCNTs

Bingel<sup>162, 163</sup>

(1.6.2.1).



1.6.2.1

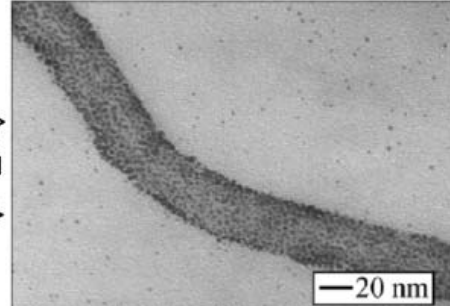
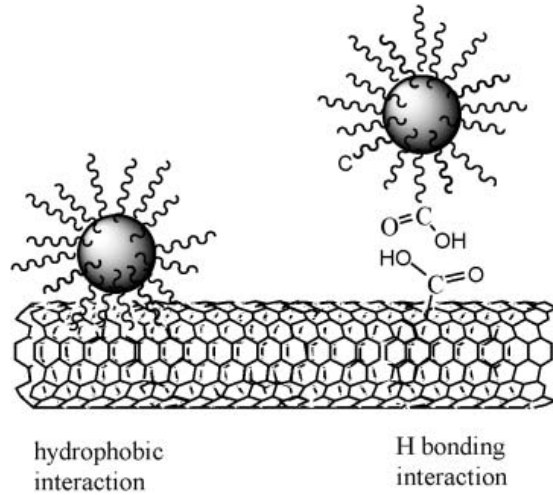
Bingel

Au

### 1.6.2.2

$$\begin{array}{cccccccc} & & & \mu & \mu & \mu & & \mu \\ & & & & \mu & & \mu & \\ & & \mu & \mu & & \mu & & \\ & \mu & & & \mu & & & \\ \mu & & \mu & (i) & - & (ii) & & (iii) \end{array}$$





hydrophobic interaction

H bonding interaction

1.6.2.2.1.

Zhu

bamboo (BCNTs)

NPs Au

168

BCNTs

(II)-

Au-BCNT

TEM

Au

Au-N.

Fitzmaurice

( $\mu$  , van der Waals,  $\mu$  ,

and  $\mu$  )  $\mu$   $\mu$  NPs Au

MWCNTs,

CNTs  $\mu$  NPs Au

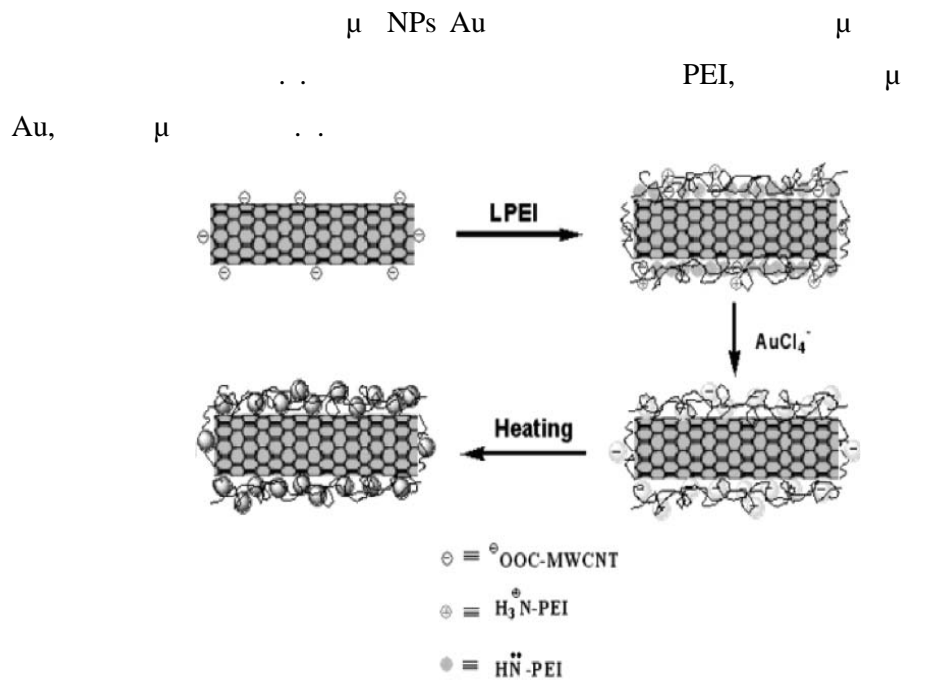
169

$\mu$  MWCNTs,  $\mu$   
 MWCNT NPs,  $\mu$   
 $\mu$  MWCNTs  $\mu$  NPs Au  
 Fitzmaurice <sup>170</sup>  
 $\mu\mu$  (crown ethers) MWCNTs  $\mu$  NPs<sup>171</sup>.  
**1.6.2.2.2 A**  
 $\mu$  CNT  $\mu$  - <sup>172-175</sup>  
 $\mu$  NPs Au  $\mu$  CNTs. H  
 $\mu$   $\mu$   $\mu$   $\mu$  Raman CNTs  $\mu$   
 $\mu$  CNTs NPs Au  $\mu$   $\mu$  ( $\mu$ ).  
 $\mu$   $\mu$   $\mu$  CNTs  
 $\mu$  SWCNT  $\mu$  Zn  
<sup>172</sup>  $\mu$   
 $\mu$   $\mu$  Fe<sub>3</sub>O<sub>4</sub>, Co CoPt SWCNT  $\mu$   
 $\mu$  NPs,  
 $\mu$  SWCNTs ( $\mu$  1.6.2.2.2). H  
 $\mu$   
 $\mu$  <sup>176</sup>.





$\mu$  « »  
 $\mu$  CNTs  $\mu$   $\mu$  NPs.  $\mu$   
 $\mu$  NPs Au<sup>179</sup>.  
 $\mu$  NPs.  
 $\mu$   $\mu$  NPs Au-MINTs  $\mu$   $\mu$  L L (layer-by-layer)  $\mu$  <sup>182</sup>.  $\mu$   $\mu$   $\mu$  MWCNTs  $\mu$   
 $\mu$  [PDDA, (  $\mu$   $\mu$   $\mu$  )]  
 $\mu$   $\mu$   $\mu$  [PSS, (4-  $\mu$  )].  
 $\mu$  Au,  $\mu$   $\mu$   
Au  $\mu$  PSS.  $\mu$  NPs  
 $\mu$  MWCNTs  
 $\mu$   $\mu$  ,  
NPs-CNTs  $\mu$   $\mu$  ,  $\mu$   
PDDA/PSS-LBL  $\mu$  .  
 $\mu$  LBL  $\mu$   
Au  $\mu$   $\mu$   $\mu$   $\mu$  MWCNTs<sup>183</sup>.  
MWCNTs  $\mu$   $\mu$   $\mu$   
(PSS)  $\mu$   $\mu$   $\mu$  (PDDA).  $\mu$   
 $\mu$   $\mu$  , Au,  
 $\mu$   $\mu$  Nikoobakht El-Sayed<sup>184</sup>.  $\mu$   $\mu$   
 $\mu$   $\mu$   $\mu$   $\mu$   
 $\mu$   $\mu$  - $\mu$  - .  
( -  $\mu$  - )  $\mu$   
 $\mu$   $\mu$   $\mu$  . PEI  
 $\mu$  «  $\mu$  » NPs  
. Dong <sup>185</sup>  
PEI  $\mu$   $\mu$  Au-CNT  $\mu$  in situ  
Au PEI MWCNTs (  $\mu$  1.6.2.2.3). H



μ 1.6.2.2.3.

*in-situ*

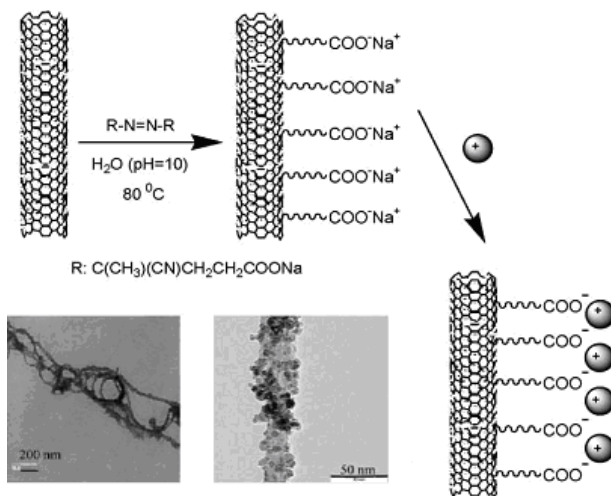
Au

Jerome

186

NPs Fe<sub>3</sub>O<sub>4</sub> ( μ 1.6.2.2.4).

MWNTs<sup>187</sup>



μ 1.6.2.2.4.

Luong <sup>188</sup>  $\mu$  Pt-

SWCNTs  $\mu$   $\mu$   $\mu$  .

$\mu$   $\mu$  (Nafion)  $\mu$   $\mu$   $\mu$

,  $\mu$

$\mu$

<sup>189</sup> . ,

NPs Pt  $\mu$

$\mu$  .

,  $\mu$   $\mu$   $\mu$  Au  $\mu$

$\mu$   $\mu$   $\mu$

$\mu$   $\mu$  NPs<sup>190</sup> .

$\mu$   $\mu$   $\mu$   $\mu$   $\mu$   $\mu$

$\mu$   $\mu$  ,  $\mu$   $\mu$   $\mu$

Au  $\mu$  ,  $\mu$

.  $\mu$   $\mu$

$\mu$   $\mu$  .

**1.8**

$\mu$  .  $\mu$  90%  $\mu$   $\mu$   
 75%  $\mu$  . ,  $\mu$  - .  
 ,  $\mu$

$C_xH_y$ .  $\mu$   $\mu$  . 0,0899 g/l  
 (14.4  $\mu$  ), -257,77°.

$\mu$  . 1 kg  $\mu$  119.972 kJ. 1 kg  
 $\mu$  2.1 kg 2.8 kg  
 $\mu$  :  $2 \mu^2 + \mu^2 + 567 J$

( $\mu$   $\mu$  ).  $\mu$   
 $\mu$   $\mu$

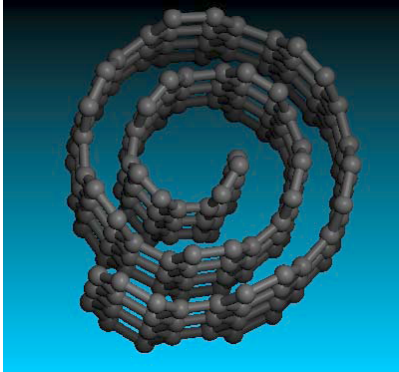
585 C 13% - 65%  $\mu$   $\mu$   
 ,  $\mu$  570 487 C  
 6.3% - 14%.  $\mu$

$\mu$   $\mu$  .  $\mu$   
 $\mu$   $\mu$   $\mu$   $\mu$   $\mu$   $\mu$   
 $\mu$  .  $\mu$  21 ,  $\mu$  20 ,  
 $\mu$  ,  $\mu$  ,  $\mu$   
 $\mu$   $\mu$  ,  $\mu$   
 $\mu$   $\mu$   $\mu$  .  $\mu$  .  
 $\mu$   $\mu$   $\mu$  ,  $\mu$  ,  
 $\mu$   $\mu$  .  $\mu$  ,  
 $\mu$   $\mu$   $\mu$  ,  $\mu$   
 $\mu$   $\mu$  .  $\mu$

Bar). .  $\mu$   $\mu$   $\mu$   $\mu$   $\mu$   $\mu$   $\mu$  (300-700  
o  $\mu$   $\mu$  !  
 $\mu$   $\mu$   $\mu$   $H_2$   $\mu$  .  
 $\mu$   $\mu$   $\mu$   $\mu$   $\mu$   $\mu$  2% . .  
 ,  $\mu$   $\mu$   $\mu$   $\mu$  ,  
Ames NASA . Srivastava  $\mu$   
 $\mu$  10% .  $H_2$   $\mu$   
 $\mu$   $H_2$   $\mu$   $\mu$  . ,  $\mu$   
 ,  
1999 Chen  
 $\mu$   $\mu$   $\mu$   $\mu$   $\mu$   $\mu$   
 ,  $\mu$   $\mu$   
 $\mu$  .  
 $\mu$   $\mu$   $\mu$   $\mu$   
 $\mu$   $\mu$  ,  $\mu$  (carbon  
nanoscrolls –  $\mu$  1.8.1), ,  $\mu$   $\mu$   
 $\mu$  .  $\mu$  .  
 $\mu$   $\mu$   $\mu$  (multi wall).  
 $\mu$   $\mu$   $\mu$   $\mu$

μ

μ



μ 1.8.1. μ

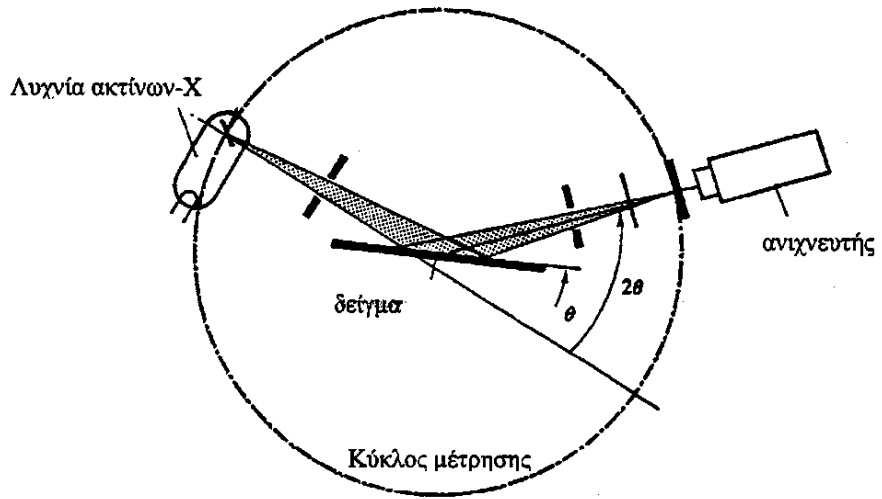
2.

2.1

-  $\mu$   $\mu$   
 $\mu$   $\mu$  .  $\mu$   
 $\mu$   $\mu$   $\mu$  .  
 $\mu$  ,  
 $\mu$   $\mu$  .  $\mu$   $\mu$  ,  
 $\mu$   $\mu$  ,  $\mu$   $\mu$   
 $\mu$   $\mu$   
 $\mu$  ,  $\mu$  : c =  $\mu$   $\mu$   
 $\mu$   $\mu$   $\mu$   
 $\mu$  .  $\mu$   $\mu$  -  $\mu$   
 0.1Å 10 nm.  $\mu$   $\mu$   
 $\mu$   $\mu$  , ,  
 .  
 -  $\mu$   
 $\mu$  ,  $\mu$  Volt,  $\mu$   $\mu$   
 $\mu$   $\mu$   $\mu$  .  $\mu$  ,  
 $\mu$  - ,  
 $\mu$  .  $\mu$  ( )  
 m . V  $\mu$   $\mu$   $\mu$   
 ( ) ( )  $\mu$   $\mu$   
 $\mu$   $\mu$   $\mu$  ,  $\mu$   
 $\mu$   $\mu$   $\mu$  .  
 -  $\mu$  (~99%)  $\mu$   
 - .  
 $\mu$   $\mu$  -  $\mu$   $\mu$   
 $\mu$  - ,  $\mu$   $\mu$



μ ( μ 2.1.1).



μ 2.1.1. μ μμ

μ

μ μ . μ μ μ μ μ 10  
eV, μ μ μ μ μ μ μ

μ

μ . μ

μ

μ μ

μ

Bragg.

$$n = 2 d \sin \theta \quad (n = 1, 2, 3, 4, \dots)$$

Bragg.

n, d

μ

,

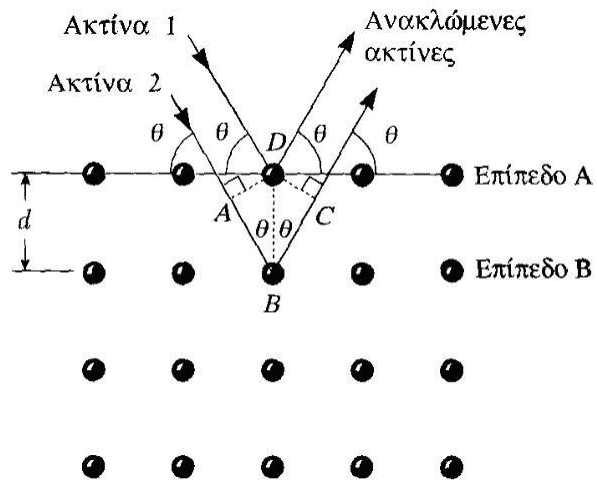
μ

μ

μ

μ

μ 2.1.2.



μ 2.1.2.

-

μ

« » :

•

( μ μ μ μ ) .

• μ μ μ

( μ ) .

• μ .

• μ μ .

μ

μ

μ .

2.2  $\mu$

$\mu$  (IR)  $\mu$   $\mu$

$\mu$   $\mu$   $\mu$   $\mu$   $\mu$

$\mu$   $\mu$   $\mu$   $\mu$   $\mu$  ,

$\mu$  ,

$\mu$   $\mu$   $\mu$

$\mu$  ,  $\mu$

$\mu$   $\mu$

$\mu$   $\mu$  ,

$\mu$   $\mu$

$\mu$  .

$\mu$   $\mu$

$\mu$   $\mu$   $\mu$  ,

$\mu$  .  $\mu$  ,

$\mu$   $\mu$

$\mu$  .  $\mu$  ,

(stretch),  $\mu$   $\mu$   $\mu$  ,

$\mu$  (deformation),  $\mu$  (bending),  $\mu$

$\mu$   $\mu$  , (rocking) (twisting).  $\mu$

$\mu\mu$   $\mu$  ,  $\mu$  ,  $\mu^3 - 6$

( $3 - 5$   $\mu$   $\mu\mu$ )<sup>191</sup>.

$\mu$  ,  $\mu$

$\mu$  Beer-Lambert-

Bouguer:

$$I = I_0 e^{-acl} \quad (2.2.1)$$

$I_0$ :  $\mu$  ,  $c$ :  $\mu$  ,  $l$ :

$\mu$   $a$ :  $\mu$  . (5.2.1)  $\mu$

$\mu$  :

$$\log(I_0/I) = c l \quad (2.2.2)$$

:  $\mu$   $\mu$   $\mu$   $\mu$

$\mu$  .  $\mu$

$$, \quad \mu \quad \mu \quad , \quad (2.2.2)$$

$\mu \quad ( ) \quad ( ) .$

$$A = \log(I_0/I) = \log(I_0/I) = \quad c l \quad (2.2.3)$$

$$\mu \quad \mu$$

$$\mu \quad , \quad \mu \mu \quad \mu \quad ,$$

$$\mu \quad \mu \quad \mu \quad \mu \quad \mu .$$

$$\mu \quad \mu \quad \mu$$

$\mu$  (normal-coordinated analysis).

$$\mu \quad \mu$$

$$\mu \quad \mu \quad 192 .$$

### 2.3 $\mu$ Mossbauer

$$\mu \quad \text{ssbauer} \quad \mu \quad \mu \quad \mu \quad \mu$$

$$\mu \quad , \quad \mu \quad 193 .$$

$$\mu \quad \mu$$

$$( \quad )$$

$$\mu \quad ( \mu \quad ) ,$$

(Recoil Free).

$$\mu \quad \mu \quad \mu \quad \mu \mu$$

$$\mu \mu \quad \mu \quad \mu \quad .$$

$$\mu$$

$, \quad \mu \quad \mu \quad$  (zero phono process),

$$\mu \mu \quad \mu \quad . \quad \mu \quad \text{Mossbauer}$$

$$\mu \quad , \quad \mu$$

$$, \quad \mu \quad ( \quad ) . \quad \mu \quad \mu$$

$$\mu \quad .$$

$$\mu \quad \mu$$

$$\mu \quad \mu \quad e, \quad \mu$$

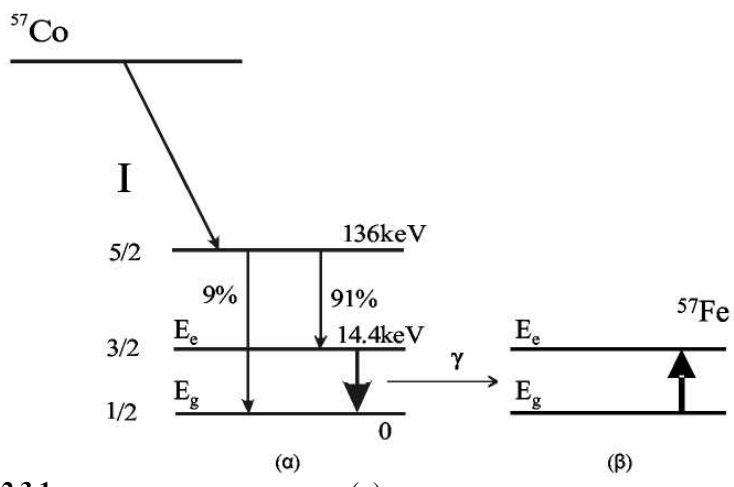
$$\mu$$

$$\sigma (\quad \mu \quad 2.3.1) . \quad \mu$$

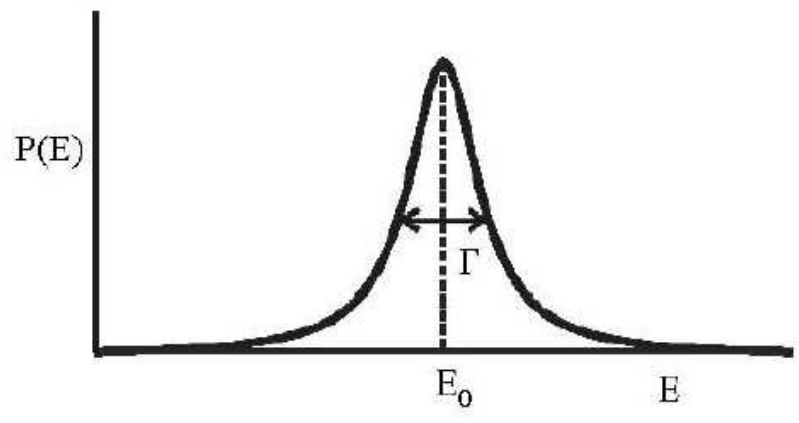
$$, \quad \mu \quad ,$$

$$\mu \quad , \quad g$$

$\mu$   $e$  ( $\mu$  2.3.1).  
 $\mu$  (  $\mu$  )  
 ossbauer),  $\mu$  ( $= e^- g$ )  
 $\mu$  ( $= e^- g$ ).  $\mu$   
 $\mu$ ,  $\mu$  (Lorentz)  $\mu$   
 $\mu$ ,  $\mu$   $\mu$   
 2.3.2.  $\mu$

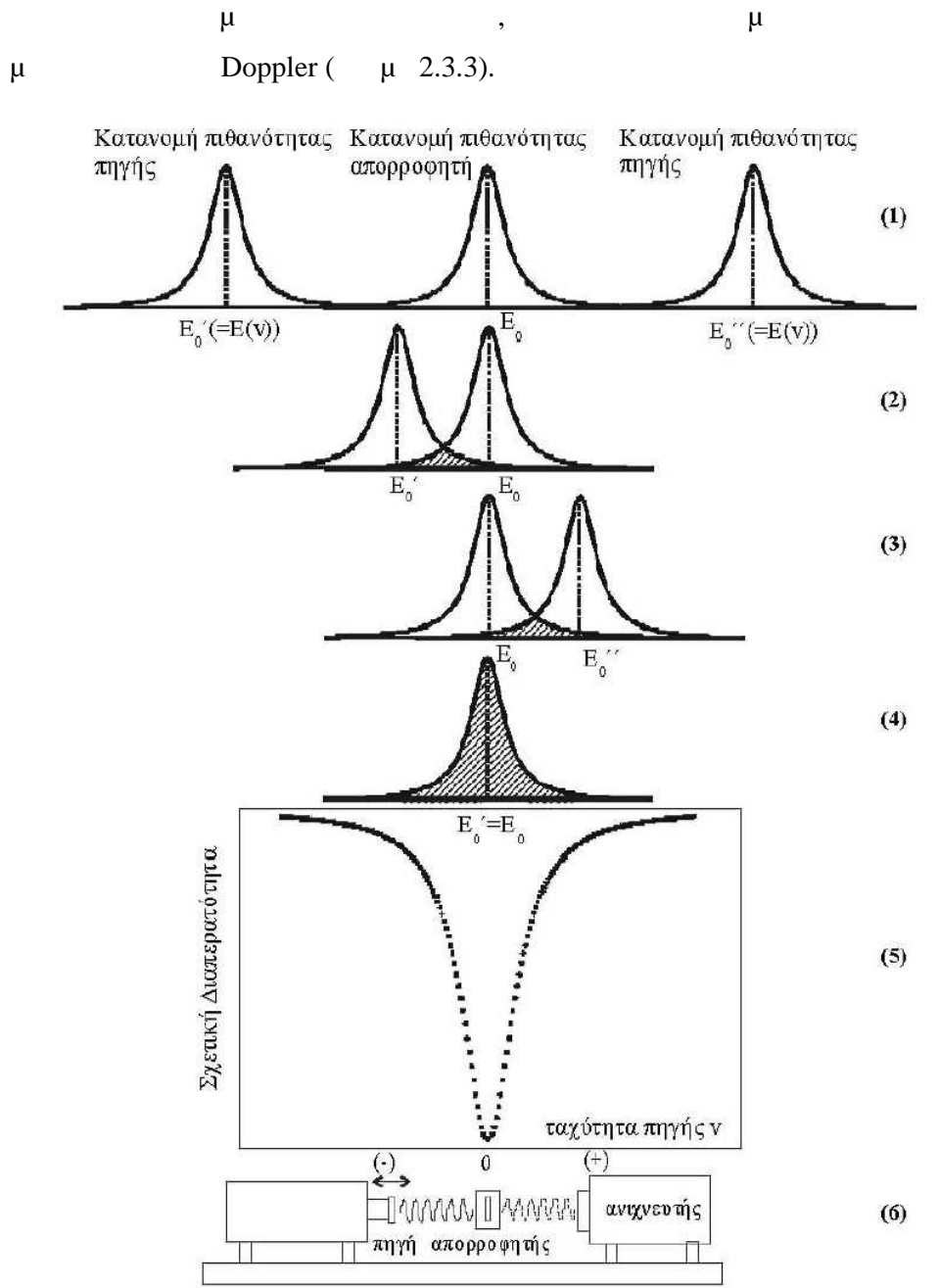


$\mu$  2.3.1. ( ) -  $\mu$  ( )



$\mu$  2.3.2.  $\mu$  Lorentz

$\mu$   
 ( ) ,  $\mu$



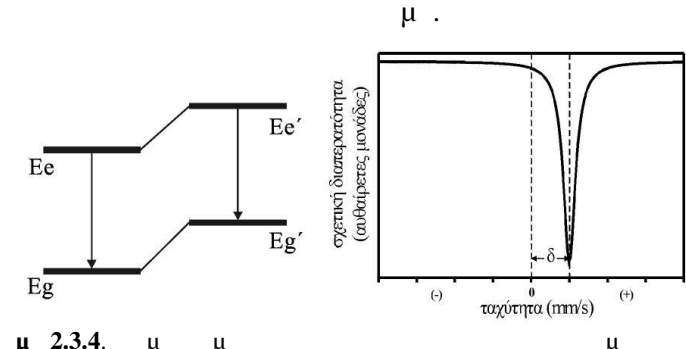
2.3.3.  $\mu$  Doppler  $\mu$   
Mossbauer

$\mu$  ,  $\mu$   $\mu$   $\mu$   
 $\mu$   $\mu$  ,  $\mu$   $\mu$   $\mu$   $\mu$   $\mu$   $\mu$

( μ 2.3.3).

μ Mossbauer μ  
 μ , μ  
 - . μ  
 -  
 μ , μ  
 . μ <sup>57</sup>Fe μ 4  
 mm/s - 15 mm/s.

μ μ , mm/s,  
 μ μ μ Mossbauer. μ  
 μ  
 ( μ 2.3.4).



μ  
 μ  
 , μ μ  
 ( μ 2.3.5).

(Electric Field

Gradient)

,  $\mu$

.  $\mu$   $\mu$   $\mu$

$\mu$

,

mm/s

$\mu$

$\mu\mu$

$\mu$  Mossbauer.

$\mu$

$\mu\mu$

$\mu$

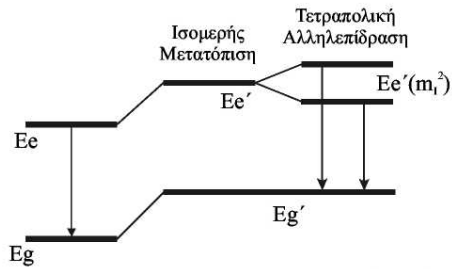
$\mu$

$\mu$

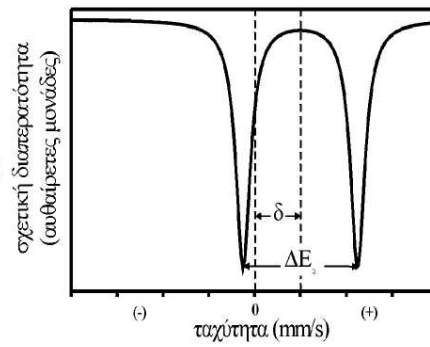
$\mu$

$\mu$

.



$\mu$  2.3.5.



$\mu$

$\mu$

$\mu$

$\mu$

$\mu$

$\mu$

$\mu$   $m_i$  ( $m_i=0, \pm 1$ )

$\mu$

$\mu$

$\mu$

$\mu$

$\mu$   $\mu\mu$

(  $\mu$  2.3.6).

$\mu$

$\mu$

$\mu$

$\mu$

$\mu$

$\mu$

$\mu$

$\mu$

$\mu$   $\mu$   $\mu$

.  $\mu$   $\mu$   $\mu$

$\mu$

$\mu$

hf.



mm/s

μ

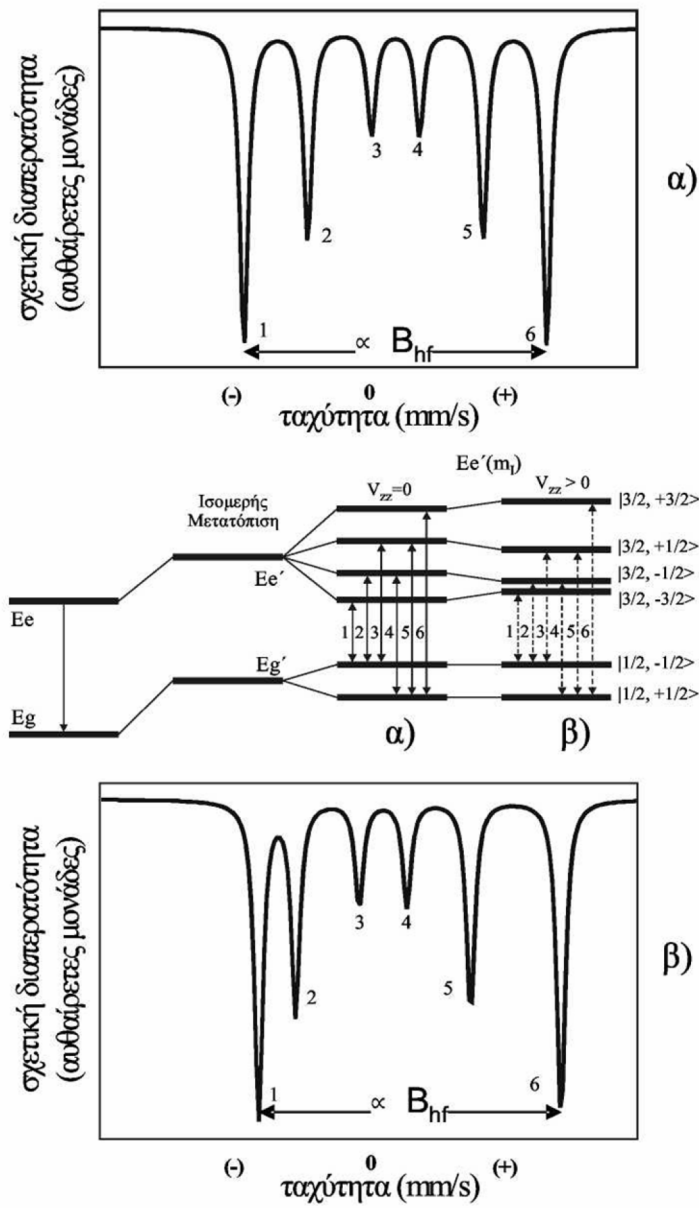
μμ

μ

μ

Mossbauer

( μ 2.3.6).



μ 2.3.6.

( ) ( )

μ μ

μ μ , μ μ

μ

μ μ μ

μ

μ 2.3.6( ).

μ μ

μ

μ

μ

μ ,

μ

μμ

2.3.6( ).  $\mu$   $\mu$  ,  $\mu$

$\mu$   $2$  ,  $\mu$

$\mu\mu$   $v_1, v_2, v_5$   $v_6$  mm/s  $[2 = (v_1 - v_2 - v_5 + v_6)]$ .  $\mu$

$\mu$   $2$  ,  $\mu$

$\mu$   $\mu$   $V_{zz}$

( ,  $\mu$

$\mu\mu$  ,  $V_{xx} = V_{yy}$ ).  $\mu$   $\mu$

$\mu$

,  $\mu$   $\mu$  (  $\mu$  ,  $\mu$

$\mu$   $\mu$   $\mu$  )  $\mu$

$\mu$   $\mu\mu$   $\mu$   $\mu$   $\mu$  .

$\mu$   $\mu$   $\mu$  (  $\mu$   $\mu$  )

$\mu$   $\mu$   $\mu$   $\mu\mu$   $\mu$   $\mu$

.

-  $\mu$   $\mu$  : )  $\mu$

$\mu$   $\mu$   $\mu$  Mossbauer

$\mu$  , )  $\mu$   $\mu$

$\mu$  Mossbauer ,

$\mu$  Mossbauer .  $\mu$

Mossbauer  $\mu$   $\mu$   $\mu$

( $\mu$  -  $\mu$  2.2.4, -  $\mu$  2.3.5, -

$\mu$  2.3.6).  $\mu$   $\mu$  Mossbauer  $\mu$

, ,

$\mu$  Mossbauer  $\mu$   $\mu$

(  $\mu$  2.3.7).  $\mu$  , ,

$\mu$  Mossbauer  $\mu$

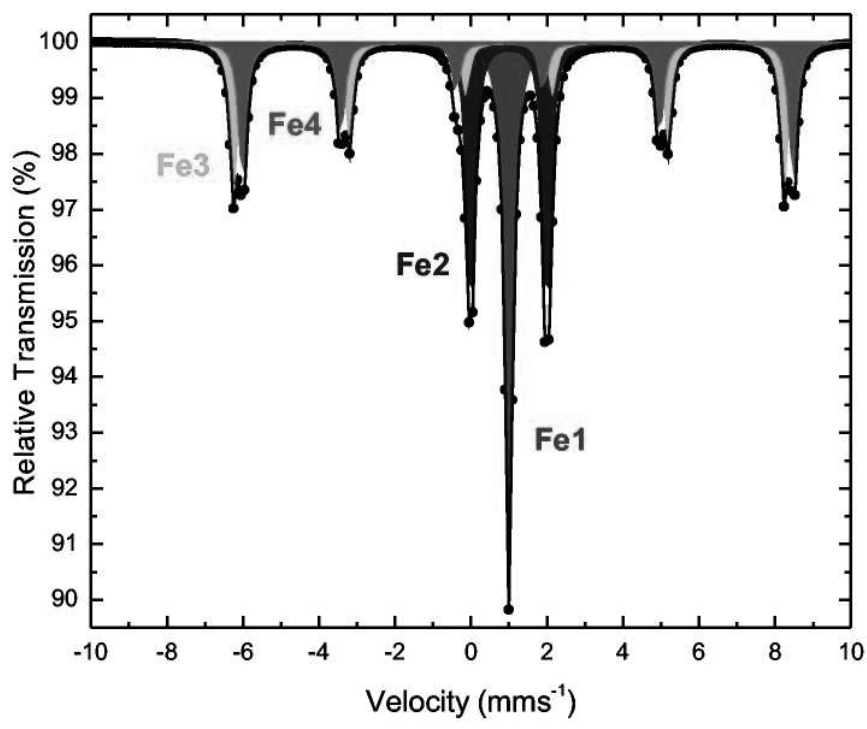
$\mu$   $\mu$   $\mu$  Mossbauer.  $\mu$  ,

$\mu$   $\mu$   $\mu$   $\mu$   $\mu$

.

$\mu$  Mossbauer  $\mu$

$\mu$   $\mu$  (Lamp-Mossbauer factor),  $\mu$   
 $\mu$   $\mu$  Mossbauer  $\mu$   
 $\mu$   $\mu$  Mossbauer  
 $\mu$   $\mu$  .



$\mu$  2.3.7.  $\mu$   $\mu$  Mossbauer  
 $\mu$  Mossbauer <sup>57</sup>Fe (Fe1,  
 Fe2, Fe3 Fe4),  $\mu$   
 $\mu$   $\mu$  =  $\mu_2 = \mu_3 = \mu_4 = 25\%$ ,  
 $\mu$   $\mu$  Fe1:Fe2 :Fe3:Fe4 = 1:1:1:1.

**2.4  $\mu$  Raman**

$\mu$   $\mu$   $\mu$   $\mu$   $\mu$   $\mu$  .  
 $\mu$  ,  $\mu$   $\mu$   $\mu$   
 $\mu$  (IR),  
 $\mu$   $\mu$  ,  
 $\mu$   $\mu$  Raman.  
 $\mu$  ,  $\mu$   $\mu$   
 $\mu$   $\mu$  .  
 $\mu$  .

Rayleigh.

Raman.

$$\left( \frac{\theta\alpha}{\theta q_i} \right)_0$$

2.5

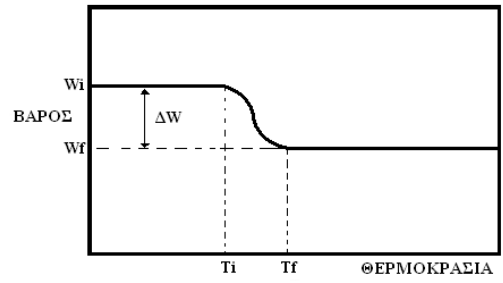
(TGA/DTA)

Analysis

GA

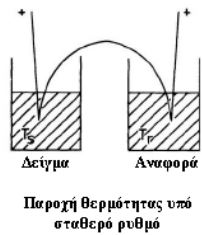
(Thermo Gravimetric

$\mu \mu \mu$   $\mu \mu$  ( $\mu$  2.5.1).  
 $\mu$   $\mu$   
 $\mu \mu \mu$  .



$\mu$  2.5.1 .  $\mu$   $\mu$  GA

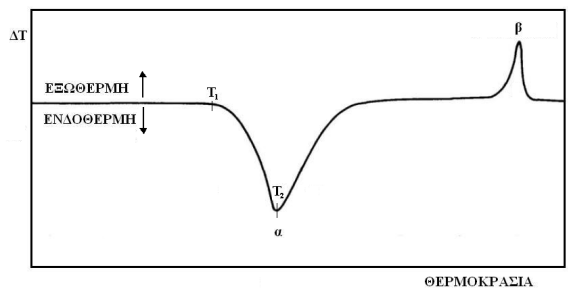
$\mu$  (DTA)  $\mu$   
 $\mu$   $\mu$   $\mu$   $\mu$   
 $\mu$  ,  $\mu$  .  $\mu$  «  $\mu$   
 $\mu$  »  
 Η  $\mu$  (Differential Thermal Analysis  $\mu$   
 DTA),  $\mu$   $\mu$   
 $\mu$   $\mu$  ,  $\mu$   
 $\mu$  t/ t-Rh,  $\mu$   $\mu$   
 ( $\mu$  2.5.2).



$\mu$  2.5.2.  $\mu$   $\mu$

$\mu$   $\mu$   $\mu$   $\mu$   $\mu$   $\mu$   
 $\mu$   $\mu$   $\mu$   $\mu$   $\mu$  .  
 $\mu$   $\mu$   $\mu$  . . ( $\mu$   $\mu$   $\mu$  ) ,  
 $\mu$   $\mu$   $\mu$   $\mu$   
 $\mu$  ,  $\mu$   $\mu$  s  $\mu$   $\mu$   
 $\mu$   $\mu$  R ,

$\mu \mu \quad \mu \quad \mu \quad . \quad \mu \quad = \quad s^{-1} \quad r$   
 $\mu \quad \mu \quad \mu \quad \mu \quad \mu \quad \mu \quad 1.11.3, \quad 1$   
 $\mu \quad \mu \quad \mu \quad .$   
 $\mu \quad \mu \quad ,$   
 $\mu \quad \mu \quad \mu \quad \mu \quad \mu \quad .$   
 $\mu \quad \mu \quad \mu \quad \mu \quad : \quad = \quad /m, \quad m: \quad \mu$   
 $\mu \quad : \quad \mu \quad \mu \quad .$   
 $\mu \quad \mu \quad \mu \quad \mu \quad \mu \quad \mu$   
 $( \quad ) \quad \mu \quad \mu \quad ( \quad \mu$   
 $\mu \quad ) .$   
 $\mu \quad \mu \quad \mu \quad \mu \quad \mu \quad \mu \quad \mu$   
 $\mu \quad \mu \quad \mu \quad \mu \quad \mu \quad \mu \quad \mu$   
 $\mu \quad \mu \quad \mu \quad ( \dots ) , \quad " \quad \mu \quad " \quad ( \mu$   
 $2.5.3 ) , \quad \mu \quad \mu \quad \mu \quad \mu \quad ( \dots ,$   
 $\mu \quad \mu \quad \mu ) , \quad " \quad \mu \quad " \quad ( \mu \quad 2.5.3 )$   
 $\mu \quad \mu \quad \mu \quad \mu$   
 $\mu \quad \mu \quad \mu \quad \mu \quad .$



**μ 2.5.3.** μ μ DTA μ μ μ μ μ μ  
μ μ D μ μ μ μ μ μ μ μ D

- μ :
- μ μ ,
  - μ
  - .
- μ μ μ μ μ μ μ μ μ μ μ μ ( . . - ) .

2.6

μ

( . . . )

μ

μ

μ

μ

μ

μ

μ

μ

μ

μ

μ

μ

μ

μ

μ

μ

μ

μ

μ

μ

μ

μ

μ

μ

μ

μ

μ

μ

μ

μ

μ

75

200 kV,

μ

μ

μ

μ

μ

μ

μ

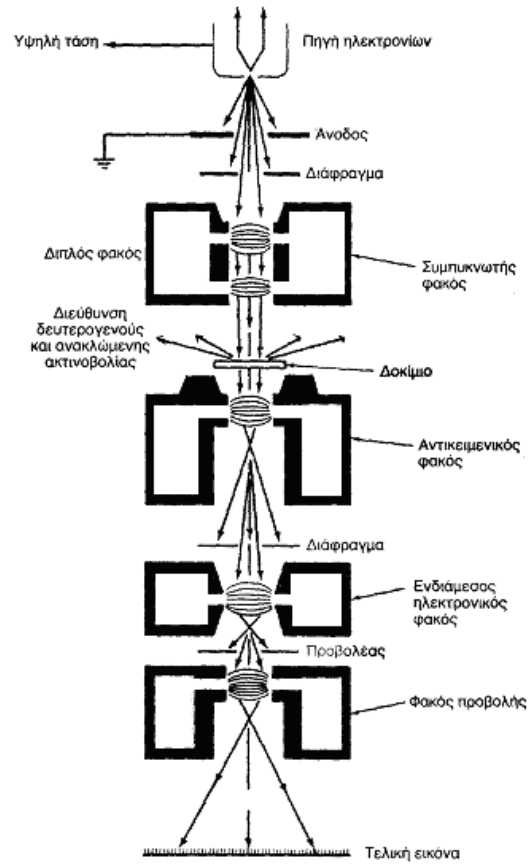
μ

μ

μ

μ

μ 2.6.1.



2.6.1).

. . . ,  $\mu$   $\mu$   $\mu$  (S. . . ),  
 $\mu$   $\mu$   $\mu$   $\mu$  ( . . . ),  $\mu$   
 S. . . .  
 $\mu$   $\mu$  , -  
 $\mu$  .  $\mu$   
 100 nm  $\mu$  ,  
 $\mu$  .  $\mu$   $\mu$   $\mu$  ,  $\mu$   
 $\mu$  ,  $\mu$   $\mu$   $\mu$   $\mu$   
 $\mu$   $\mu$   $\mu$  .  
 $\mu$   $\mu$   $\mu$   $\mu$   $\mu$  ,  
 $\mu$   $\mu$  - -  $\mu$   $\mu$   
 $\mu$  500 000 0.2 nm.  
 $\mu$   $\mu$   $\mu$  150 000 3-  
 6nm.  $\mu$   $\mu$   $\mu$   
 ( R )  $\mu$   $\mu$   
 x 1 000 000.

- $\mu$   $\mu$   $\mu$   
 :  
 •  $\mu$   $\mu$  ,  
 $\mu$  .  
 •  $\mu$   $\mu$   $\mu$   $\mu$  .  
 •  $\mu$   $\mu$   $\mu$   $\mu$  .  
 •  $\mu$   $\mu$   $\mu$  .

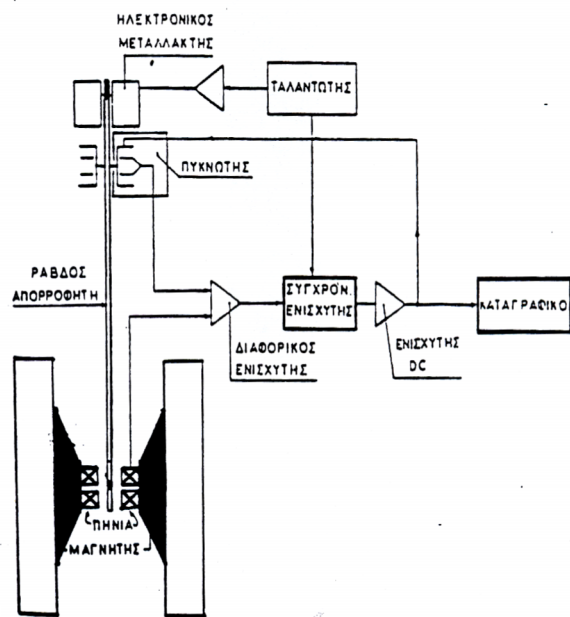
$\mu$  (S.E.M.)  
 $\mu$  (SEM)  
 $\mu$  2.6.2.  $\mu$   
 30 kV,  $\mu$   $\mu$  ( ),  $\mu$   $\mu$   $\mu$  -  
 $\mu$  , ,







2.  $\mu$   $\mu$  2 -300
- $\mu$   $\mu$  300 -1200
3.  $\mu$   $\mu$
- $\mu$   $\mu$   $\mu$   $\mu$
- $\mu$  0-2
4.  $\mu$   $\mu$  45
- $\mu$   $\mu$   $\mu$
- $\mu$   $\mu$   $\mu$   $\mu$
- $\mu$   $\mu$   $\mu$   $\mu$
5.  $\mu$   $\mu$   $\mu$   $\mu$
- $\mu$   $\mu$   $\mu$   $\mu$   $\mu$  2.7.3:



$\mu$  2.7.3  $\mu$   $\mu$   $\mu$

1.

μ μ μ , μ

1.

SWCNTs	90%	Texas Carbon NT
MWCNTs	95%	Aldrich
C <sub>16</sub> H <sub>33</sub> Cl <sub>3</sub> Si	Technical	Fluka
FeCl <sub>2</sub>	99.99%	Aldrich
H <sub>2</sub> O <sub>2</sub>	30% μ	Aldrich
SOCl <sub>2</sub>	90%	Fluka
Ru(C <sub>5</sub> H <sub>7</sub> O <sub>2</sub> ) <sub>3</sub>	97%	Aldrich
Pt(C <sub>5</sub> H <sub>7</sub> O <sub>2</sub> ) <sub>2</sub>	99.9%	Aldrich
Fe(CO) <sub>5</sub>	99.999%	Aldrich
HCl	36-38% μ	Aldrich
SnO <sub>2</sub>	>99.99%	Aldrich
NH <sub>3</sub>	>99.9%	Aldrich
FeH <sub>8</sub> N <sub>2</sub> O <sub>8</sub> S <sub>2</sub> ·6H <sub>2</sub> O	>99%	Merck
Montmorillonite		Clay Min. Soc
Laponite		Clay Min. Soc

NiCl <sub>2</sub> 6H <sub>2</sub> O	>98%	Aldrich
H <sub>2</sub> SO <sub>4</sub>	95-97%     μ	Riedel de Haen
Fe(NO <sub>3</sub> ) <sub>3</sub> 9H <sub>2</sub> O	>99%	Merck
C <sub>14</sub> H <sub>11</sub> N	96%	Aldrich
(HO) <sub>2</sub> C <sub>6</sub> H <sub>3</sub> CHO	>97%	Aldrich
NH <sub>2</sub> CH <sub>2</sub> COOCH <sub>3</sub>	99%	Aldrich
CH <sub>3</sub> COCH <sub>3</sub>	>99%	Aldrich
CH <sub>3</sub> CH <sub>2</sub> OH	>99%	Aldrich
HCON(CH <sub>3</sub> ) <sub>2</sub>	99.5%	Aldrich
(CH <sub>3</sub> CH <sub>2</sub> ) <sub>2</sub> O	99.7%	Aldrich
C <sub>6</sub> H <sub>5</sub> CH <sub>3</sub>	99.8%	Aldrich
C <sub>9</sub> H <sub>4</sub> O <sub>5</sub>	97%	Aldrich
4-(HO)C <sub>6</sub> H <sub>4</sub> CH <sub>2</sub> CH(NH <sub>2</sub> )CO <sub>2</sub> H	>99%	Aldrich
NH <sub>2</sub> (CH <sub>2</sub> ) <sub>6</sub> NH <sub>2</sub>	99%	Fluka
(C <sub>6</sub> H <sub>5</sub> ) <sub>2</sub> O	>98%	Fluka
CH <sub>3</sub> (CH <sub>2</sub> ) <sub>9</sub> CH(OH)CH <sub>2</sub> OH	90%	Aldrich
CH <sub>3</sub> (CH <sub>2</sub> ) <sub>7</sub> CH=CH(CH <sub>2</sub> ) <sub>7</sub> CH <sub>2</sub> NH <sub>2</sub>	>70%	Fluka
CH <sub>3</sub> (CH <sub>2</sub> ) <sub>7</sub> CH=CH(CH <sub>2</sub> ) <sub>7</sub> COOH	99%	Aldrich
CHCl <sub>3</sub>	99%	Sigma
C <sub>17</sub> H <sub>13</sub> N HCl	95%	Aldrich
CH <sub>3</sub> CO <sub>2</sub> H	99.7%	Aldrich
C <sub>2</sub> H <sub>2</sub>	Technical	Linde
Ar	99.999%	Linde
Oxygen	99.99%	Linde

## 2.

### 2.1 1,3-

#### 2.1.1 1,3-

20 mg SWCNTs, 200 mg 200 mg  $\mu$  -  
50 ml DMF  $\mu$  120 °C 5  $\mu$  .  
 $\mu$  Millipore (0.45  $\mu$ m FG) (3 )  $\mu$  DMF.

$\mu$  DMF 60 min,  $\mu$   
 $\mu$  Millipore.

i) DMF, ii)  $\mu$   $\mu$  (1:1) EtOH-CHCl<sub>3</sub> iii) - .  
 $\mu$   $\mu$  (SWCNT-f-OH)

$\mu$  3  $\mu$  (10<sup>-2</sup> bar).

#### 2.1.2 1,3-

20 mg MWCNTs, 200 mg 200 mg  $\mu$  -  
50 ml DMF.  $\mu$   $\mu$   $\mu$  120 °C 5  $\mu$   
 $\mu$  (3.500 rpm, 5 min)

$\mu$  20 ml DMF  $\mu$  20 ml  $\mu$   
 $\mu$  .  $\mu$   $\mu$

$\mu$  100 ml  
 $\mu$  Millipore (0.45  $\mu$ m FG),  
 $\mu$  ( WCNT-f-OH)  $\mu$   
(10<sup>-2</sup> bar).

**2.1.3 X μ** **μ**  
 μ  
 10 mg μ μ MWCNT-f-OH 0.5 ml  
 C<sub>16</sub>H<sub>33</sub>Cl<sub>3</sub>Si μ (20 ml).  
 μ μ μ

**2.1.4 μ** **μ**  
 μ  
 10 mg μ μ MWCNT-f-OH 50 mg  
 μ 12 μ μ  
 μ DMF (20 ml). μ  
 μ

## 2.2 $\mu$ $\mu$

---

$\mu$  10 mg SWCNTs 150 ml  $\mu$   $\mu$   
 $\mu$  2 min.  $\mu$  50 ml  
 $\mu$  (312.8 mg).  $\mu$   
 $\mu$  120 min. 15  
 $\mu$  FeCl<sub>2</sub>  $\mu$   $\mu$  H<sub>2</sub>O<sub>2</sub>.  
 $\mu$  ( 65 °C) 2  $\mu$  ,  
 $\mu$  (4500 rpm, 30 min)  
 $\mu$  ,  $\mu$   $\mu$  .



### 3

#### 3.1 μ -

#### μ μ **FePt**

**3.1.1** μ μ

100 mg MWCNTs, 40 ml μ μ H<sub>2</sub>SO<sub>4</sub>/HNO<sub>3</sub> (3:1  
(v/v)) 3 .

μ , μ μ

50 °C 18 . 50

mg , 40 ml μ μ SOCl<sub>2</sub>

DMF (20:1 . .) μ 70 °C 24 h. μ

, μ , μ

50 °C. 20 mg

μ μ - μ ( μ 50% . . ) μ

μ 80 °C 3 μ μ

μ . μ μ μ

μ μ μ F

μ .

#### 3.1.2 μ **FePt**

μ FePt μ μ .

, 20 ml - - , 10 mmol 5 mmol

μ μ 140 °C 10 min. 1 mmol

Pt(C<sub>5</sub>H<sub>7</sub>O<sub>2</sub>)<sub>2</sub>, 2 mmol Fe(CO)<sub>5</sub> 5 mmol , μ

μ 180 °C.

3 μ μ μ .

μ FePt μ (40

ml)  $\mu$  .  $\mu$

### 3.1.3

#### FePt

10 mg  $\mu$  FePt 10 ml - -  
50 ml  $\mu$   $\mu$   $\mu$   
MWCNTs (2 mg) - - .  $\mu$  60 min  
3  $\mu$  . MWCNTs-FePt  
 $\mu$   $\mu$  .  
FePt ,  $\mu$   
 $\mu$  700 °C 30 min.  
 $\mu$   $\mu$   
 $\mu$   $\mu$  .

## 3.2

μ

μ

### 3.2.1

μ

μ

100 mg MWCNTs, 40 ml μ μ H<sub>2</sub>SO<sub>4</sub>/HNO<sub>3</sub> (3:1)

(v/v) 3 .

μ , μ μ

μ 50 °C 18 .

### 3.2.2

μ

μ

μ

μ

μ μ μ

50 mg SWCNTs, 40 ml μ μ H<sub>2</sub>SO<sub>4</sub>/HNO<sub>3</sub> (3:1)

(v/v) 3 .

μ , μ μ

μ 50 °C 18 .

### 3.2.3

μ

μ

μ

μ

μ μ μ

12 mg SWCNTs, 150 ml DMF μ

μ 60 min. 1 ,

μ 30 mg μ - 60 ml DMF

μ SWCNTs μ 3

μ . μ μ μ

μ DMF

μ 60 C μ μ .

### 3.2.4

μ

μ

μ

μ μ μ μ μ μ

μ μ (μ - - μ )

1:5)  
(FeNO<sub>3</sub>)

μ μ μ μ μ μ μ μ  
μ μ , μ . μ μ  
, μ μ  
(μ . . -  
μ μ μ μ  
. . FeNO<sub>3</sub>:  
2:1. μ μ ,  
60 min μ μ μ .  
- μ μ  
120 min. ,  
μ μ μ μ 80 C.  
, μ μ μ μ μ μ  
μ μ μ μ μ μ μ μ  
, ) 400 C 60 min μ μ  
μ .

3.3  $\mu$   $\mu$  Sn-

-  $\mu$  -Fe<sub>2</sub>O<sub>3</sub>

3.3.1  $\mu$  Sn

Sn (Sn@CNTs)

$\mu$   $\mu$   $\mu$   $\mu$  (CCVD),  $\mu$

$\mu$  3.3.1.1. ,

100 mg (SnO<sub>2</sub>)  $\mu$   $\mu$

,  $\mu$   $\mu$

$\mu$   $\mu$  (700 °C).  $\mu$  ,

$\mu$   $\mu$  10 sccm  $\mu$  30 min.

$\mu$   $\mu$   $\mu$   $\mu$

$\mu$   $\mu$  . Sn@CNTs

$\mu$  .



$\mu$  3.3.1.1. CCVD

3.3.2  $\mu$  Sn@CNTs

Sn@CNTs  $\mu$  CCVD  $\mu\mu$

CCVD  $\mu$   $\mu$  .

$\mu$  , 100 mg Sn@CNTs, 35 ml

$\mu$  HNO<sub>3</sub> 1N.  $\mu$  30 min,  
 $\mu$  Sn@CNTs  $\mu$  (3500 rpm, 30 min)  
 $\mu$   $\mu$   $\mu$  .

### 3.3.3 $\mu$ -Fe<sub>2</sub>O<sub>3</sub>

$\mu$  -Fe<sub>2</sub>O<sub>3</sub>, 1.75 ml NH<sub>3</sub>  
 $\mu$  (60 ml) 1.41 gr FeH<sub>8</sub>N<sub>2</sub>O<sub>8</sub>S<sub>2</sub>·6H<sub>2</sub>O.  
 NH<sub>3</sub>, 0.125 ml  $\mu$  H<sub>2</sub>O<sub>2</sub> 25 ml  
 3 ml  $\mu$   $\mu$   
 95 °C 45 min. ,  
 $\mu$  50  
 ml .  $\mu$  -Fe<sub>2</sub>O<sub>3</sub>  $\mu$   $\mu$   
 ,  $\mu$   $\mu$   $\mu$  .

### 3.3.4 $\mu$ $\mu$ Sn-

$\mu$  -Fe<sub>2</sub>O<sub>3</sub>  
 50 mg  $\mu$  Sn@CNTs 200 ml  $\mu$   
 $\mu$  - (200 mg)  $\mu$  / (1:1).  $\mu$   
 18 . 15 mg  $\mu$  -Fe<sub>2</sub>O<sub>3</sub> 15 ml  
 CHCl<sub>3</sub>  $\mu$  200ml  $\mu$   
 Sn@CNTs  $\mu$  2  $\mu$  .  
 $\mu$   $\mu$  Sn-  
 $\mu$  -  $\mu$  -Fe<sub>2</sub>O<sub>3</sub>  $\mu$   $\mu$  ,  
 $\mu$   $\mu$   $\mu$   $\mu$  .

### 3.4

$\mu$

$\mu$

**RuPt**

#### 3.4.1 $\mu$

$\mu$

100 mg MWCNTs, 40 ml  $\mu$   $\mu$  H<sub>2</sub>SO<sub>4</sub>/HNO<sub>3</sub> (3:1  
(v/v) 3 .  
 $\mu$  ,  $\mu$   $\mu$   $\mu$   $\mu$   
50 °C 18 . ,  
50 mg , 40 ml  $\mu$   $\mu$   
SOCl<sub>2</sub> DMF (20:1 . .)  $\mu$  70 °C 24 h.  
 $\mu$   $\mu$  ,  $\mu$  ,  
 $\mu$  50 °C. 20 mg  
 $\mu$   $\mu$   $\mu$  -  $\mu$  (  $\mu$  50% . . )  $\mu$   
 $\mu$  80 °C 3  $\mu$   $\mu$   $\mu$   
 $\mu$  .  $\mu$   $\mu$   $\mu$   
 $\mu$   $\mu$   $\mu$   $\mu$  F  
 $\mu$  50 C.

#### 3.4.2

$\mu$

**RuPt**

$\mu$  RuPt  $\mu$   $\mu$  .  
, 20 ml - - , 10 mmol 5 mmol  
 $\mu$   $\mu$  140 °C 10 min. 1 mmol  
Pt(C<sub>5</sub>H<sub>7</sub>O<sub>2</sub>)<sub>2</sub>, 1 mmol Ru(C<sub>5</sub>H<sub>7</sub>O<sub>2</sub>)<sub>3</sub> 5 mmol ,  $\mu$   
 $\mu$  180 °C.  
3  $\mu$   $\mu$   
 $\mu$  .  $\mu$  FePt  $\mu$   $\mu$   
(40 ml)  $\mu$  .  
 $\mu$   $\mu$   $\mu$   $\mu$   
 $\mu$  .

### 3.4.3

MWCNTs (2 mg)      10 mg      50 ml      3 μg      RuPt      μg      RuPt      μg      10 ml      -      -      60 min      MWCNTs-RuPt

μg      μg      μg      μg      μg      μg



### 3.5

$\mu$

$\mu$

#### 3.5.1 $\mu$

$\mu$

$\mu$  1,3-

20 mg MWCNTs, 200 mg

200 mg  $\mu$  -

50 ml DMF.  $\mu$   $\mu$   $\mu$

120 °C 5  $\mu$

$\mu$  (3.500 rpm, 5 min)

$\mu$  20 ml DMF

$\mu$  20 ml

$\mu$

$\mu$

100 ml

$\mu$

Millipore (0.45  $\mu$ m FG),

$\mu$  ( WCNT-f-OH)

$\mu$

(10<sup>-2</sup> bar).

#### 3.5.2

$\mu$

-

$\mu$

100 mg

10 ml

$\mu$

18

2-30 mg MWCNT-f-OH

4-10 ml  $\mu$   $\mu$

- (80:20 (v/v))

$\mu$

$\mu$

$\mu$

-

18

$\mu$

$\mu$

-

$\mu$

$\mu$

$\mu$

$\mu$

$\mu$

$\mu$

3.6 

---

---

 -  $\mu$   $-Fe_2O_3$  

---

**3.6.1**

$\mu$   $\mu$   $\mu$   $\mu$   $\mu$   $\mu$

$\mu$   $\mu$  Ni  $\mu$   $\mu$   $\mu$   $\mu$   $\mu$

,  $\mu$   $NiCl_2$  .

$\mu$   $\mu$   $\mu$  (SW<sub>y</sub>) 1% . .  $\mu$

[NiCl<sub>2</sub>]/[ $\mu$   $\mu$  ]  $\mu$  5.  $\mu$   $\mu$

3 ,  $\mu$   $\mu$  ,  $\mu$  ,

$\mu$  450 °C 4.5 . ,

250 mg  $\mu$   $\mu$

,  $\mu$   $\mu$   $\mu$

$\mu$   $\mu$  (800 °C).  $\mu$  ,

$\mu$   $\mu$  10 sccm  $\mu$  30 min.

$\mu$  -  $\mu$   $\mu$

$\mu$   $\mu$   $\mu$

$\mu$  . SW<sub>y</sub>-CNTs  $\mu$  .

**3.6.2**  $\mu$   $\mu$  SW<sub>y</sub>-CNTs

100 mg  $\mu$  SW<sub>y</sub>-CNTs, 40 ml  $\mu$   $\mu$

H<sub>2</sub>SO<sub>4</sub>/HNO<sub>3</sub> (3:1 (v/v)) 3 .

$\mu$  ,  $\mu$

$\mu$  50 °C 18 .

50 mg , 40 ml

$\mu$   $\mu$  SOCl<sub>2</sub> DMF (20:1 . .)  $\mu$  70 °C 24

h.  $\mu$  ,  $\mu$  ,

$\mu$  50 °C. 20

mg  $\mu$  ,  $\mu$   $\mu$  -  $\mu$  (

$\mu$  50% . . )  $\mu$   $\mu$  80 °C 3  
 $\mu$   $\mu$   $\mu$  .  $\mu$   
 $\mu$   $\mu$   $\mu$   $\mu$   $\mu$  F  
 $\mu$   $\mu$   $\mu$   $\mu$  SW<sub>y</sub>-CNTs  $\mu$

**3.6.3**  $\mu$   $\mu$  -Fe<sub>2</sub>O<sub>3</sub>  
 $\mu$  -Fe<sub>2</sub>O<sub>3</sub>, 1.75 ml NH<sub>3</sub>  
 $\mu$  (60 ml) 1.41 gr FeH<sub>8</sub>N<sub>2</sub>O<sub>8</sub>S<sub>2</sub>·6H<sub>2</sub>O.  
 NH<sub>3</sub>, 0.125 ml  $\mu$  H<sub>2</sub>O<sub>2</sub> 25 ml  
 3 ml .  $\mu$   $\mu$   
 95 °C 45 min. ,  
 $\mu$  50  
 ml .  $\mu$  -Fe<sub>2</sub>O<sub>3</sub>  $\mu$   $\mu$   
 ,  $\mu$   $\mu$   $\mu$  .

**3.6.4**  $\mu$   $\mu$  -Fe<sub>2</sub>O<sub>3</sub>  
 $\mu$  -  $\mu$  -Fe<sub>2</sub>O<sub>3</sub>  
 $\mu$   $\mu$  -Fe<sub>2</sub>O<sub>3</sub>, 86 mg  $\mu$  -Fe<sub>2</sub>O<sub>3</sub>  
 $\mu$  . . 1:1 - - .  $\mu$   $\mu$   
 160 ml - -  $\mu$  43  
 mg  $\mu$   $\mu$   $\mu$  SW<sub>y</sub>-CNTs.  $\mu$   
 60 min  $\mu$  45 C  
 7  $\mu$  . -  $\mu$   
 -  $\mu$  -Fe<sub>2</sub>O<sub>3</sub>  $\mu$  ,  
 $\mu\mu$   $\mu$   $\mu$   $\mu$  .

## 4.

### 4.1

$\mu\mu$  -  
 $\mu$   $\mu$   $\mu$  -  $\mu$   $\mu$   
 $\mu$  D8 Advance Brüker.  $\mu$  CuK (40 kV, 40  
mA)  $\mu$   $\mu$   $\mu$   $\mu$   $\mu$   $\mu$   $\mu$   $\mu\mu$   
-  $\mu$   $\mu$  2 10 90 ,  $\mu$   $\mu$  0.02  
 $\mu$  2 sec  $\mu$   $\mu$   $\mu$   $\mu$   
 $\mu$   $\mu$   $\mu$  .

### 4.2 $\mu$ Raman

$\mu$  Raman  $\mu$  Micro-Raman Renishaw system RM  
1000,  $\mu$  laser 532 nm (Nd – YAG).  $\mu$   
0.5 1 mW  $\mu$  1  $\mu\text{m}$ ,  $\mu$   
 $\mu$   $\mu$   $\mu$  .

### 4.3 $\mu\mu$ $\mu$

$\mu$   $\mu$  (TGA)  $\mu$  (DTA)  
 $\mu$   $\mu$  Perkin Elmer Pyris Diamond TG/DTA.  $\mu$  ,  
5 mg,  $\mu$   $\mu$  2  
 $\mu$   $\mu$  850 C,  $\mu$   $\mu$   $\mu$  5 C/min.  
 $\mu$  -  $\mu$  .

### 4.4

(SEM).

$\mu$   $\mu$   
 $\mu$  SEM JEOL JSM - 5600 V.  $\mu$   $\mu$   $\mu$   
 $\mu$   $\mu$   $\mu$  (Au),  $\mu$

**4.5** -  $\mu$  (STM).

$\mu$  STM  $\mu$   $\mu$   $\mu$   
 $\mu$  STM Schaefer  $\mu$  Pt/Ir.  $\mu$   
 $\mu$   $\mu$  ,  $\mu$   $\mu$   
,  $\mu$   $\mu$   $\mu$   
 $\mu$   $\mu$  .

**4.6**  $\mu$  - (UPS).

$\mu$   $\mu$   
 $\mu$   $\mu\mu$  ELETTRA ,  
 $\mu$   $\mu$  95 eV  $\mu$   $\mu$  1 lm.

**4.7** ( )

$\mu$   $\mu$   $\mu$   
 $\mu$  JEOL JEM-2010F ( $\mu$  200 kV),  
 $\mu$   $\mu$  EDAX.  $\mu$   $\mu$   $\mu$   
 $\mu$  -  $\mu$   
 $\mu$  (holey carbon grid)  
 $\mu$   $\mu$   $\mu$  .  
 $\mu$  .

**4.8**  $\mu$  Mössbauer.

$\mu$  Mössbauer  $\mu$   $\mu$  , 77  
13  $\mu$   $\mu$   $\mu$   $^{57}\text{Co}(\text{Rh})$   
 $\mu$   $\mu$  , Mössbauer  $\text{N}_2$  (Oxford)  
Mössbauer He (ARS).

#### 4.9 (VSM).

$\mu$   $\mu$   $\mu$   $\mu$   $\mu$   $\mu$  ,  
 $\mu$   $\mu$   $\mu$   $\mu$   $\mu$   $\mu$  77 K  $\mu$   
 $\mu$   $\mu$   $\mu$   $\mu$  (Vibrating Sample Magnetometer VSM)  
LakeShore 7300  $\mu$   $\mu$   $\mu$   $\mu$   
(Janis).

#### 4.10 (FT-IR).

$\mu$   $\mu$  -  $\mu$   $\mu$  FT-IR 8400  
SHIMADZU,  $\mu$  DTGS.  $\mu$   $\mu$  64  
 $\mu$  ,  $\mu$   $\mu$  400-4000  $\text{cm}^{-1}$   $\mu$   
 $\mu$   $2 \text{ cm}^{-1}$ .  $\mu$   $\mu$   $\mu$   $\mu$  r.

#### 4.11 (AFM).

AFM  $\mu$  ( DMF)  $\mu$   
 $\mu$   $\mu$   $\mu$  spin coating (3000  
rpm 3 min)  $\mu$  Digital Instruments (Veeco) Nanoscope IIIa.

#### 4.12 (EPR).

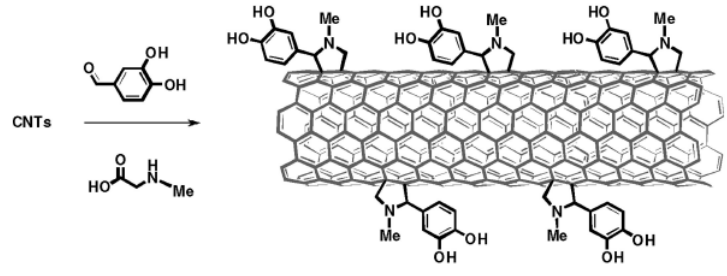
$\mu$  EPR  $\mu$   $\mu$   $\mu$  Bruker ER 200D-  
SRC  $\mu$   $\mu$  Oxford ESR 9  $\mu$   
Gauss Bruker 035M NMR. To DPPH  $\mu$   
 $\mu$  g.



# 1. $\mu$

## 1.1. $\mu$ $\mu$ 1,3-

(MWCNTs)  $\mu$  (SWCNTs)  $\mu$   
 $\mu$   $\mu$  1,3-  $\mu$   
 $\mu$  1,3-  $\mu$   
 $\mu$  (SWCNTs)  $\mu$   
 $\mu$   $\mu$   $\mu$   
 $\mu$   $\mu$  N- $\mu$  3,4-  
 $\mu$   $\mu$   $\mu$   $\mu$   
 $\mu$  (  $\mu$  1.1.1).  $\mu$   $\mu$   $\mu$   
 $\mu$   $\mu$   $\mu$



$\mu$  1.1.1:  $\mu$  1,3-  $\mu$   
 $\mu$   $\mu$   $\mu$   $\mu$   
 $\mu$  (  $\mu$  1.1.2).  $\mu$   $\mu$   
 $\mu$  (SWCNT-f-OH)  $\mu$   
 $\mu$   $\mu$   $\mu$   $\mu$   $\mu$  Raman,  
 $\mu$  -  $\mu$  ,  $\mu$   $\mu$



SWCNTs (WCNTs), MWCNTs, SWCNTs, MWCNTs (MWCNT-f-OH) (silylation) (hexadecyltrichlorosilane) (trimellitic anhydride).



**1.1.2:** SWCNT, MWCNTs-f-OH in DMF

**1.1.1. Raman**

SWCNTs (Pristine SWCNTs) Raman (1.1.1.1). SWCNTs (SWCNT-f-OH) Raman 1200-1800, 1340 1590 cm<sup>-1</sup>

Graphite (Highly Ordered Purolitic  $sp^2$ )

D  $E_{2g}$  G  $\mu\mu$  G  $\mu$  (sp<sup>2</sup>)

HOPG), D  $\mu$  CNTs

194-196  $\mu$  G (R= $I_D/I_G$ )  $\mu$   $\mu$  199  $\mu$

$\mu$  197, 198  $\mu$  200-202 (  $\mu$  )  $\mu$   $\mu$   $\mu$

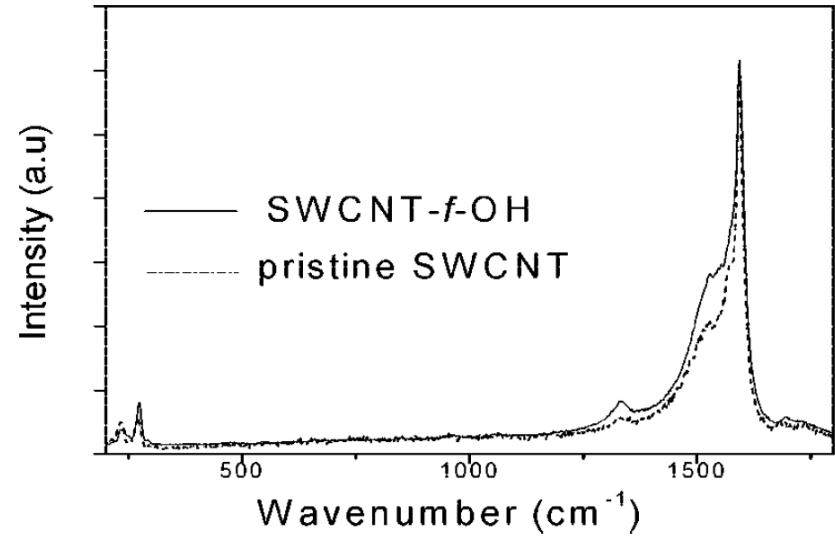
$\mu$  )  $\mu$  G  $\mu$   $\mu$   $\mu$   $\mu$

$\mu$   $\mu$   $\mu$   $\mu$   $\mu$   $\mu$   $\mu$   $\mu$

Breathing Mode RBM)<sup>203, 204</sup>  $\mu$  RBM ( RBM = (A/d<sub>t</sub>) + , ,

$\mu$   $\mu$   $\mu$   $\mu$  , d<sub>t</sub>  $\mu$  CNTs

RBM )<sup>205, 206</sup>  $\mu$



1.1.1.1:  $\mu$  Raman  $\mu$   $\mu$  (Pristine SWCNT)  $\mu$

$\mu$  SWCNT-f-OH  $\mu$   $I_D/I_G$  0.1

0.035 Pristine-SWCNTs.



SWCNT-f-OH

1.1.2.

μ

van Hove

SWCNTs

μ

μ

μ

μ

μ

μ

(band gap).

μ

μ

μ

MWCNTs

μ

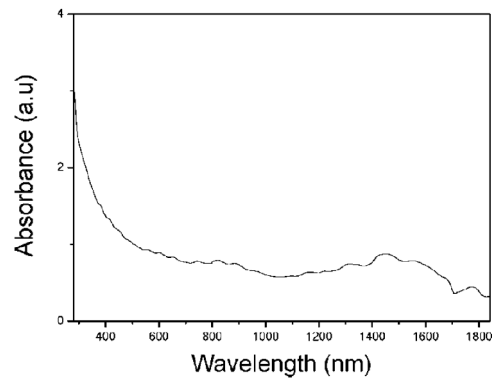
μ

μ

μ

μ

μ UV.



μ 1.1.2: μ UV-Vis μ μ SWCNT-f-OH

### 1.1.3.

μ

μ

&

μ

μ

μ

μ

μ

(AFM)

μ

(TEM).

SWCNTs μ

μ

μ

SWCNT-f-OH

μ

#### 1.1.3.1.

μ

μ

μ

μ

μ

μ

μ

μ

μ

μ

μ

SWCNT-f-OH

Pristine SWCNTs

μ

μ

μ

μ

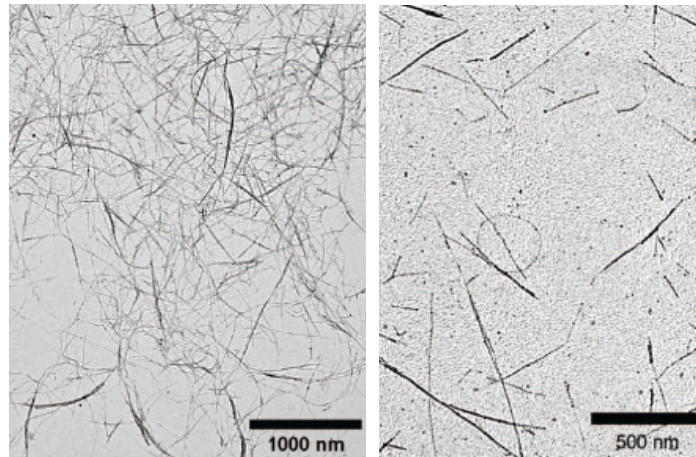
μ

μ

SWCNTs

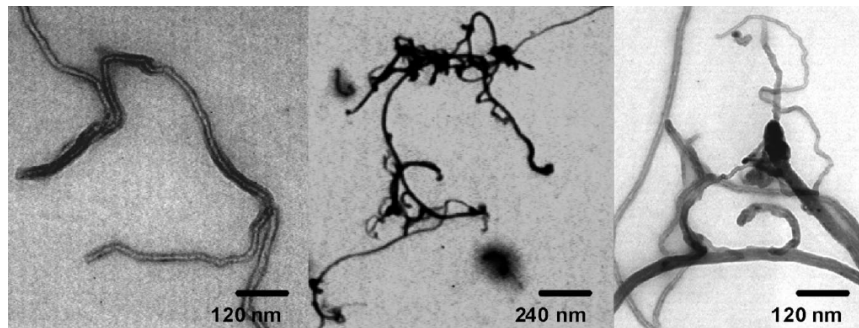
μ μ

SWCNTs.



μ 1.1.3.1: AFM μ μ SWCNTs

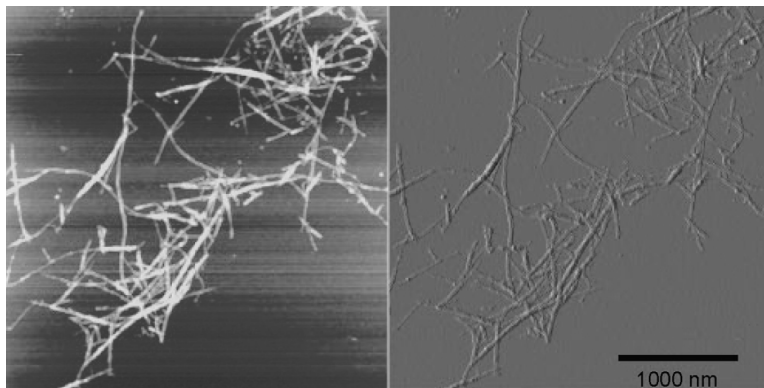
μ μ μ  
 ( μ 1.1.3.2) μ μ  
 μ . μ μ μ MWCNTs  
 μ ~ 30 nm μ μ μ μ.  
 μ μ  
 μ



μ 1.1.3.2: TEM μ μ MWCNTs

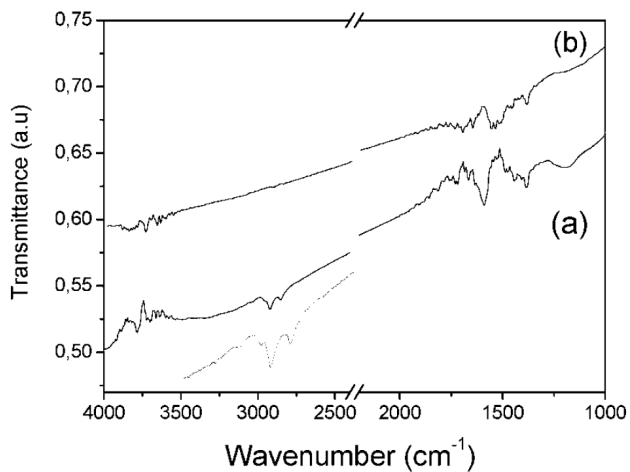
μ μ μ  
 μ μ AFM μ μ  
 μ μ μ ( μ 1.1.3.3)  
 μ μ μ ( μ , μ )  
 μ . μ

μ μ μ μ μ Raman.



μ 1.1.3.3 : AFM μ μ SWCNTs

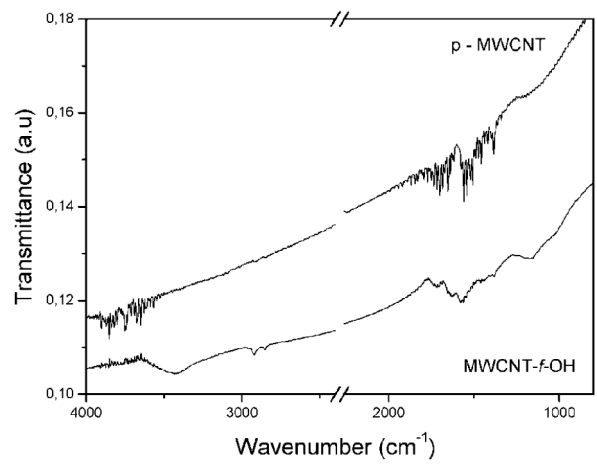
1.1.4. μ μ (FT-IR) SWCNT-f-OH pristine  
 μ μ μ 1.1.4.1.  
 SWCNT



μ 1.1.4.1 : μ FT-IR μ μ μ (a) μ (b) μ

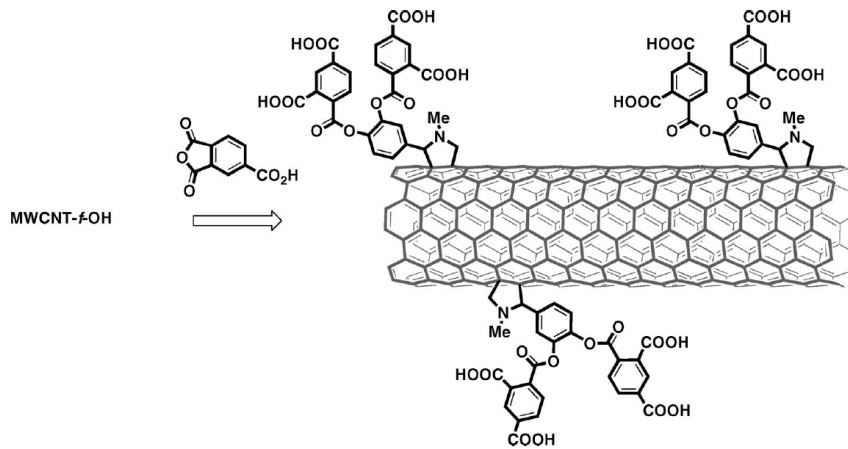
1.1.4.1a) μ μ μ μ μ ( μ C-H  
 2950, 2920, 2850 cm⁻¹ μ μ Pristine  
 SWCNT ( μ 1.1.4.1b). μ SWCNT-f-OH  
 μ μ , C-H  
 C=C 3040 ( ) 1380-1600 cm⁻¹ .

O-H 3600–3700 cm<sup>-1</sup>,  
 C-O 1200 cm<sup>-1</sup>  
 MWCNTs (1.1.4.2).  
 MWCNT-f-OH  
 MWCNT, C-H  
 2922 2853 cm<sup>-1</sup>.  
 C=C C-  
 O (1400-1600 ~1190 cm<sup>-1</sup>)  
 MWCNTs  
 MWCNTs,



1.1.4.2: FT-IR (MWCNT-f-OH) (p-MWCNT)

MWCNT-f-OH  
 MWCNT-f-OH  
 MWCNT-f-OH  
 MWCNT-f-OH  
 (1.1.4.3).



MWCNT-f-OH

μ 1.1.4.3: μ

MWCNT-f-OH μ

μ

MWCNT-f-OH

μ μ μ

μ μ μ μ

μ μ μ

μ μ

C-O-Si

MWCNT-f-OH

μ

μ FT-IR

μ

840, 1150 μ

3000 cm<sup>-1</sup>

Si-O-Si Si-O-C, CH<sub>3</sub>-

CH<sub>3</sub>-, -CH<sub>2</sub>-

( μ 1.1.4.4).

μ

MWCNT-f-OH

μ

μ

NaOH

μ

μ

μ

μ

μ

(MWCNT-f-OSiR)

μ

μ

(MWCNT-f-ArCOOH),

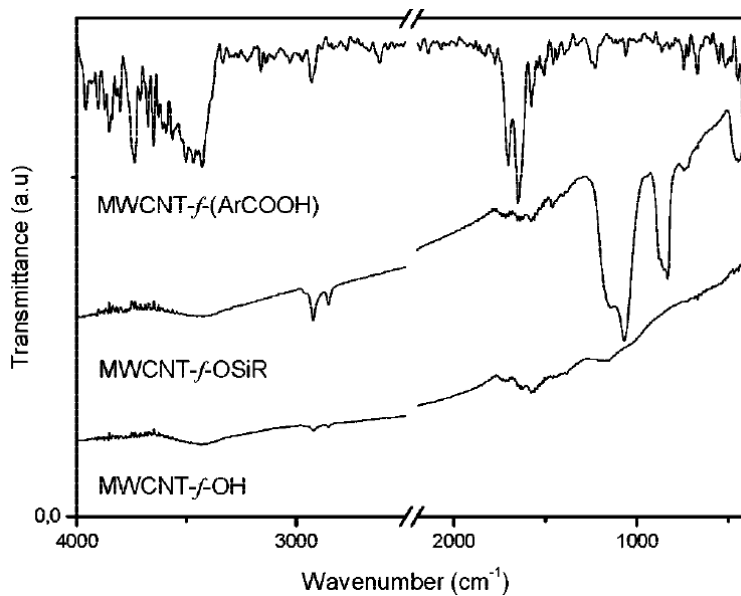
1703 1651 cm<sup>-1</sup>

μ

μ

( μ 1.1.4.4).

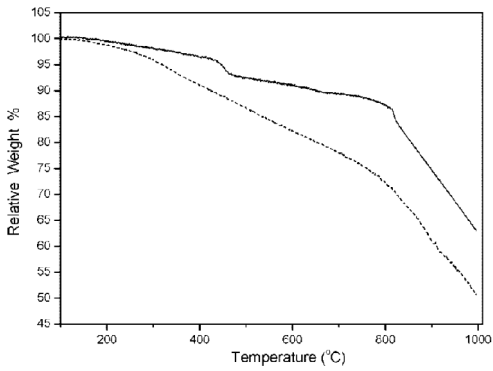




μ 1.1.4.4: μ FT-IR μ μ μ μ

1.1.5.

(TGA). 1.1.5  
 TGA SWCNT-f-OH Pristine SWCNT.  
 ( 300-400 C)  
 (> 400 C)<sup>213-217</sup>.  
 218, 219.  
 TGA SWCNT-f-OH  
 28% 800  
 Pristine SWCNT (< 14%). H



**1.1.5:** ( TGA ) SWCNT-f-OH Pristine SWCNT ( TGA )



## 1.2

Figure 1.2 shows the structure of a single-walled carbon nanotube (SWCNT) and its interaction with a protein. The SWCNT is a cylindrical structure composed of carbon atoms arranged in a hexagonal lattice. The protein is shown as a complex structure with various amino acid side chains. The interaction between the SWCNT and the protein is shown as a binding site where the SWCNT is attached to the protein structure. The figure is labeled with the number 1.2.

*situ* (SWCNTs),

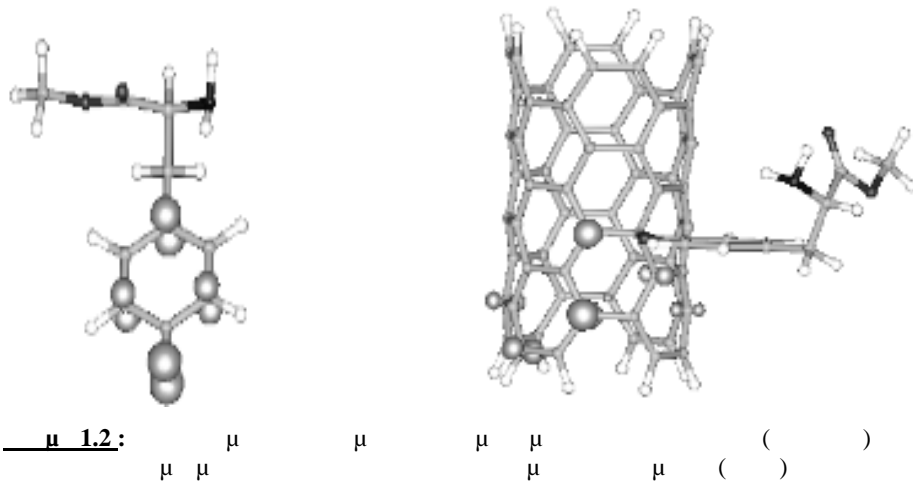
CNTs

CNTs.

(SWCNTs)

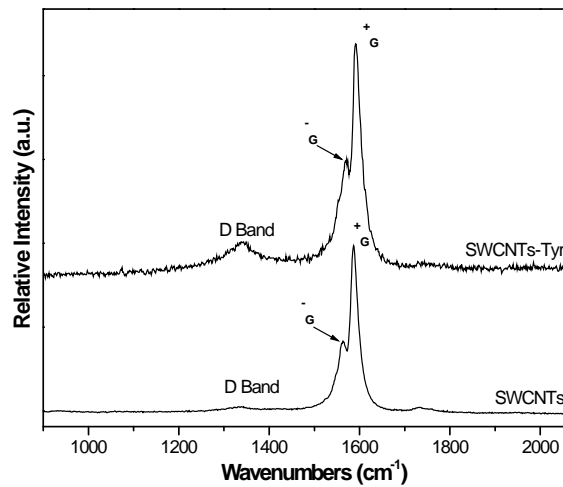
SWCNTs (1.2)

(...)



### 1.2.1 Raman

SWCNTs Raman. (SWCNTs-Tyr, 1.2.1) 1200-1800  $\mu$ , D G  $\sim 1350$   $\sim 1580$   $\text{cm}^{-1}$ .  $E_{2g}$   $sp^2$   $D$   $sp^2$ , CNTs 194-196.  $(R=I_D/I_G)$   $\mu$   $197, 198$ ,  $\mu$   $199$  200-202 (  $\mu$  G  $\mu$   $^+_G$  (  $\mu$   $^-_G$  (  $\mu$  ).

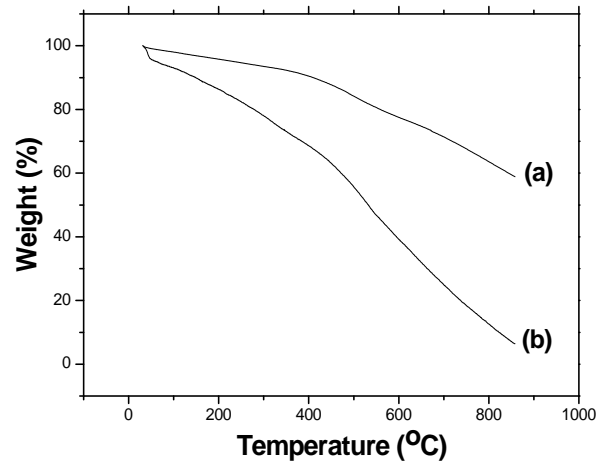


1.2.1: Raman SWCNTs SWCNTs-Tyr

SWCNTs  
 $I_{G/D}$ ,  $I_{G/D}$   
 6 ( 44.8 SWCNT 7.6 SWCNT-Tyr),  
 $(I_{G^+})/(I_{G^-})$  1.4.  
 Raman, CNTs  
 $I_{G/D}$   $(I_{G^+})/(I_{G^-})$   
<sup>223</sup>.

1.2.2

SWCNTs  
 (TGA). 1.2.2, TGA SWCNTs  
 SWCNTs-Tyr.  
 200 °C  
 800 °C 90%.  
 SWCNTs 300  
 C ~ 30%.

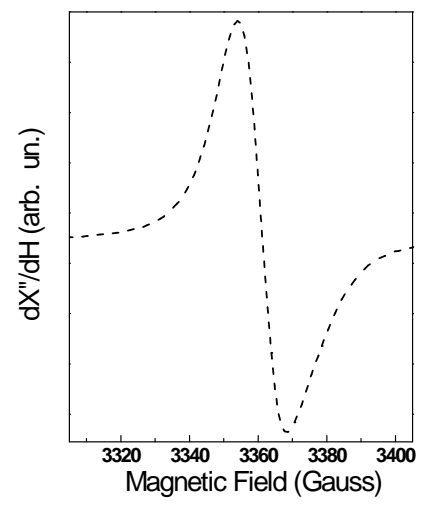


1.2.2: TGA SWCNTs (a) SWCNTs-Tyr (b)

200 °C.

μ , μ μ μ  
 μ μ μ μ  
 μ μ μ μ 218, 219  
 μ μ μ μ SWCNTs μ μ μ  
 μ μ μ μ SWCNTs.

**1.2.3** μ μ μ  
 o μ μ (EPR) SWCNT-  
 Tyr ( μ 1.2.3) μ μ g 2.0024  
 μ μ μ g μ  
 μ μ g μ  
 SWCNT-Tyr  
 μ g μ  
 , μ 2.0140 μ 2.0110<sup>224</sup> μ 2.0111-2.0206<sup>225</sup>  
 μ μ



**μ 1.2.3:** μ EPR SWCNT-Tyr

μ EPR μ μ  
 μ -

(spin-orbit, SO) SU(2)  $\mu\mu$  <sup>226</sup>  
 , Hpp  $\mu$   $\mu$   $\mu$  9-20 Gauss. <sup>224, 226, 227</sup>  
 SWCNT-Tyr  $\mu$   $\mu$   $\mu$   
 $\mu$   $\mu$   $\mu$   $\mu$   
 $\mu$  SWCNTs  $\mu$   
 $\mu$   $\mu$   $\mu$  g  $\mu$  EPR  
 $\mu$   $\mu$   $\mu$   $\mu$   $\mu$   $\mu$   
 $\mu$   $\mu$   $\mu$   $\mu$  .

**1.2.4.  $\mu$   $\mu$  -**

$\mu$   $\mu$   $\mu$   $\mu$   
 .  
 ( . . ).  
 $\mu$   $\mu$   $\mu$  - (XPS) (  
 $\mu$  ),  
 $\mu$   $\mu$   $\mu$  Raman, TGA EPR.  
 $\mu$   $\mu$   $\mu$  EPR  $\mu$   $\mu$   
 $\mu$  (DFT)  $\mu$  (  
 $\mu$  )  $\mu$   
 .  $\mu$   $\mu$   
 $\mu$   $\mu$   $\mu$   $\mu$   $\mu$   
 30  $\mu$  35%  $\mu$   $\mu$   $\mu$   $\mu$  .  
 $\mu$   $\mu$  (  
 )  
 $\mu$  -  $\mu$   $\mu$   $\mu$   
 , (C<sub>60</sub>).



2

μ

2.1

μ

μ

μ

FePt

(NPs) FePt

μ

μ

μ

μ

(MWCNTs)

μ

μ

NPs FePt.

μ

μ

μ

μ

μ

μ

228. T  
229

μ

μ

FePt

μ

μ

μ

MWCNTs

μ

μ

μ

L1<sub>0</sub> FePt

μ

FePt (

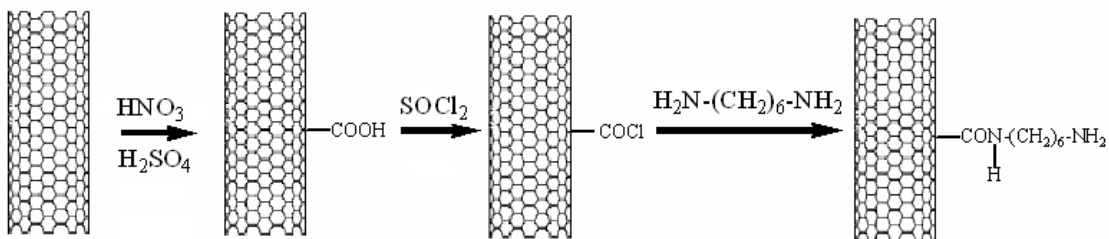
)

μ

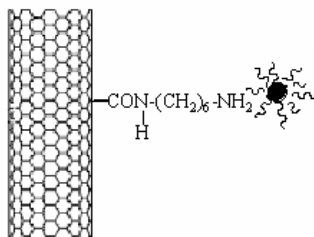
FePt (MWCNTs-FePt)

700 C. H

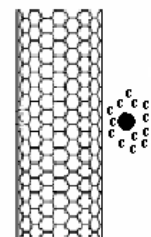
μ



Νανοσωματίδια



Ανόπτηση



μ 2.1.

μ 2.1:

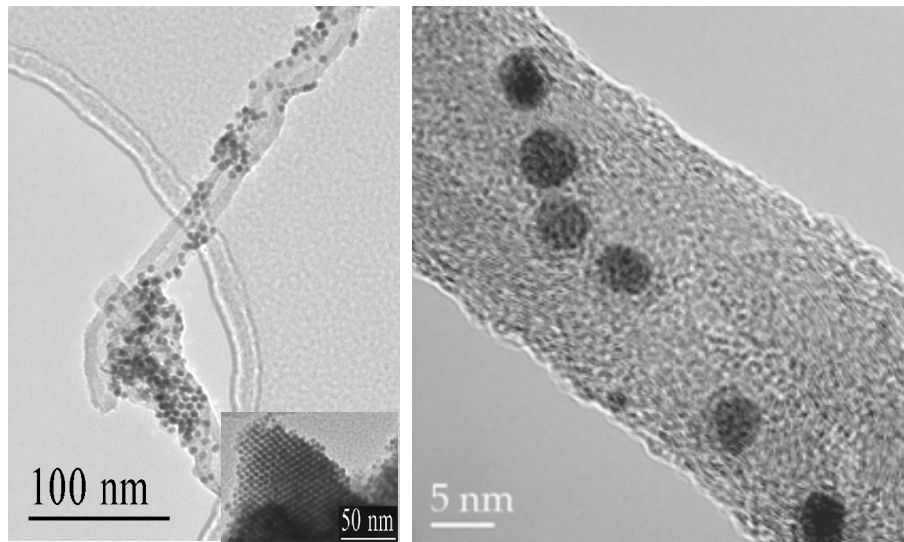
μ

μ

FePt

MWCNTs-





(a)

(b)

μ 2.1.1:

. . . MWCNTs-NPs

### 2.1.2

$\mu$   $\mu$   $\mu$  FePt  $\mu$   
 $L_{10}$  FePt  $\mu$ ,  $\mu$   $\mu$  550 °C 800 °C<sup>230</sup>,  
<sup>231</sup>  $\mu$   $\mu$   $\mu$ ,  
 $\mu$   $\mu$   $\mu$   $\mu$   $\mu$   
 $\mu$   $\mu$   $\mu$  FePt<sup>229</sup>  
 $\mu$   $\mu$   $\mu$   $\mu$   
650 °C.  $\mu$  FePt  
 $\mu$   $\mu$ ,  $\mu$   $\mu$   $\mu$   
- (XRD),  $\mu\mu$  XRD NPs FePt  
MWCNTs-FePt  $\mu$   
 $\mu$  2.1.2.  $\mu$  -  
, FePt FePt  $\mu$   
MWCNTs-FePt FCC (Face Centered Cubic)  
(disorder)  $\mu$  .

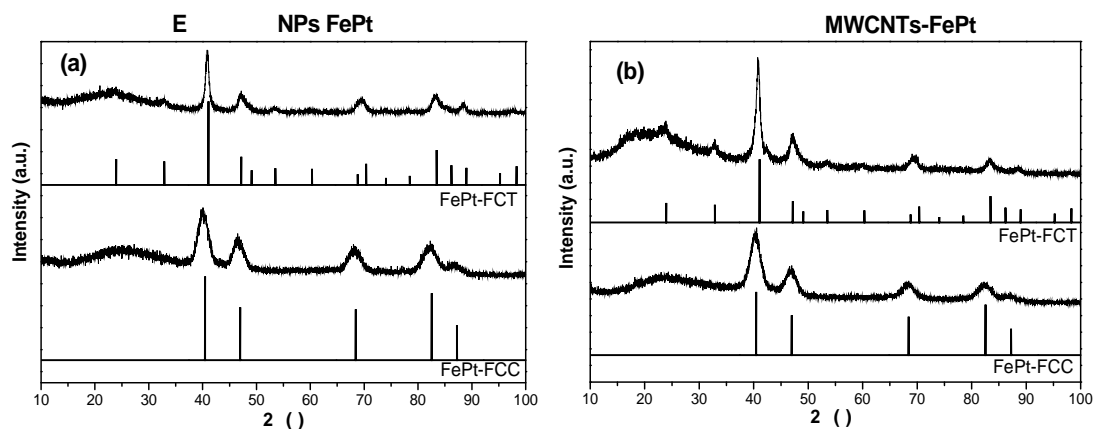


Figure 2.1.2: XRD patterns of (a) FePt NPs and (b) MWCNTs-FePt. The patterns show peaks corresponding to the FePt-FCT and FePt-FCC phases. The sintering temperature for (b) is 700 °C. Reference patterns for FePt-FCT (JCPD # 29-0717) and FePt-FCC (JCPD # 43-1359) are also shown.

M FePt FCT (Face Centered Tetragonal)  $L1_0$   $\mu$  (*ordered*)  $\mu$   $\mu$  XRD

$\mu$   $\mu$   $\mu$   $\mu$  Scherrer<sup>232</sup>,  $\mu$   $\mu$

$\mu$  FePt ( $\mu$  2.1.2a),  $\mu$   $\mu$  4 nm 13 nm.  $\mu$  ,  $\mu$

$\mu$  FePt ( $\mu$  2.1.2b) 4 nm 11 nm  $\mu$

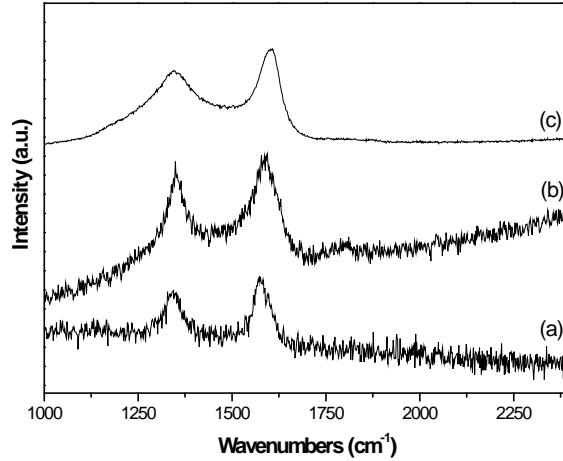
$\mu$   $\mu$   $\mu$   $\mu$   $\mu$   $\mu$

MWCNTs-FePt (sintering)  $\mu$   $\mu$   $\mu$   $\mu$   $\mu$  FePt

$\mu$   $\mu$   $\mu$   $\mu$   $\mu$

**2.1.3 Raman**

MWCNTs MWCNTs-FePt  
 (2.1.3a)  
 MWCNTs<sup>195, 233</sup>

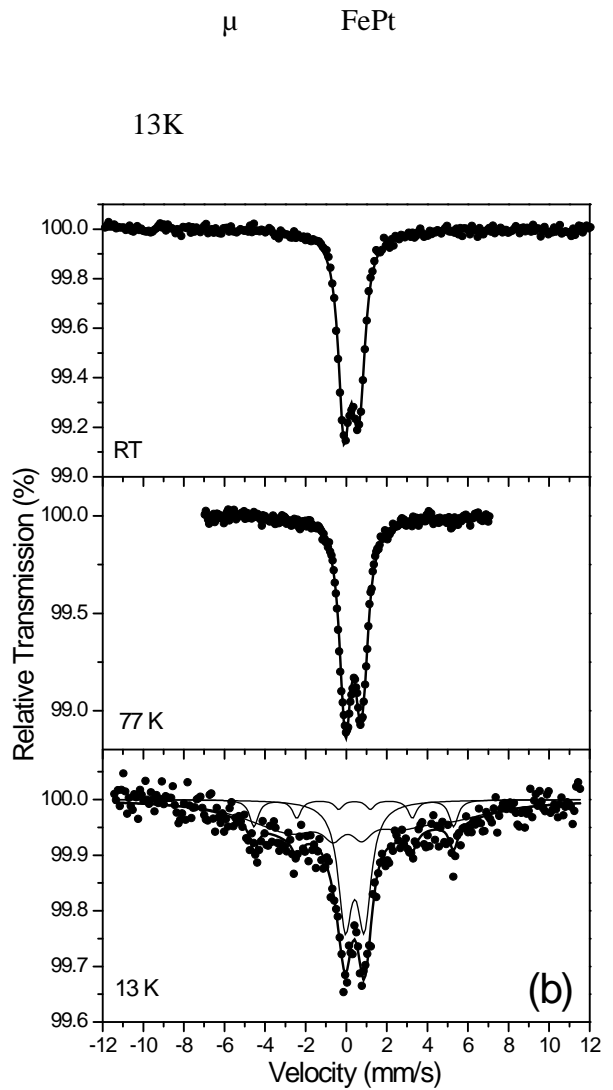
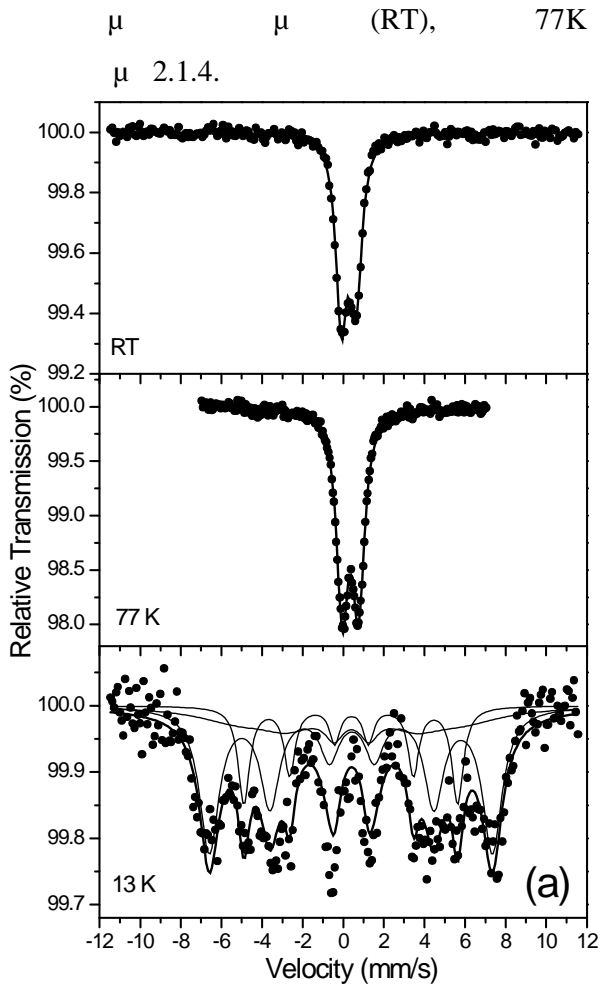


**2.1.3:** Raman spectra of (a) MWCNTs, (b) MWCNTs-FePt, and (c) MWCNTs-FePt at 700 C.

The Raman spectra show the characteristic G and D bands. The G band is located at  $1580\text{ cm}^{-1}$  ( $E_{2g}$  sp<sup>2</sup>) and the D band is located at  $1342\text{ cm}^{-1}$  (D band, sp<sup>3</sup>). The intensity ratio  $I_D/I_G$  is a measure of the defect density. For MWCNTs,  $I_D/I_G$  is 0.95. For MWCNTs-FePt,  $I_D/I_G$  is 0.66. The decrease in  $I_D/I_G$  for MWCNTs-FePt indicates a higher degree of graphitization compared to MWCNTs.

$\mu$  MWCNTs-FePt 700 C.  
 $\mu$   $I_D/I_G$   
 $\mu$  (0.77)  $\mu$   
 $\mu$  Endo  $\mu$  MWCNTs  
 $\mu$   $\mu$   $\mu$   
 $\mu$  238

2.1.4  $\mu$  ssbauer  
 $\mu$  Mössbauer (MS)  
 MWCNTs-FePt



$\mu$  2.1.4:  $\mu$  Mössbauer  
 MWCNTs-FePt (b)

$\mu$  FePt (a)  
 $\mu$

$\mu$  RT 77 K  
 $\mu$   $\mu$   $\mu$   $\mu$  ,  $\mu$   
 $\mu$   $\mu$   $\mu$  13K.  $\mu$   
 $\mu$   $\mu$   $\mu$   $\mu$  ,  
 $\mu$   $\mu$   $\mu$   $\mu$   $\mu$  .  
 $\mu$   $\mu$   $\mu$   $\mu$   $\mu$   
 $\mu$   $\mu$   $\mu$   $\mu$  RT 77K.  
 $\mu$   $\mu$  13K  $\mu$   $\mu$  3  $\mu$   
 $\mu$   $\mu$   $\mu$   $\mu$  FePt  
 $\mu$   $\mu$   $\mu$   $\mu$   
 MWCNTs-FePt  $\mu$  Mössbauer (MPs)  
 $\mu$   $\mu$

2.1.4.

**2.1.4:**  $\mu$  Mössbauer  $\mu$   
 $\mu$   $\pm 0.02$  mm/s  $/2, IS, 2$  ,  $\pm 0.5$   $B_{hf}$   
 $B_{hf}$   $\pm 3\%$   $\mu$  A

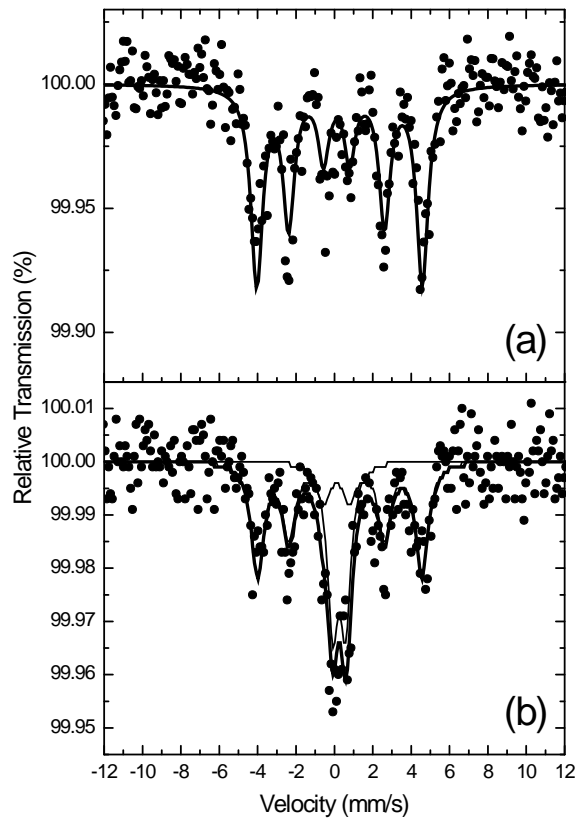
	T	$I/2$	IS	2 -	$B_{hf}$	$B_{hf}$	A
	K	mm/s	mm/s	mm/s	T	T	%
FePt $\mu$	300	0.31	0.36	0.70	-	-	100
	77	0.32	0.46	0.79	-	-	100
	13	0.56	0.51	-0.05	43.5	0.1	55
		0.30	0.50	-0.04	32.8	0.2	22
		0.16	0.49	-0.05	34.0	14.8	23
MWCNTs-FePt	300	0.32	0.36	0.71	-	-	100
	77	0.36	0.46	0.80	-	-	100
	13	0.41	0.53	0.94	-	-	36
		0.24	0.49	0.64	27.9	14.4	54
		0.25	0.50	-0.04	30.7	0	10
FePt $\mu$	300	0.33	0.30	0.15	26.9	0.2	100
FePt $\mu$ MWCNTs-	300	0.32	0.35	0.67	-	-	37
		0.40	0.31	0.17	26.6	0	63

2.1.4 Mössbauer  
 (isomer shift) 77K. FePt<sup>239</sup>  
 300K) FePt<sup>239</sup>  
 Doppler<sup>240</sup>.  
 77 K MWCNTs-FePt 13 K.  
 FePt  
 (B<sub>hf</sub>) 31.0 T<sup>241</sup>  
 (2) ~ 0 mm/s.  
 77K FePt  
 FePt RT  
 77K FePt  
 (locking emperature T<sub>B</sub>),  
 (A)<sup>212</sup> T<sub>B</sub> 77K  
 13K ~ 36 %  
 13K  
 T



$T_B$   $\mu$   $\mu$   $V$   $\mu$   
 $K$   $\mu$  <sup>242</sup>,  $\mu$   $\mu$   
 $\mu$   $\mu$   $\mu$   $FePt$   
 $\mu$  ,  $\mu$  ,  
 $\mu$   $\mu$   $FePt$   $\mu$   $\mu$   $\mu$   
 $\mu$   $\mu$   $K$   $\mu$   $\mu$   
 $\mu$  .  $\mu$   $\mu$   $\mu$   
 $\mu$   $FePt$  ,  
XRD ( $\sim 4$  nm),  
.  $\mu$   $\mu$   $\mu$   $\mu$   $\mu$   $\mu$   
13  $\mu$   $\mu$   $K$   
 $\mu$   $\mu$  .  $\mu$   $\mu$   
 $\mu$   $\mu$   $\mu$   $fcc$   $FePt$   $\mu$   
 $\mu$   $\mu$   $\mu$   $\mu$  .  
 $\mu$  (  $\mu$   
 $\mu$  ),  $\mu$   $\mu$   $\mu$   
 $\mu$   $\mu$   
.  $\mu$   $FePt$   
 $\mu$  :  $\mu$   $\mu$   $\mu$   
 $\mu$   $\mu$   $\mu$   
 $\mu$   $\mu$   $\mu$  .  $\mu$   
 $\mu$   $\mu$   
 $\mu$   $\mu$  .  $\mu$   
 $\mu$   $\mu$   $\mu$   $\mu$   $\mu$   
 $\mu$   $\mu$   $\mu$   $\mu$   $\mu$   
 $\mu$  .  $\mu$   
 $\mu$   $\mu$   $\mu$   
 $\mu$   $M\ddot{o}ssbauer$  13  $\mu$   $\mu$   $\mu$   
 $\mu$

Mössbauer RT  
 2.1.4.2. « »  
 FePt  
 RT,  
 (A ~ 37%,  
 2.1.4) μ  
 13K



2.1.4.2: Mössbauer FePt (a)  
 MWCNTs-FePt (b)

Mössbauer fct FePt  $B_{hf}$   
 27.1 T and 0.15 mm/s

241, 243 . μ μ μ

μ Mössbauer μ μ

μ μ μ

μ μ μ

μ FePt μ S μ ,

μ μ <sup>239</sup> .

μμ XRD μ μ

fcc ,

μ μ μ

fcc μ fct ( μ 2.1.2).

μ FCT

μ μ c/a

μ . - μ μ

μ μ μ ,

μμ -

μ . μ ( 11 4

nm) μ μ

μ ( 13 4 nm),

μ μ μμ XRD

μ fct , μ

μ μ μ μ .

μ fcc

μ FePt μ μ μ

13 , μ μ

μ μ μ

μ fct μ μ .

μ μ μ μ μ

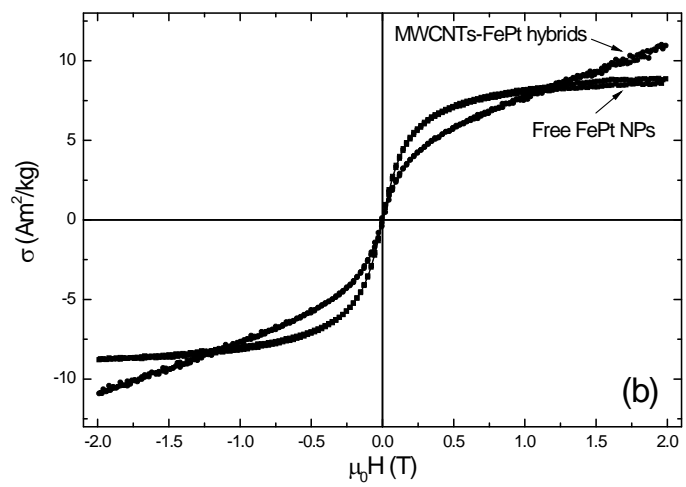
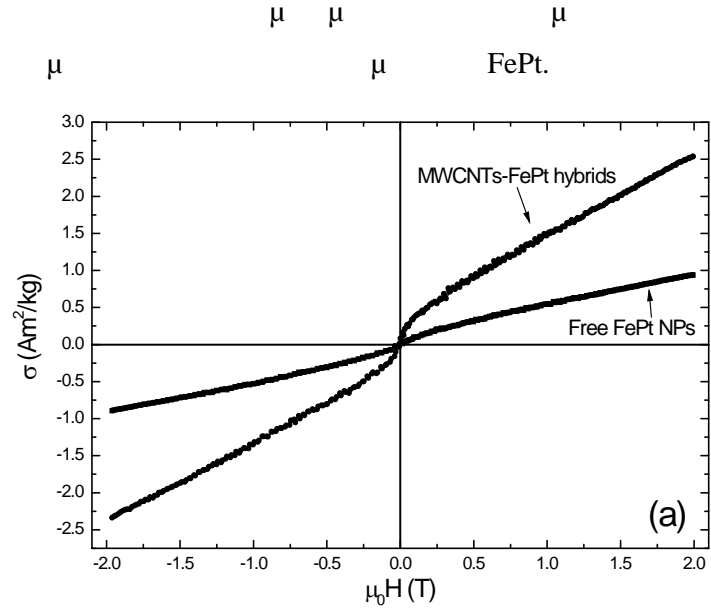
μ μ μ .

μ μ μ μ ,

μ μ μ μ

μ μ

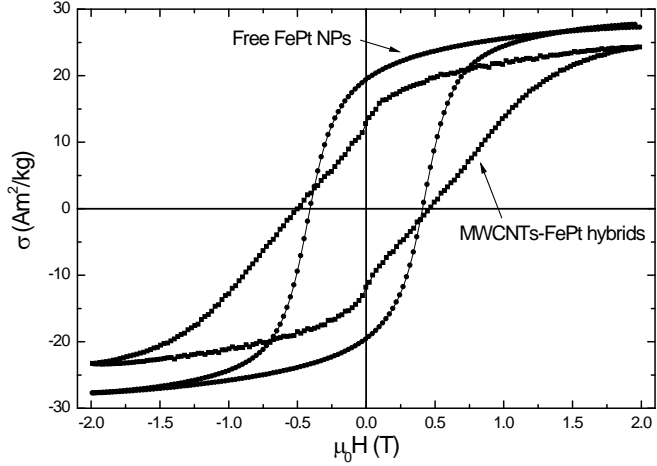




**2.1.5.1:** MWCNTs-FePt (MWCNTs-FePt hybrids) FePt (Free FePt NPs) (a) 77K (b).

TEM Mössbauer

Figure 2.1.5.2 shows the magnetic hysteresis loops for FePt, MWCNTs-FePt hybrids, and Free FePt NPs at 77K and room temperature (RT). The plot shows saturation magnetization  $\sigma$  (Am<sup>2</sup>/kg) versus magnetic field  $\mu_0 H$  (T). The curves for Free FePt NPs and MWCNTs-FePt hybrids are nearly identical and show a higher saturation magnetization compared to FePt. The FePt curve shows a much lower saturation magnetization. The hysteresis loops for FePt and MWCNTs-FePt hybrids are wider than those for Free FePt NPs. The MWCNTs-FePt hybrids exhibit a higher coercivity than Free FePt NPs and a similar coercivity to FePt.



**Figure 2.1.5.2:** Magnetic hysteresis loops for FePt (solid line), MWCNTs-FePt hybrids (dotted line), and Free FePt NPs (dashed line) at 77K and room temperature (RT). The curves show saturation magnetization  $\sigma$  (Am<sup>2</sup>/kg) versus magnetic field  $\mu_0 H$  (T). The FePt curve shows a lower saturation magnetization compared to the other two. The MWCNTs-FePt hybrids and Free FePt NPs show higher saturation magnetization and similar hysteresis widths. The MWCNTs-FePt hybrids exhibit a higher coercivity than Free FePt NPs. The curves were recorded after annealing at 700 °C.







## 2.2

μ

μ

μ - (SWCNTs)

μ (MWCNTs)

μ

- μ

μ

μ

μ

( -Fe<sub>2</sub>O<sub>3</sub>, -Fe<sub>2</sub>O<sub>3</sub> Fe<sub>3</sub>O<sub>4</sub>) μ μ

μ

μ

μ

μ

μ

μ , SWCNTs

μ

μ

, 2- μ - , μ

- ( μ

2.2.1a).

μ

μ

SWCNTs

,

μ

/

μ

,

μ

(

)

μ

μ

μ

( μ 2.2.1b)

μ

μ

μ

μ

( μ 2.2.1c) μ

μ

400 °C

μ

μ

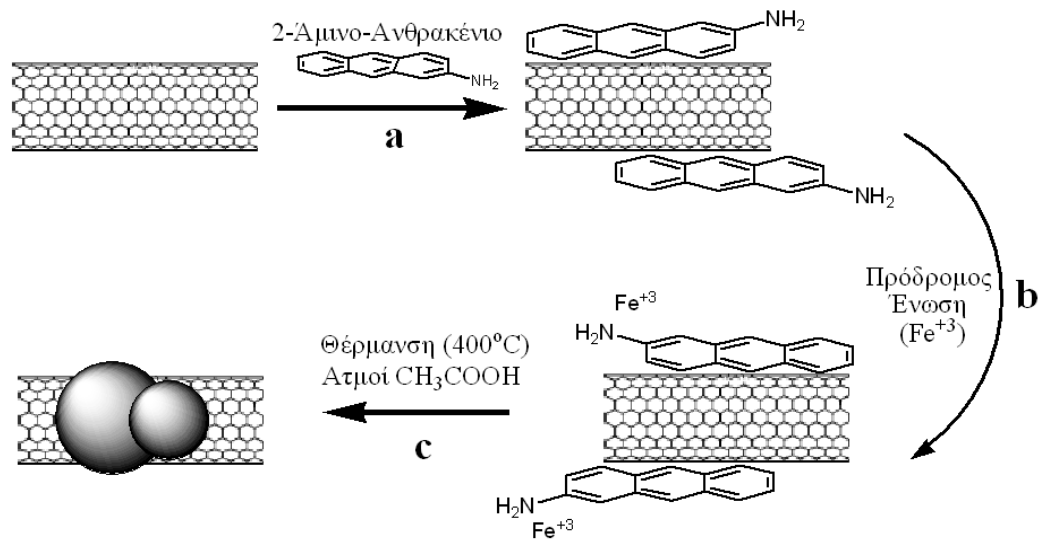
( μ

) μ

μ

μ

SWCNTs.



μ 2.2.1:

μ

μ

μ

2- μ

-

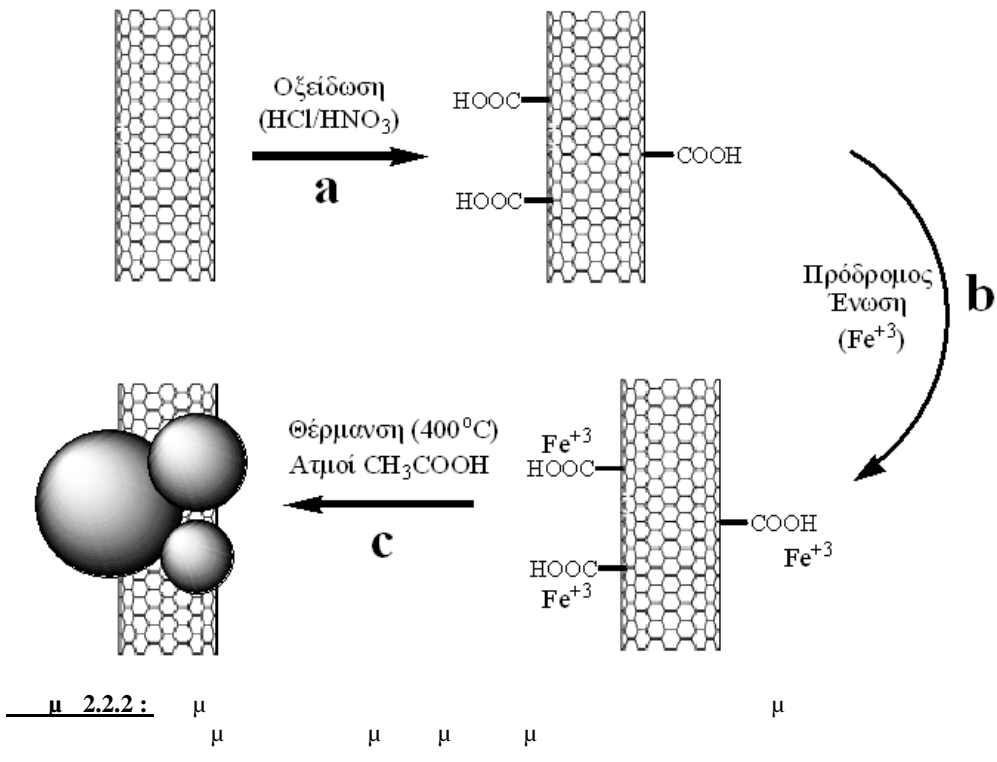
μ

μ

μ

.

$\mu$   $\mu$   $\mu$  , SWCNTs MWCNTs  $\mu$   $\mu$   
 $\mu$   $\mu$   $\mu$  (  $\mu$  2.2.2a).  $\mu$   $\mu$   
 (  $\mu$  2.2.2b)  $\mu$   
 $\mu$   $\mu$   $\mu$  400 °C  $\mu$  (  $\mu$   $\mu$   
 MWCNTs  $\mu$   
 ) (  $\mu$  2.2.2c).



$\mu$  Raman Mössbauer,  $\mu$   $\mu$   $\mu$

## 2.2.1 μ o Raman

μ Raman μ μ 2- μ -

(Pristine-SWCNTs) μ μ μ 2.2.1.1. G

(Anthracene-SWCNTs) sp<sup>2</sup> μ μ E<sub>2g</sub>, D

sp<sup>2</sup> μ μ sp<sup>3</sup>

μ μ , μ

μ μ /

194-196 μ G

μ , <sup>+</sup>G ( ) <sup>-</sup>G ( μ

) μμ

μ 1G μ μ μ μ

μ μ

(Radial Breathing Mode RBM)<sup>203, 204</sup>

μ μ 199 μ

μ μ 200-202 μ

μ μ μ RBM

μ μ μ ( RBM = (A/d<sub>t</sub>) + , ,

μ μ , d<sub>t</sub> μ CNTs

RBM )<sup>205, 206</sup>.

G<sup>+</sup> D ( G<sup>+</sup>/D)

G<sup>+</sup> G<sup>-</sup> ( G<sup>+</sup>/ G<sup>-</sup>) μ μ

μ μ SWCNTs

μ μ 245-247 .

μ μ G<sup>+</sup>/D G<sup>+</sup>/ G<sup>-</sup>

14.7 1.85 . μ

μ μ .

μ G<sup>+</sup>/D 7.2 G<sup>+</sup>/ G<sup>-</sup> 1.59.

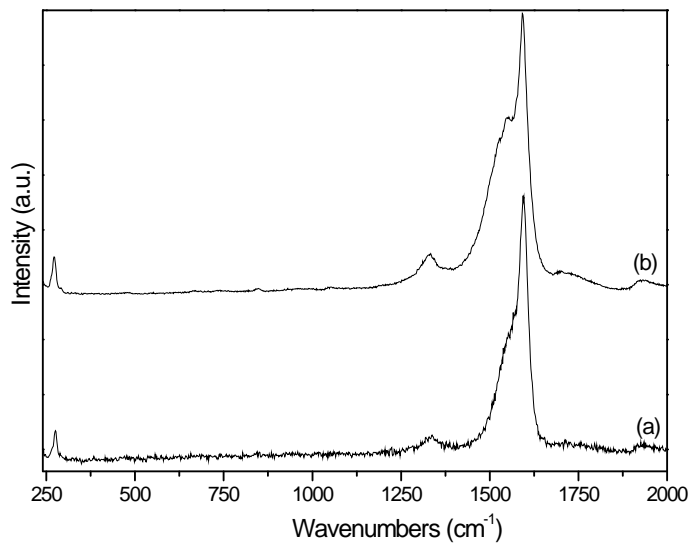
μ μ

Anthracene-SWCNTs μ .

RBM

Anthracene-SWCNTs μ

μ μ .



2.2.1.1 Raman Pristine-SWCNTs (a) Anthracene-SWCNTs (b)

SWCNTs

SWCNTs

Argon)

Raman,

D G RBM

400 °C

400 °C,

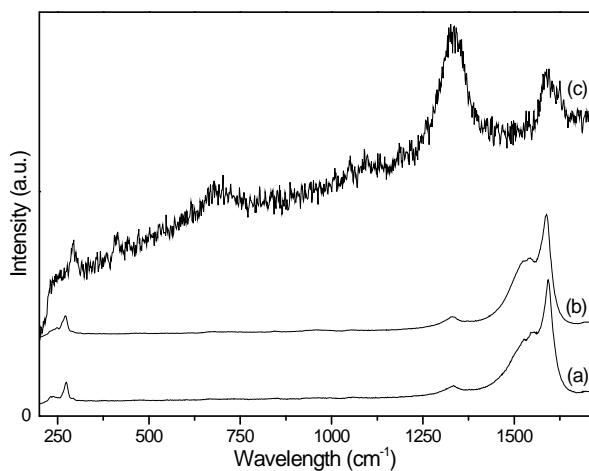
(Anthracene-SWCNTs-Fe-Air).

(Anthracene-SWCNTs-Fe-Argon)

Raman

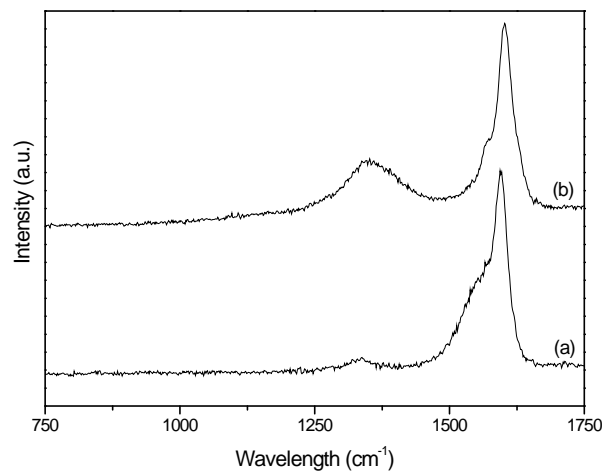
G

400 °C,



2.2.1.2. Raman Anthracene-SWCNTs (a), Anthracene-SWCNTs-Fe-Argon (b) Anthracene-SWCNTs-Fe-ir (c)

Raman  
 (Pristine-SWCNTs)  
 (Acids-SWCNTs)  
 Acids-SWCNTs  
 G, D  
 G D ( $I_G/I_D$ ) 3.1  
 14.7  
 sp<sup>3</sup>  
 248, 249



μ 2.2.1.3: μ Raman Pristine-SWCNTs (a) Acids-SWCNTs (b)

Acids-SWCNTs, μ μ μ 400 C  
 ( μ ) μ μ  
 SWCNTs μ μ μ

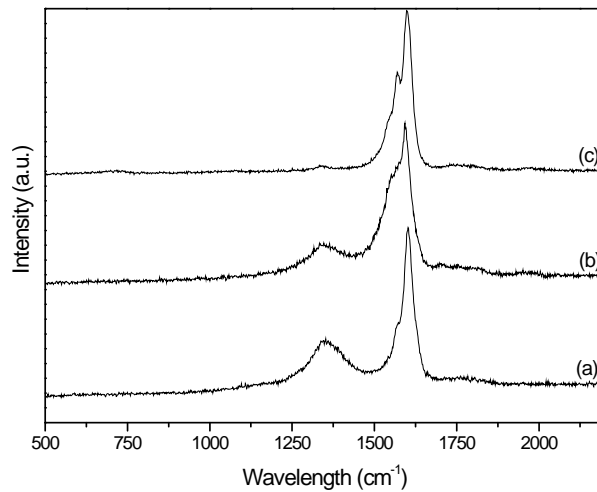
μ 2.2.1.4

μ Raman Acids-SWCNTs

μ μ μ 400 C  
 μ (Acids-SWCNTs-Fe-Argon) (Acids-SWCNTs-Fe-  
 Air). μ μ 400 C,  
 D G μ

μ G 200-202

μ μ μ  
 μ μ D  
 μ μ μ μ



**2.2.1.4:** Raman Acids-SWCNTs (a), Acids-SWCNTs-Fe-Argon (b)  
Acids-SWCNTs-Fe-Air (c)

Raman (Pristine-MWCNTs) (Acids-MWCNTs)

2.2.1.5.

( $I_G/I_D$ )

Acids-MWCNTs

1.19

1.30

Pristine-

MWCNTs.

,

,

,

,

,

,

,

,

,

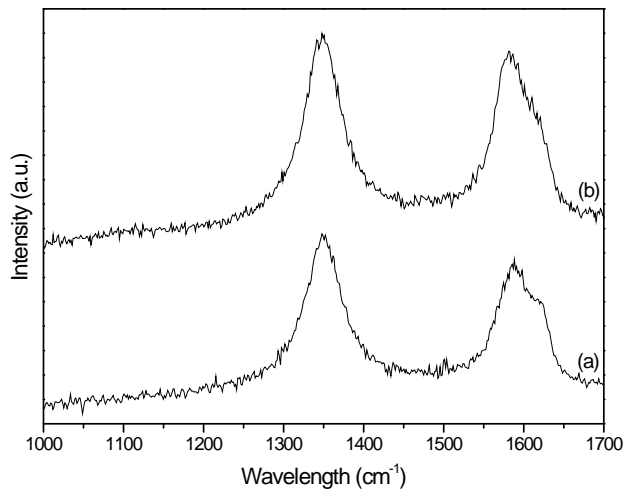
210, 211.

D

D

$sp^3$

$sp^3$



**2.2.1.5:** Raman Pristine-MWCNTs (a) Acids-MWCNTs (b)

$I_D/I_G$  (Acid-MWCNTs-Fe-Argon), (Acid-MWCNTs-Fe-Air) (Acid-MWCNTs-Fe-Oxygen)

400 C

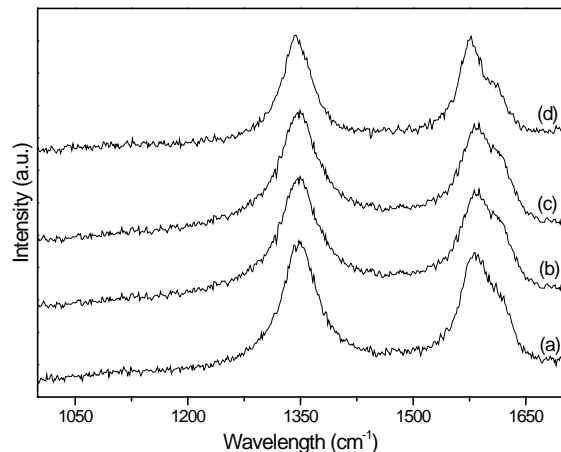
D G

Acids-SWCNTs (1.19).

1.21, 1.22 1.11

Acid-MWCNTs-Fe-Argon, Acid-MWCNTs-Fe-Air Acid-MWCNTs-Fe-Oxygen



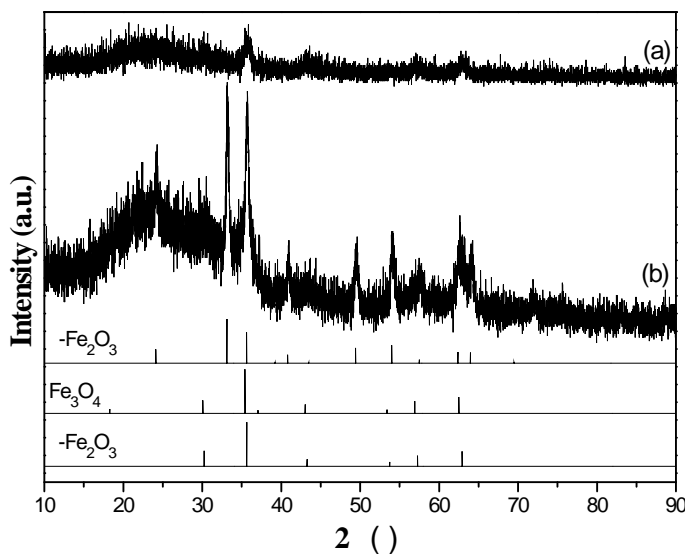


**2.2.1.6:** Raman spectra of Acid-MWCNTs (a), Acid-MWCNTs-Fe-Argon (b), Acid-MWCNTs-Fe-Air (c), and Acid-MWCNTs-Fe-Oxygen (d).

## 2.2.2

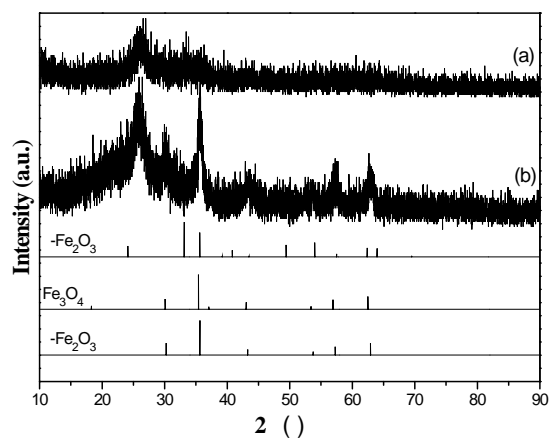
Figure 2.2.2 shows the XRD patterns of Anthracene-SWCNTs-Fe-Argon (a) and Anthracene-SWCNTs-Fe-Air (b) after being heated at 400 °C. The x-axis represents the diffraction angle  $2\theta$  (degrees) and the y-axis represents Intensity (a.u.). The patterns show characteristic peaks for iron oxides. Reference patterns for  $\text{Fe}_2\text{O}_3$  and  $\text{Fe}_3\text{O}_4$  are provided for comparison.

### 2.2.2.1.



**2.2.2.1:** XRD patterns of Anthracene-SWCNTs-Fe-Argon (a) and Anthracene-SWCNTs-Fe-Air (b) after being heated at 400 °C. The reference patterns for  $\text{Fe}_2\text{O}_3$  and  $\text{Fe}_3\text{O}_4$  are shown for comparison.

(  $\mu$  Anthracene-SWCNTs-Fe-Argon),  $\mu$   
 $35.7^\circ$ .  $2$   $\mu$   
 $\mu$   $\mu$   $\mu$   $-\text{Fe}_2\text{O}_3$   $\text{Fe}_3\text{O}_4^{250}$ .  $\mu$   
 $\mu$   $(-\text{Fe}_2\text{O}_3 \text{ Fe}_3\text{O}_4)$   $\mu$   
 $\mu\mu$  -  
 $\mu$   $\mu\mu$   $\mu$   $\mu$   $\mu$   $\mu$   
 $\mu$  Mössbauer .  
 $\mu$   $\mu$   $\mu$   $\mu$   $\mu$   $\mu$   $\mu$   
 $\mu$  Anthracene-SWCNTs-Fe-Air),  
 $33.1^\circ$   $35.7^\circ$ .  $2$   $\mu$   
 $\mu$   $\mu$   $-\text{Fe}_2\text{O}_3$ .  $\mu$   
 $\mu$   $\mu$  ,  $\mu$  ,  
 $\mu$   $\mu$   $2$   $57.5$  ,  
 $-\text{Fe}_2\text{O}_3$   $\text{Fe}_3\text{O}_4$ .  $\mu$   $\mu$   $\mu$   
 $\mu$   $\mu$  Scherrer ,  $\mu$   $\mu$   
 $\mu$   $-\text{Fe}_2\text{O}_3 \text{ Fe}_3\text{O}_4$   $\mu$   $9 \text{ nm}$ .  
 $\mu\mu$  XRD Acids- WCNTs-Fe-Argon  
 Acids- WCNTs-Fe-Air  $\mu$   $\mu$   
 $\mu$   $\mu$   $\mu$   $\mu$  WCNTs,  
 $\mu$  2.2.2.2.



$\mu$  2.2.2.2 :  $\mu\mu$  - Acids- WCNTs-Fe-Argon (a) Acids- WCNTs-Fe-Air (b)

2.2.2.2 ,

( Acids- WCNTs-Fe-Air),

002 ~26

( Acids- WCNTs-Fe-Argon),

002 35.7°

~30 . 2

220 311 ,

-Fe<sub>2</sub>O<sub>3</sub> Fe<sub>3</sub>O<sub>4</sub>.

Mössbauer

( 2.2.3)

Scherrer μ 14.3 nm. μμ XRD

Acids-MWCNTs-Fe-Oxygen

WCNTs, 2.2.4.3.

400 C.

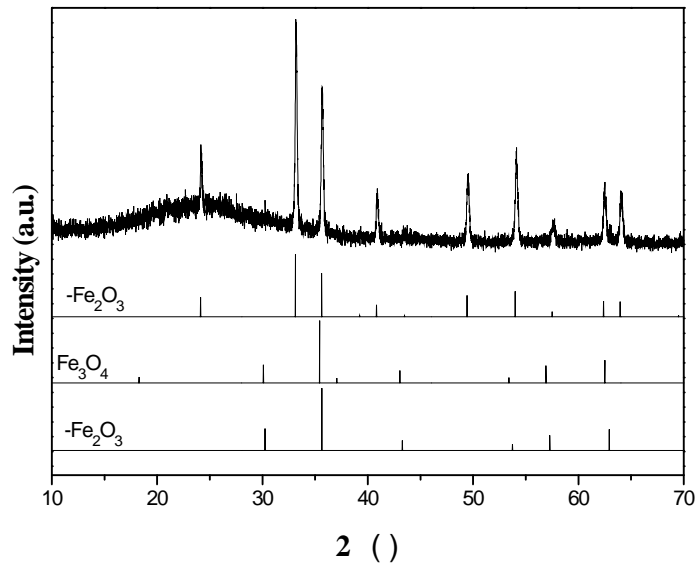
Acids-MWCNTs-Fe-Oxygen

~24 , ~33.2 , ~35.7 , ~49.5

~54 -Fe<sub>2</sub>O<sub>3</sub>.

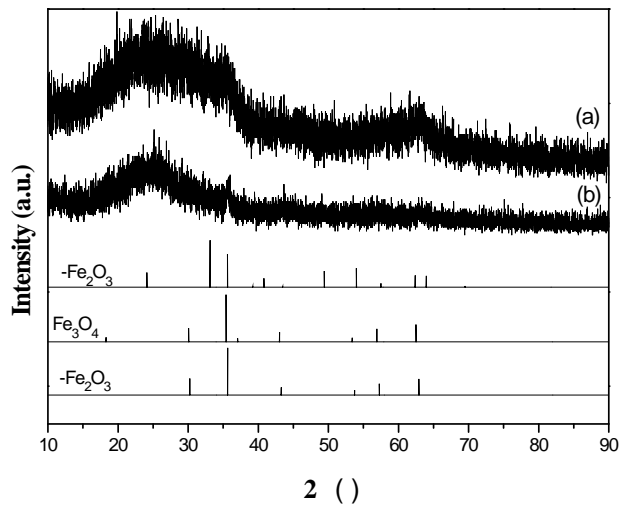
Scherrer μ μ μ

μ 126 nm.



μ 2.2.2.3 : μμ - Acids-MWCNTs-Fe-Oxygen

μ 2.2.2.4. μμ XRD  
Acids-SWCNTs-Fe-Air Acids-SWCNTs-Fe-Argon  
μ μ μ μ  
μ μ SWCNTs.



μ 2.2.2.4 : μμ - Acids-SWCNTs-Fe-  
Air (a) Acids-SWCNTs-Fe-Argon (b)

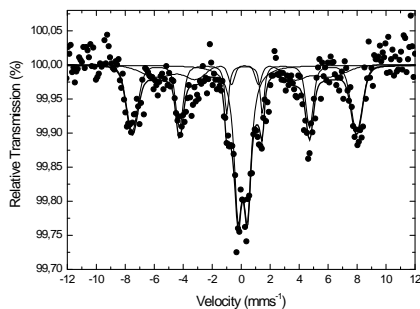
Acids-SWCNTs-Fe-Air

μ

30 40 μμ XRD  
 μ  
 μμ Acids-SWCNTs-Fe-Argon , μ μ μ  
 ~35.6  
 Fe<sub>2</sub>O<sub>3</sub> Fe<sub>3</sub>O<sub>4</sub> μ μ μ μ  
 μ Mössbauer ( 2.2.3), μ  
 Scherrer, μ μ μ μ 27 nm.

### 2.2.3 μ o Mössbauer

μ Mössbauer μ Anthracene-SWCNTs-Fe-Argon ( μ 2.2.3.1)  
 μ μ μ  
 μ μ Mössbauer μ  
 μ 2.2.3,  
 μ μ μμ - μ μ  
 μ μ Fe μ Fe<sub>3-x</sub>O<sub>4</sub>  
 μ μ Fe<sub>3</sub>O<sub>4</sub> (x = 0) Fe<sub>2</sub>O<sub>3</sub> (x = 1/3). μ  
 Fe μ  
 μ μ Fe<sup>3+</sup>. μ μ  
 ( μ ~ 37%), μ μ  
 μ (MF) μ μ *bulk*  
 μ μ μ  
 μ μ μ μ μ μ  
 μ μ μ



μ 2.2.3.1: μ Mössbauer μ Anthracene-SWCNTs-Fe-Argon

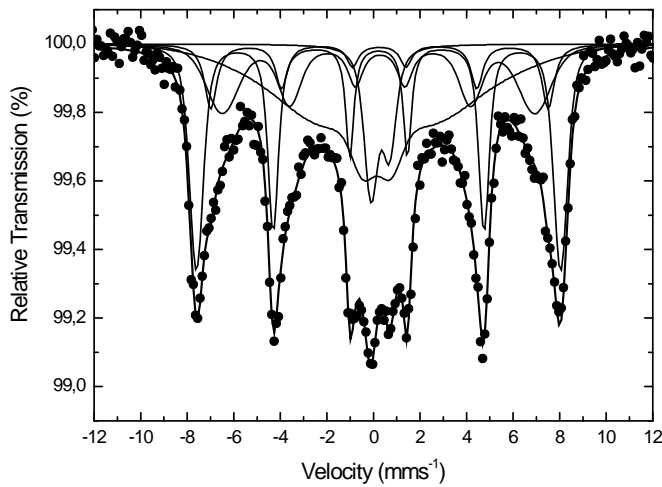
**2.2.3:**      μ      Mössbauer      μ

μ	T (K)	I.S. Fe (mm/s)	/2 (mm/s)	Q.S./2 (mm/s)	M.F. kG	Spread (kG or mm/s)	Area (%)
Anthracene-SWCNTs-Fe-Argon	300	0.33	0.15	-0.01	482	21	42
		0.22	0.32	0.65	0	0	37
		0.31	0.08	-0.11	366	71	21
Anthracene-SWCNTs-Fe-Air	300	0.38	0.14	-0.21	521	6	42
		0.34	0.13	-0.18	491	22	12
		0.38	0.35	-0.20	365	137	14
		0.33	0.35	0.70	0	0	32
Acids-SWCNTs-Fe-Air	300	0.35	0.25	0.77	0	0.17	100
	77	0.48	0.37	0.86	0	0.10	100
Acids-SWCNTs-Fe-Argon	300	0.37	0.24	0.90	0	0.25	70
		0.36	0.19	-0.19	501	22	15
		0.35	0.14	-0.23	334	108	15
	77	0.50	0.21	0.92	0	0.36	68
		0.47	0.27	0.00	526	14	21
Acids-WCNTs-Fe-Argon	300	0.45	0.14	-0.01	363	105	11
		0.33	0.20	-0.01	486	13	29
		0.36	0.30	0.01	450	4	9
		0.36	0.37	-0.07	417	32	19
		0.35	0.20	0.18	224	166	35
Acids-MSWCNTs-Fe-Oxygen	300	0.40	0.23	0.79	0	0.35	8
		0.39	0.14	-0.20	520	8	94
Acids-MSWCNTs-Fe-Air	300	0.41	0.32	0.79	0	0	6
		77	0.36	0.18	0.77	0	0.24
		0.49	0.20	0.84	0	0.42	100

I.S.: μ μ      μ μ      Fe μ μ  
/2: 1/2      μμ  
Q.S.: ( μ      ), 2 : μ ( μ )  
) )  
M.F.: μ  
Spread: μ (M.F. μ kG)  
Q.S. ( μ mm/s)  
Area: μ  
μ : ±0.01 mm/s      I.S., /2, Q.S. 2 , ±5 kG      M.F. ±5%      Area



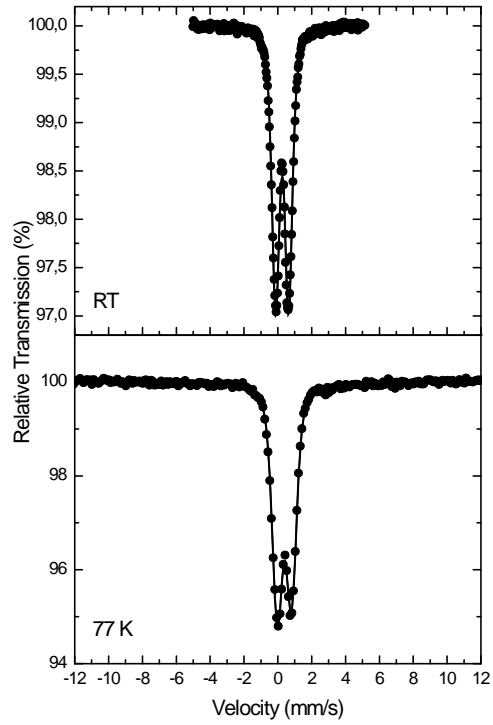
$Fe_2O_3$   
 μ μ μ μ μ μ  
 μ μ 8% μ μ  
 μ μ μ Anthracene-SWCNTs-Fe-Air  
 Anthracene-SWCNTs-Fe-Argon μ μ  
 μ μ μ μ μ μ



μ 2.2.3.3: μ Mössbauer μ Acids- WCNTs-Fe-Argon

μ Mössbauer μ Acids- WCNTs-Fe-Air  
 μ μ μ ( μ 2.2.3.4).  
 μ μ μ μ μ μ  
 μ μ μ μ μ μ  
 μ μ μ Mössbauer ( μ 2.2.3),  
 μ μ μ Acids-  
 WCNTs - $Fe_2O_3$  - $Fe_2O_3$ .  
 77 μ μ μ μ  
 μ μ μ  
 μ





μ 2.2.3.4: μ Mössbauer μ Acids- WCNTs-Fe-Air μ  
μ (RT) μ (77 ) μ

μ μ Acids- WCNTs-Fe-Oxygen ( μ 2.2.3.5)

μ μ , μ  
μ -Fe<sub>2</sub>O<sub>3</sub> μ μ

μμ

μ

μ

-

μ -Fe<sub>2</sub>O<sub>3</sub> μ *bulk*

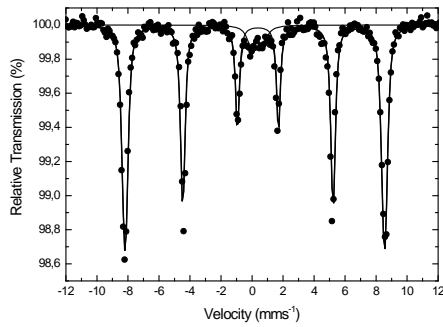
μ

,

μ

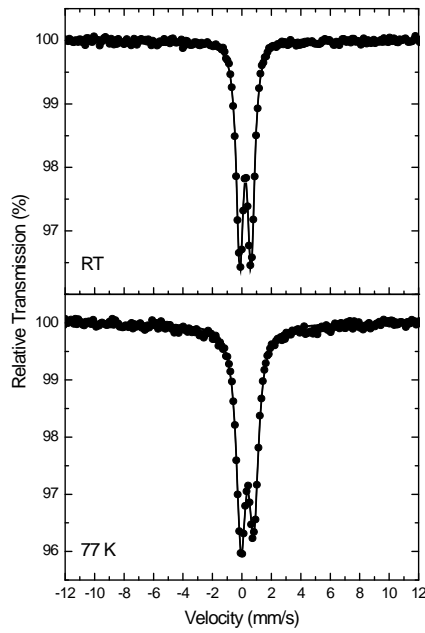
μ

.



μ 2.2.3.5: μ Mössbauer μ Acids- WCNTs-Fe-Oxygen

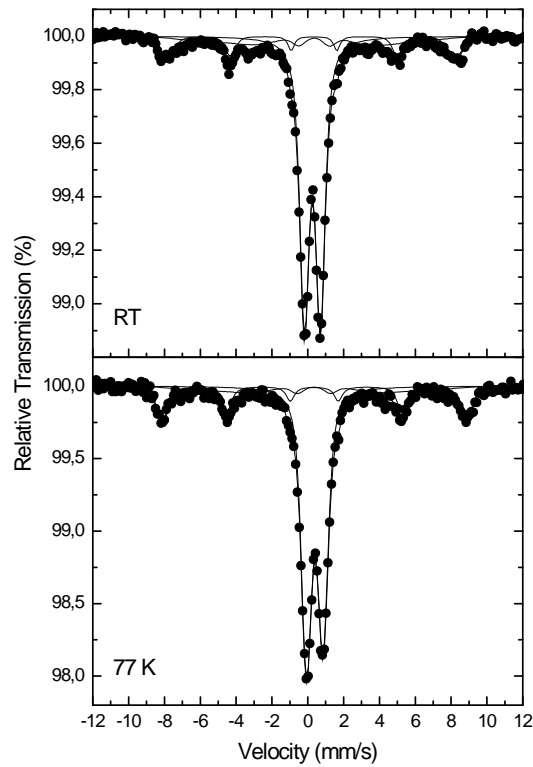
2.2.3.6 Mössbauer Acids-SWCNTs-Fe-Air  
 Acids-SWCNTs-Fe-Air, Mössbauer Acids-SWCNTs-Fe-Air



2.2.3.6: Mössbauer Acids-SWCNTs-Fe-Air (RT) (77 K)

2.2.3.7 Mössbauer Acids-SWCNTs-Fe-Argon  
 Acids-SWCNTs-Fe-Air, Mössbauer Acids-SWCNTs-Fe-Air  
 Acids-SWCNTs-Fe-Air, Mössbauer Acids-SWCNTs-Fe-Air

$\mu$  Mössbauer  $\mu$   $\mu$   $\mu$  Acids- WCNTs-Fe-  
 Argon  $\mu$  -Fe<sub>2</sub>O<sub>3</sub>  $\mu$   
 $\mu$   $\mu$   $\mu$   $\mu$   
 $\mu$  Mössbauer  $\mu$  -Fe<sub>2</sub>O<sub>3</sub>  $\mu$   $\mu$   
 20-30 nm.  $\mu$   
 $\mu$  -Fe<sub>2</sub>O<sub>3</sub>  $\mu$  ( 10 nm).



$\mu$  2.2.3.7:  $\mu$  Mössbauer  $\mu$  Acids-SWCNTs-Fe-Argon  $\mu$   
 $\mu$  (RT)  $\mu$  (77 )

2.2.4  $\mu$   $\mu$  -  $\mu$  - (SWCNTs) -  $\mu$  (MWCNTs)

$\mu$  -  $\mu$

$\mu$   $\mu$   $\mu$

( $-\text{Fe}_2\text{O}_3$ ,  $-\text{Fe}_2\text{O}_3$ )  $\mu$   $\mu$   $\mu$   $\mu$  .

$\mu$   $\mu$  .  $\mu$  ,

SWCNTs  $\mu$   $\mu$

, 2-  $\mu$  - ,  $\mu$  - .

$\mu$  , SWCNTs MWCNTs  $\mu$   $\mu$   $\mu$

$\mu$   $\mu$  .  $\mu$

$\mu$  ,

$\mu$   $\mu$   $\mu$  .

$\mu$   $\mu$   $\mu$  400 °C  $\mu$  (  $\mu$

MWCNTs  $\mu$

).  $\mu$   $\mu$   $\mu$

$\mu$   $\mu$   $\mu$   $\mu$  .

$\mu$  .

$\mu$   $\mu$   $\mu$  ,

$\mu$   $\mu$   $\mu$   $\mu$   $\mu$  .  $\mu$   $\mu$

$\mu$  ,  $\mu$

$\mu$   $\mu$   $\mu$   $\mu$   $\mu$

$\mu$   $\mu$   $\mu$

### 2.3

μ

μ

Sn-

-

μ

-Fe<sub>2</sub>O<sub>3</sub>

μ

μ

(CCVD)

μ

Sn

μ

<sup>197</sup> ( μ 2.3a).

Sn-

(Sn@CNTs)

μμ

CCVD ( μ 2.3b),

μ

μ

μ

μ

μ

μ

μ

μ

μ

(1- μ - )

μ

( μ 2.3c)<sup>251</sup>.

μ

-Fe<sub>2</sub>O<sub>3</sub>

μ

μ

μ

<sup>252</sup>,

μ

μ

Sn@CNTs.

μ

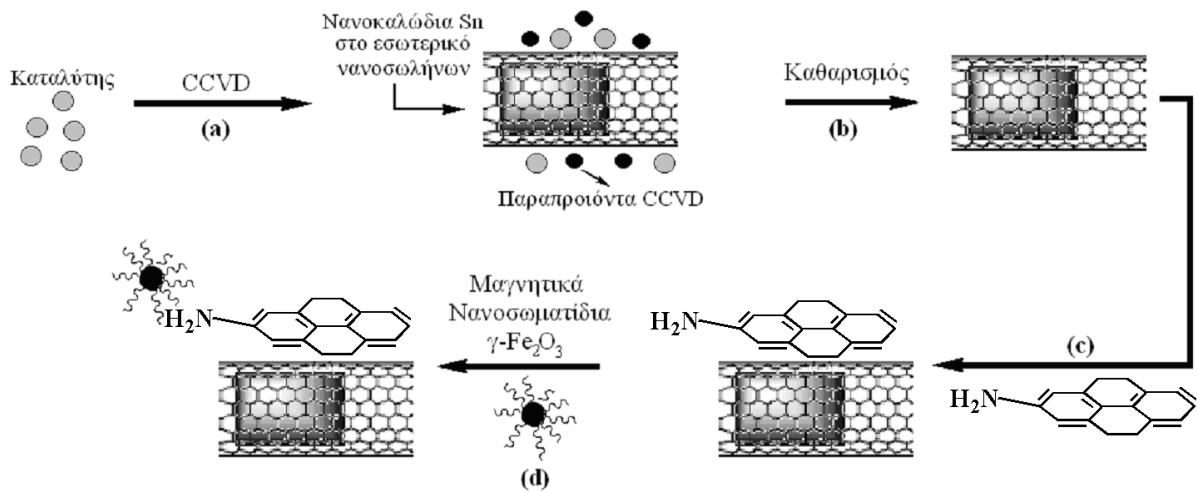
μ

μ

μ

μ

( μ 2.3d).



μ 2.3: μ

μ

Sn-

μ -Fe<sub>2</sub>O<sub>3</sub>

,

μ

μ

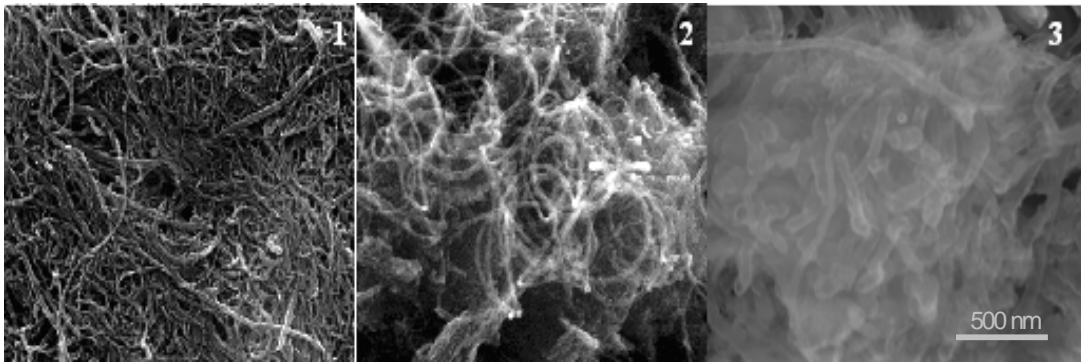
μ

μ

μ μ μ μ μ , Raman, Mössbauer  
 - μ (Scanning Tunneling spectroscopy),  
 - μ μ , - μ  
 (Scanning Tunneling Microscopy)

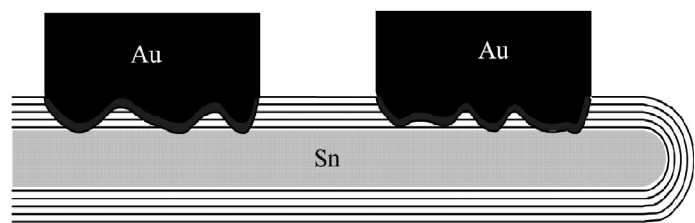
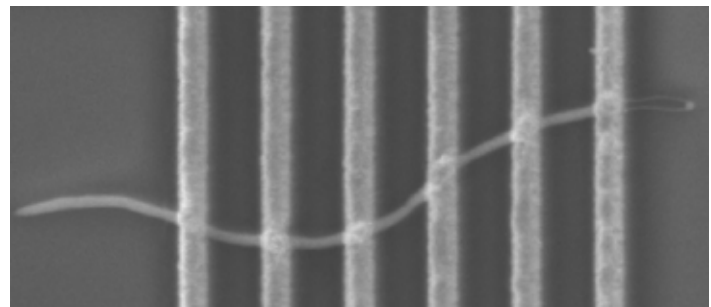
2.3.1

μ CCVD μ (SEM) Sn@CNTs  
 μ 2.3.1. μ  
 SEM ( « »)  
 μ μ μ CCVD.



μ 2.3.1: μ (1)  
 μ (2) Sn@CNTs (3).  
 μ ( μ 2.3.1.1  
 2.3.1.2) μ μ μ  
 μ μ μ Sn@CNTs  
 μ μ  
 μ  
 Sn  
 253 μ μ μ  
 μ μ μ  
 μ  
 μ CCVD. μ μ  
 μ μ μ 25%  
 , μ .

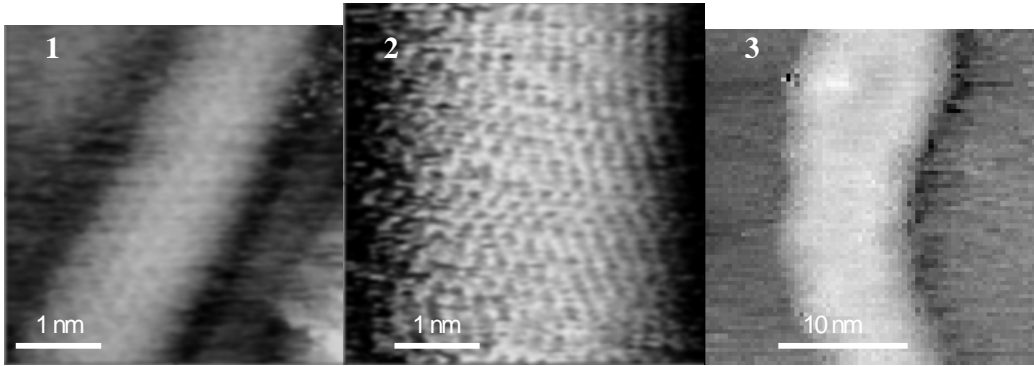
$\mu$  .  $\mu$   $\mu$   $\mu$   $\mu$   $\mu$   $\mu$   
 % ,  $\mu$  Sn@CNTs  
 : C (74 %), Sn (16 %) O (10 %),  $\mu$   
 (  $\mu$  Sn  
 ),  
 (SnO<sub>2</sub>)  $\mu$  . To  
 $\mu$   $\mu$  Sn  
 $\mu$   $\mu$  SnO<sub>2</sub> Sn - <sup>254</sup> Sn  
 $\mu$   $\mu$  (  $\mu$  )  
 $\mu$   $\mu$  )  
 (  $\mu$  2.3.2).  
 ~25nm)  $\mu$   $\mu$   $\mu$   $\mu$   $\mu$   
 bulk Sn  $\mu$   $\mu$   $\mu$   $\mu$  Sn<sup>255</sup> (  $\mu$  2.3.2).



$\mu$  2.3.2: SEM Sn@CNTs  $\mu$   
 $\mu$  Sn@CNTs ( )  $\mu$  Au  
 $\mu$   $\mu$  ( ).

### 2.3.2

STM),  
 ( μ 2.3.2.1  
 2.3.2.2). Sn@CNTs ( μ 2.3.2.3)  
 ( μ 12nm).  
 SEM μ<sup>254</sup>,  
 μ STM μ μ μ μ  
 μ  
 Sn@CNTs μ

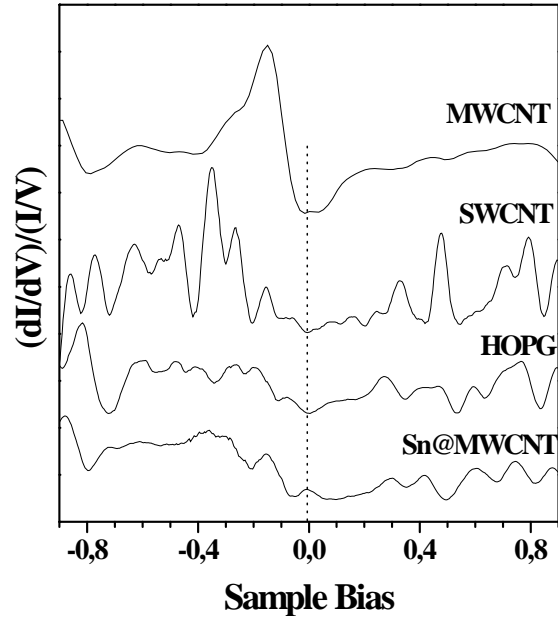


μ 2.3.2: STM μ (2) μ Sn@CNTs (1), (3).

### 2.3.3

μ 2.3.3 μ I-V μ 2.3.2.  
 μ μ μ μ  
 (Density of States μ DOS)  
 μ<sup>256</sup>.





**Figure 2.3.3:** A plot of differential conductance  $(dI/dV)/(dV)$  versus sample bias for (SWCNT), (MWCNT), (HOPG), and Sn@CNTs. The bias ranges from -0.8 V to 0.8 V. The Fermi level is indicated by a vertical dashed line at 0.0 V. The conductance curves show characteristic features for each material, with a sharp peak at 0.0 V for SWCNT and a broader peak for HOPG. The Sn@MWCNT curve shows a peak at approximately -0.1 V, indicating the presence of Sn on the MWCNT surface.

**2.3.4 Mössbauer**

Mössbauer spectroscopy was used to study the iron (Fe) content of the samples. The Mössbauer spectra show a characteristic doublet for Fe<sub>2</sub>O<sub>3</sub>, indicating the presence of iron in the samples.

Fe<sub>2</sub>O<sub>3</sub>.

(a)

-Fe<sub>2</sub>O<sub>3</sub>

Fe<sub>2</sub>O<sub>3</sub>,

(b)

μ

μ

μ

μ

Mössbauer

μ

μ

μ

μ

μ

μ

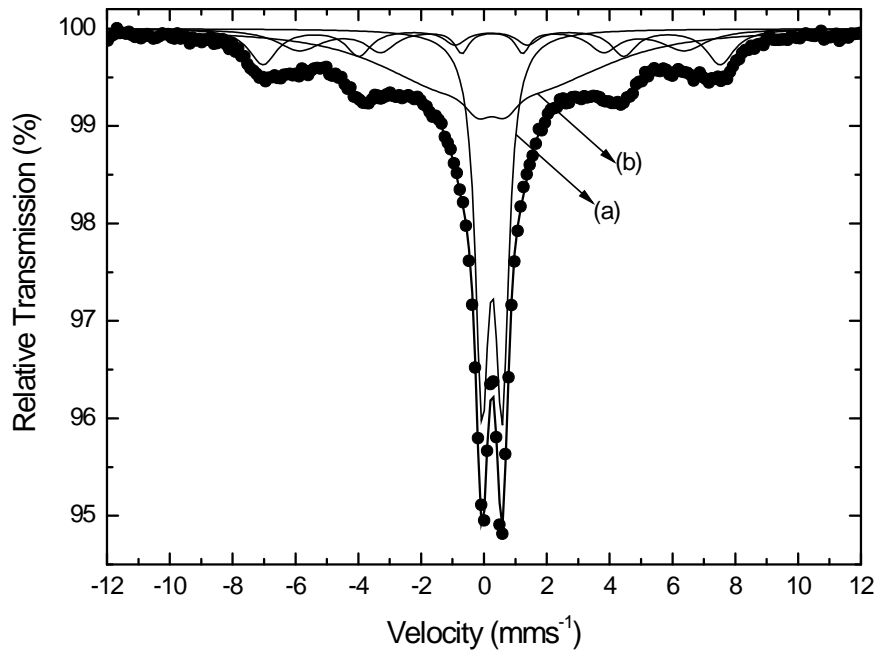
μ

μ

μ

~15 nm. H

( 2.3.5).



2.3.4: Mössbauer -Fe<sub>2</sub>O<sub>3</sub>

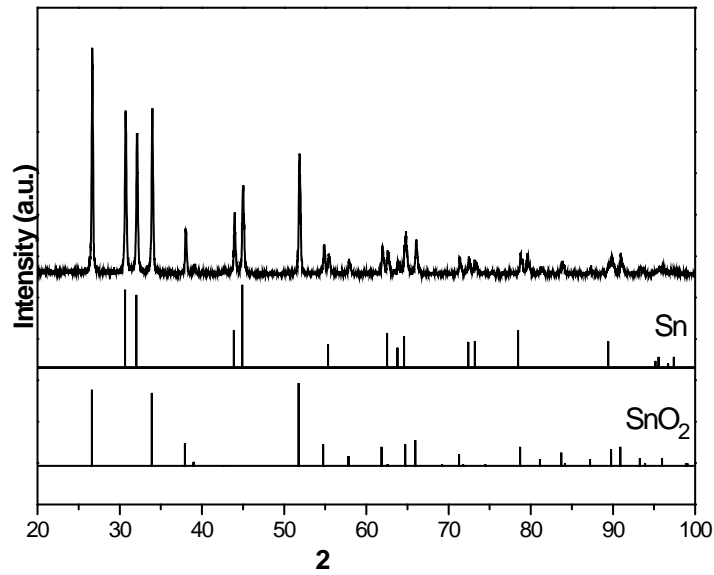
### 2.3.5

μμ

Sn@CNTs

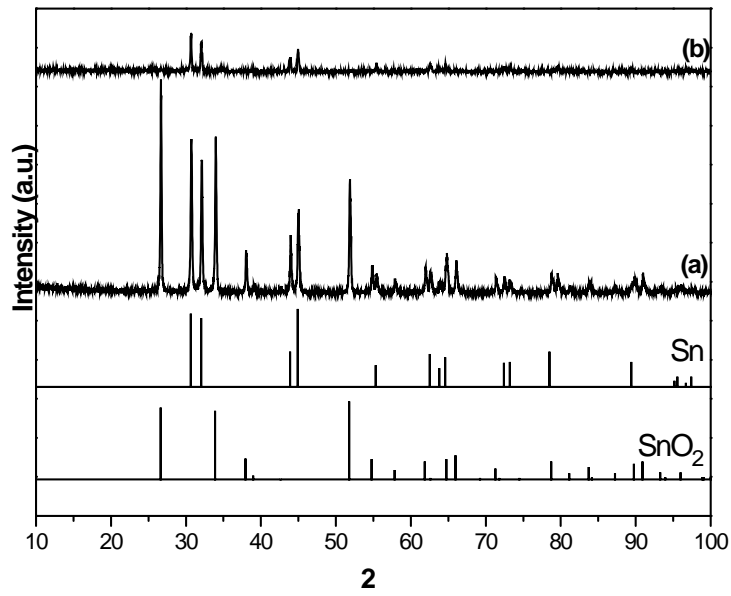
CCVD

μ 2.3.5.1.



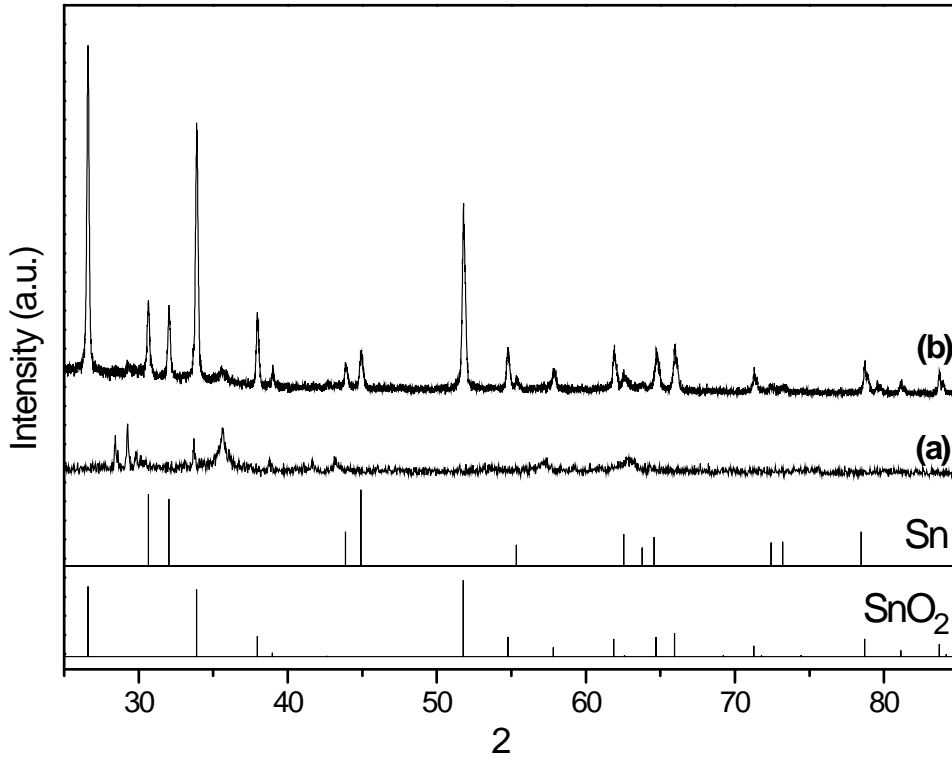
μ 2.3.5.1: μμ - Sn@CNTs μ CCVD (SnO<sub>2</sub>:  
JCPD # 41-1445, Sn: JCPD # 04-0673)

μμ Sn@CNTs ( μ 2.3.5.1)  
μ Sn  
~30 , ~32 , ~43 ~45 .  
μμ (SnO<sub>2</sub>) μ .  
μ Sn μ μ μ μ μ μ<sup>254</sup>  
STM SEM μ μ μ SnO<sub>2</sub> CCVD  
μ μ μ Sn  
Sn@CNTs μ CCVD,  
Sn, μ  
SnO<sub>2</sub> ~26 , ~34 ~51 ( CCVD.  
) μ μ μ  
SEM μ μ μ .  
μ 2.3.5.2 μμ -  
Sn@CNTs μ μ μ  
μ SnO<sub>2</sub> CCVD.



**Figure 2.3.5.2:** XRD patterns of Sn@CNTs (a) and SnO<sub>2</sub> (b). (SnO<sub>2</sub>: JCPD # 41-1445, Sn: JCPD # 04-0673)

Figure 2.3.5.2d shows the XRD patterns of Sn@CNTs (a) and SnO<sub>2</sub> (b). The patterns are compared with the reference patterns for Sn (JCPD # 04-0673) and SnO<sub>2</sub> (JCPD # 41-1445). The Sn@CNTs pattern shows a broad peak at approximately 20° 2θ, which is characteristic of the amorphous carbon nanotubes. The SnO<sub>2</sub> pattern shows sharp peaks at approximately 28°, 32°, 35°, 45°, and 52° 2θ, which are characteristic of the SnO<sub>2</sub> phase. The inset shows the XRD pattern of Sn@CNTs-μ, which shows a broad peak at approximately 20° 2θ, indicating the presence of amorphous carbon nanotubes.



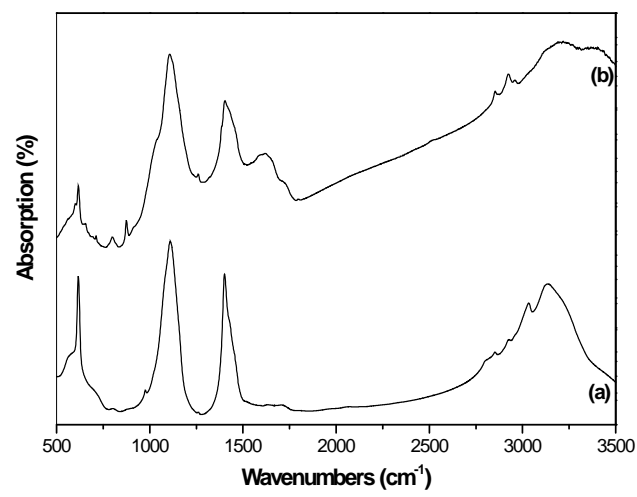
$\mu$  2.3.5.3:  $\mu\mu$  -  $\mu$   $\mu$  (a)  
 Sn@CNTs- $\mu$   $\mu$  (b). (SnO<sub>2</sub>: JCPD # 41-1445, Sn: JCPD # 04-0673)

$\mu\mu$   $\mu$   $\mu$   $\mu$  (  $\mu$  2.3.5.3a),  
 220, 311, 222, 400, 511 440  
 ~30 , ~36 , ~38 , ~42 , ~57 ~63 <sup>258</sup>.

$\mu$   $\mu$   $\mu$  Fe<sub>3</sub>O<sub>4</sub> -  
 Fe<sub>2</sub>O<sub>3</sub>.  $\mu$   $\mu$   $\mu$  Mössbauer  
 $\mu$  ( 2.3.4)  $\mu$   
 $\mu$   $\mu$   $\mu$   $\mu$   $\mu$   $\mu$   $\mu$   
 $\mu$   $\mu$   $\mu$   $\mu$  (311) ,  
 ~36  $\mu$  Scherrer<sup>232</sup>.  $\mu$   
 $\mu$   $\mu$   $\mu$  21 nm.  $\mu\mu$   
 Sn@CNTs- $\mu$   $\mu$  (  $\mu$  2.3.5.3b)  
 $\mu$  Sn  
 ~30 , ~32 , ~43 , ~45 , ~55 ~78 .  
 $\mu$  SnO<sub>2</sub> ~26 , ~33 ,  
 ~38 , ~39 , ~51 ~55 ,

Sn@CNTs  
 SnO<sub>2</sub>  
 Sn@CNTs-μ  
 (311)  
 2 ~36 μμ  
 Sn SnO<sub>2</sub>  
 2 μ μ

2.3.6 μ -  
 μ μ μ μ Sn@CNTs-  
 μ μ μ μ  
 ( μ 2.3.6b).



μ 2.3.6: μ μ μ μ (a)  
 Sn@CNTs-μ μ (b).

μ 2.3.6a μ μ  
 μ -Fe<sub>2</sub>O<sub>3</sub>.  
 610 cm<sup>-1</sup>  
 μ μ Fe μ Fe<sub>2</sub>O<sub>3</sub><sup>252</sup>.  
 ~1400 cm<sup>-1</sup>  
 μ μ -COO<sup>-</sup> μ  
 μ -Fe<sub>2</sub>O<sub>3</sub>

3015 cm<sup>-1</sup>  
 2920 cm<sup>-1</sup> μ C=CH<sup>260</sup>.  
 2850 cm<sup>-1</sup> μ -CH<sub>2</sub> -CH<sub>3</sub><sup>252</sup>.  
 1100 cm<sup>-1</sup> μ μ μ<sup>261</sup> μ μ μ  
 μ μ μ μ μ μ μ μ  
 Sn@CNTs-μ μ ,  
 μ μ μ μ .

### 2.3.7 μ μ

μ μ μ -Fe<sub>2</sub>O<sub>3</sub> μ  
 μ μ μ  
 Sn. μ μ  
 μ Sn, μ -Fe<sub>2</sub>O<sub>3</sub>  
 μ μ μ μ μ  
 μ μ μ Sn  
 μ μ μ μ μ  
 μ ( ε) μ *bulk* Sn .  
 μ μ μ μ -Fe<sub>2</sub>O<sub>3</sub> μ  
 μ μ μ μ μ μ  
 μ μ μ μ μ μ μ μ  
 μ μ μ μ μ μ μ μ  
 μ μ .

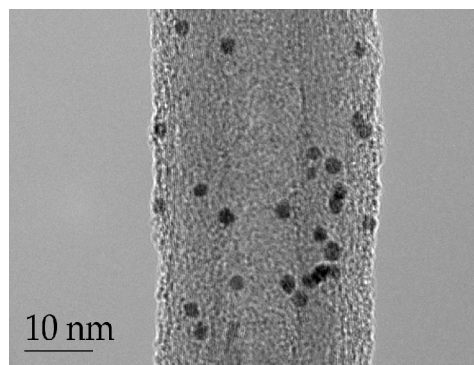
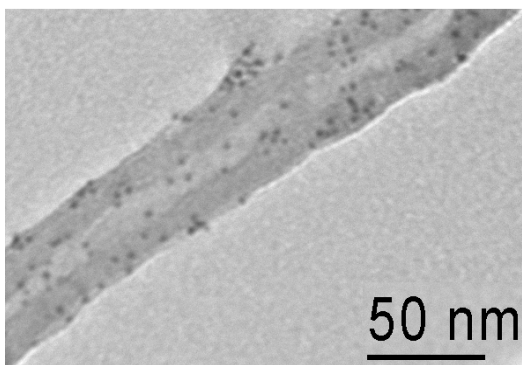




RuPt (MWCNTs-RuPt) Raman,

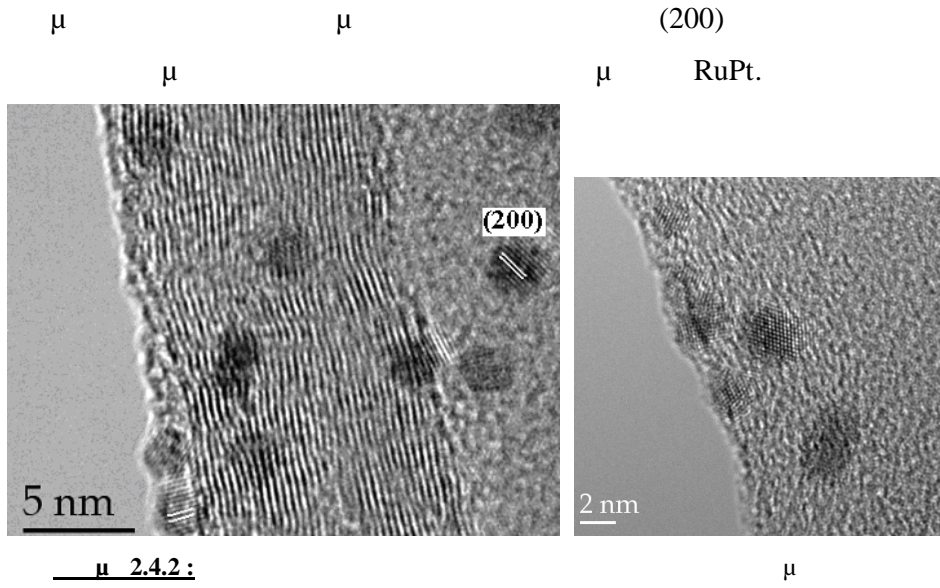
2.4.1

(T.E.M.)  
 MWCNTs-RuPt  
 RuPt MWCNTs. T.E.M.  
 ( 2.4.1)  
 RuPt MWCNTs  
 ~35 nm  
 RuPt MWCNTs.  
 nm.



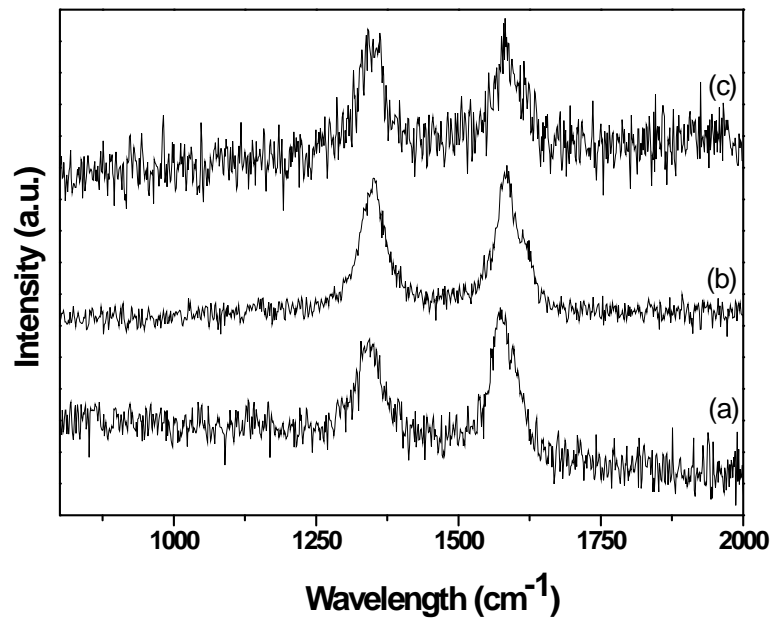
μ 2.4.1 :

( μ 2.4.2), μ μ RuPt μ  
 μ ~2.3 nm.



2.4.2 μ Raman

μ Raman MWCNTs, μ μ  
MWCNTs MWCNTs-RuPt  
μ 2.4.2. μ  
MWCNTs<sup>195, 233</sup>.



μ 2.4.2: μ Raman MWCNTs (a), μ μ μ  
μ -μ MWCNTs (b) MWCNTs-RuPt (c)

$1580\text{ cm}^{-1}$  (G-Band)  
 $E_{2g}$   $sp^2$   
 $1342\text{ cm}^{-1}$  (D band)  
 $sp^3$   
 $198, 234, 235$   
 D G  
 $(I_D/I_G)$   
 MWCNTs  $0.71$   
 MWCNTs  $0.95$   
 $237$   
 $sp^3$   
 D  
 MWCNTs-FePt  
 $I_D/I_G$   
 $0.98$   
 $I_D/I_G$

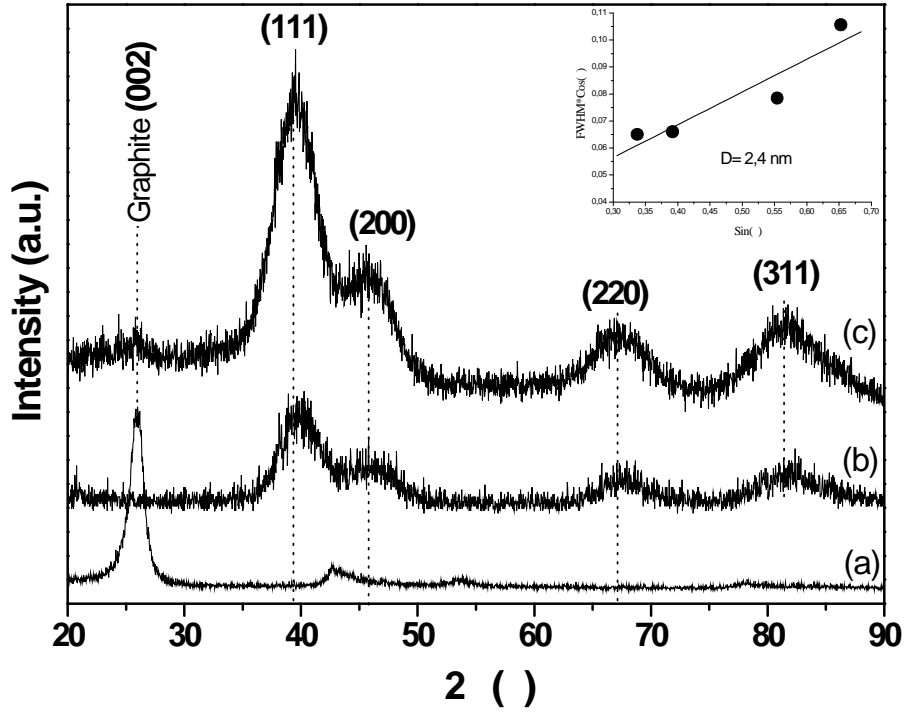
### 2.4.3

(XRD).  
 NPs RuPt  
 MWCNTs-RuPt  $2.4.3$   
 XRD  
 RuPt (111), (200), (220) (311)  $\sim$   
 $39, 45, 67$   $81$   
 $\mu\mu$  XRD  $\mu$  RuPt

MWCNTs (002)  $\mu$   $\mu$   $\mu$

2 26 ,  $\mu\mu$   $\mu$   $\mu\mu$

MWCNTs/NPs (1:10)



$\mu$  2.4.3:  $\mu\mu$   $\mu$   $\mu$   $\mu$   $\mu$   $\mu$

(a),  $\mu$  RuPt (b)

WCNTs-RuPt (c)

(101) MWCNTs,  $\mu$  (100)

$\mu$   $\mu$   $\mu\mu$

$\mu$  -  $\sim 42$   $\sim 43$   $\mu\mu$

(111) (200) RuPt  $\mu$  2  $\mu$  RuPt

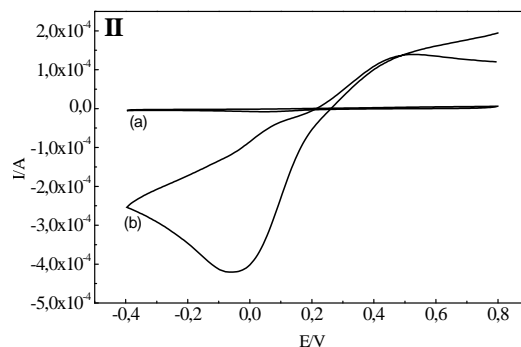
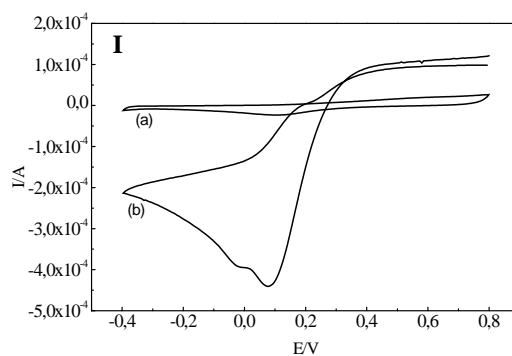
$\mu$   $\mu$   $\mu$   $\mu$   $\mu$  Scherrer<sup>232</sup>

(  $\mu$  2.4.3. - ).  $\mu$  2.4 nm.  $\mu$   $\mu$

(2.3 nm)

## 2.4.4

MWCNTs-RuPt NPs RuPt  
 2, 2,  $\mu$   $\mu$   
 $\mu$   $\mu$   $\mu$   $\mu$   $\mu$  pH 7.0,  
 20 mM  $H_2O_2$ .  
 $\mu$   $\mu$  [ NPs  
 RuPt (  $\mu$  2.4.4 ) MWCNTs-RuPt (  $\mu$  2.4.4 )  $\mu$   $\mu$   
 F  $\mu$  (6:4 v/v).  $\mu$   $\mu$   $\mu$   
 $\mu$  0.42 mA.  
 $\mu$   $\mu$   $H_2O_2$   $\mu$   $\mu$   
 0 V  $\mu$   $\mu$



**2.4.4:**  $\mu$  (a)  $H_2O_2$  (b) ( )  $\mu$  ( ) MWCNTs-RuPt  $\mu$  RuPt  $\mu$  (a)  $H_2O_2$  (b)

## 2.4.5

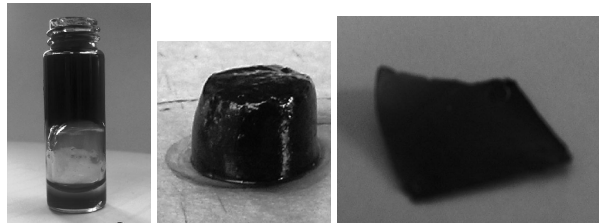
$\mu$   $\mu$  -  
 $\mu$   $\mu$   $\mu$   $\mu$   $\mu$   $\mu$   $\mu$   $\mu$   
 $\mu$  RuPt.  $\mu$   $\mu$   
 $\mu$  RuPt  $\mu$   $\mu$   
 $\mu$   $\mu$  .  
 $\mu$   $\mu$   $\mu$   $\mu$   $\mu$   $\mu$   
RuPt  $\mu$   $\mu$   $\sim 2.3$  nm  
 $\mu$   $\mu$  XRD  
RuPt . Raman,  $\mu$   
 $\mu$   $\mu$  ,  $\mu$   
 $\mu$   $\mu$   
 $\mu$   $\mu$   $\mu$  NPs RuPt  
 $\mu$   $\mu$  .







( $\mu$  2.5c). T  $\mu$  ,  
 $\mu$  -  $\mu$   
 $\mu$   $\mu$   $\mu$   $\mu$   
 ( . .  $\mu$  ,  $\mu$  . .).  $\mu$   
 -  $\mu$  ,  $\mu$   $\mu$   
 (film) Laponite-MWCNTs  $\mu$  ( $\mu$  2.5c). ,  
 $\mu$   
 $\mu$  ,  $\mu$  -  $\mu$   $\mu$   $\mu$   
 $\mu$  .  $\mu$   $\mu$   $\mu$   $\mu$   $\mu$   
 $\mu$   $\mu$   $\mu$  ,  
 $\mu$   $\mu$   $\mu$  .

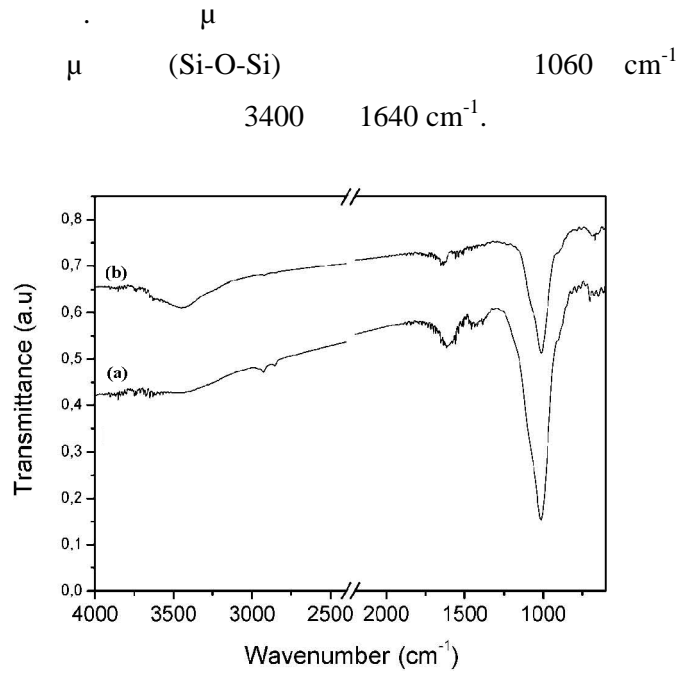


$\mu$  2.5c:  $\mu$  ( ,  $\mu$  )  $\mu$  ( ) Laponite-MWCNTs

### 2.5.2 $\mu$ $\mu$

$\mu$   $\mu$   
 $\mu$   $\mu$  (Laponite-MWCNTs)  $\mu$   
 $\mu$   $\mu$   $\mu$   $\mu$   $\mu$   $\mu$   
 (Laponite-Pristine MWCNTs)  $\mu$  2.5.2.  
 $\mu$   $\mu$   $\mu$   
 $\mu$   $\mu$   $\mu$   $\mu$   
 $\mu$  . ,  $\mu$   $\mu$   
 Laponite-MWCNTs  $\mu$  1063  $\text{cm}^{-1}$   
 $\mu$  Si-O Si-O-Si  $\mu$   
 C-H 2920  
 2850  $\text{cm}^{-1}$  C=C  $\mu$  1400  
 1600  $\text{cm}^{-1}$ . C-H C=C  $\mu$   $\mu$   
 $\mu$   $\mu$   $\mu$   
 $\mu$   $\mu$   $\mu$

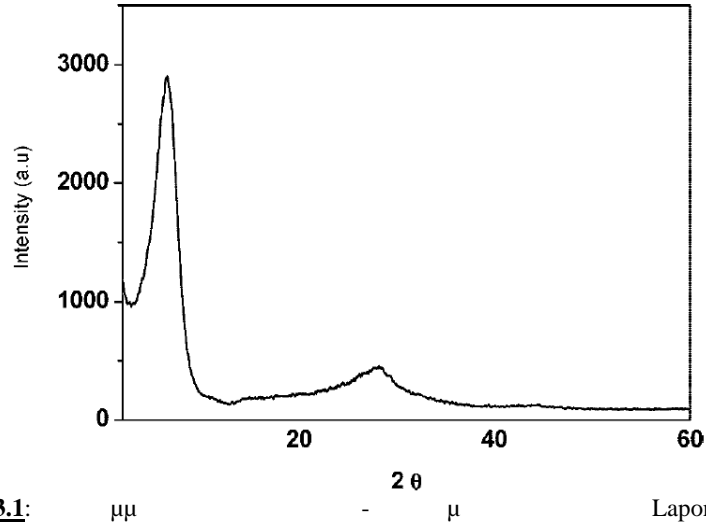
Laponite-Pristine MWCNTs



**2.5.2:** FTIR spectra of Laponite-MWCNTs (a) and Laponite-Pristine MWCNTs (b). The spectra show characteristic absorption bands for both samples, with the 1060 cm<sup>-1</sup> band being particularly prominent in the Laponite-MWCNTs sample.

### 2.5.3

Figure 2.5.3.1 shows the XRD patterns of Laponite-MWCNTs (a) and Laponite-Pristine MWCNTs (b). The patterns exhibit a broad peak at approximately 2θ = 10°, corresponding to the (001) plane of the Laponite clay. The d<sub>001</sub> spacing is calculated to be approximately 13.2 Å for the Laponite-MWCNTs sample and approximately 9.6 Å for the Laponite-Pristine MWCNTs sample. The difference in d<sub>001</sub> spacing is attributed to the presence of MWCNTs between the Laponite layers, which increases the interlayer distance. The intensity of the (001) peak is significantly higher in the Laponite-MWCNTs sample, indicating a higher degree of layer stacking and exfoliation.



μ 2.5.3.1:

μμ

Laponite-MWCNTs

μ

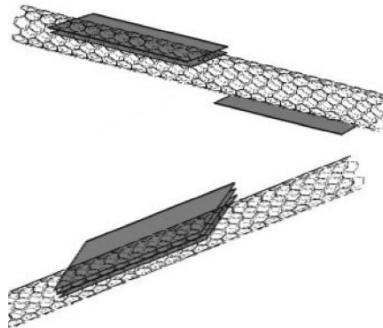
μ

μ

μ

Laponite-MWCNTs

μ 2.5.3.2.



μ 2.5.3.2:

μ

μ

μ

μ

μ

## 2.4.4 $\mu$ $\mu$ -

$\mu$   $\mu$   $\mu$   $\mu$   $\mu$   $\mu$  ,  
 $\mu$  ,  $\mu$   $\mu$   $\mu$   $\mu$   
 .  $\mu$   $\mu$   $\mu$   $\mu$  ,  
 $\mu$   $\mu$   $\mu$  /  $\mu$   $\mu$  -  
 $\mu$   $\mu$   $\mu$   $\mu$  .  
 $\mu$   $\mu$   $\mu$   $\mu$   
( . .  $\mu$  ) .  $\mu$   $\mu$   $\mu$   
 ,  
 $\mu$   $\mu$   $\mu$   $\mu$   $\mu$   
 $\mu$  (  $\mu$  . . )  $\mu$   $\mu$   $\mu$   
 .  $\mu$   
 $\mu$   $\mu$   $\mu$  ,  
 $\mu$   $\mu$   $\mu$  ,  
 ,  $\mu$   $\mu$   $\mu$   
 $\mu$  -  $\mu$   $\mu$   $\mu$   
 $\mu$   $\mu$   $\mu$  Coulomb

(segregative Coulombic repulsions)<sup>266, 267</sup>.

## 2.6

μ - μ -Fe<sub>2</sub>O<sub>3</sub>

-Fe<sub>2</sub>O<sub>3</sub>.

μ (CCVD)

μ ( μ μ μ ) μ

,  
<sup>236, 268</sup> ( μ 2.6.1a).

μ (Clay-CNTs) μ CCVD,

CCVD μ μ

μ 350 C, μ μ

μ μ μ <sup>228</sup>. , μ μ

μ μ μ μ μ μ μ μ

μ μ - - μ μ

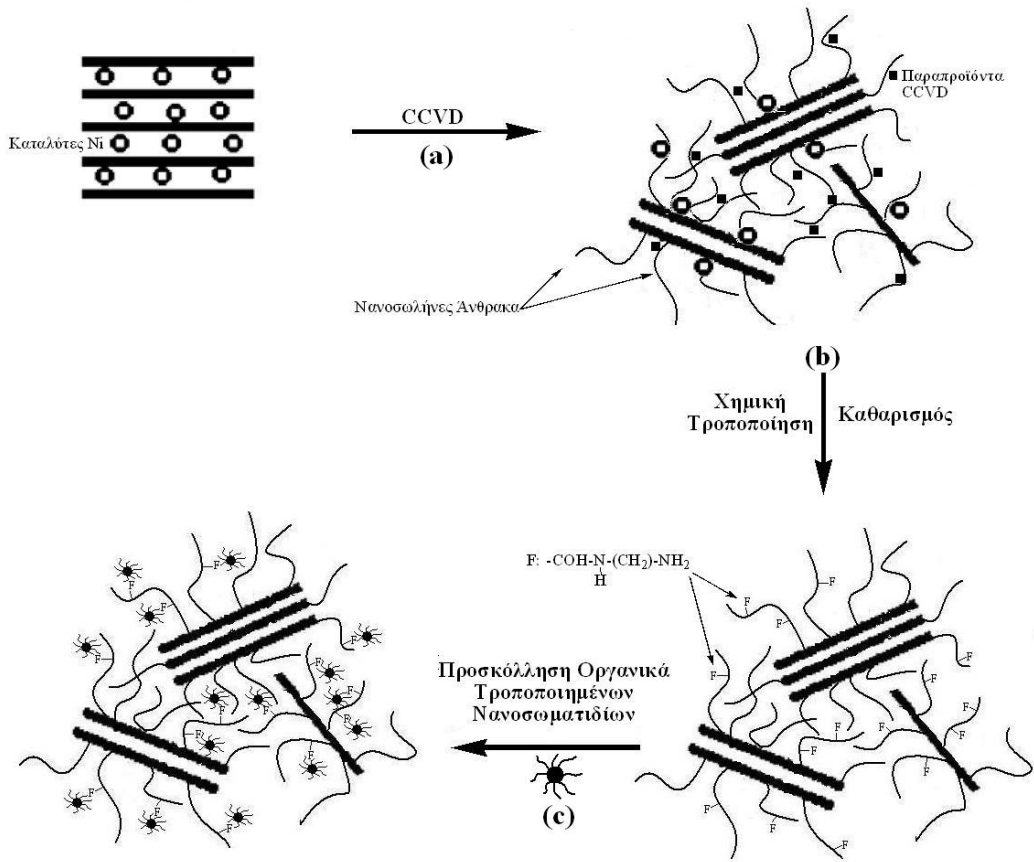
, μ μ

μ μ μ μ <sup>269, 270</sup> ( μ 2.6.1b). μ

μ -Fe<sub>2</sub>O<sub>3</sub> μ μ μ <sup>252</sup>.

-Fe<sub>2</sub>O<sub>3</sub> μ μ μ μ

μ ( μ 2.6.1c).



**μ 2.6.1:** μ

- μ -Fe<sub>2</sub>O<sub>3</sub>.

- μ -Fe<sub>2</sub>O<sub>3</sub>

μ

μ μ μ μ μ μ

, Raman, Mössbauer μ

**2.6.1**

H μ

μ μ μ μ μ μ (XRD).

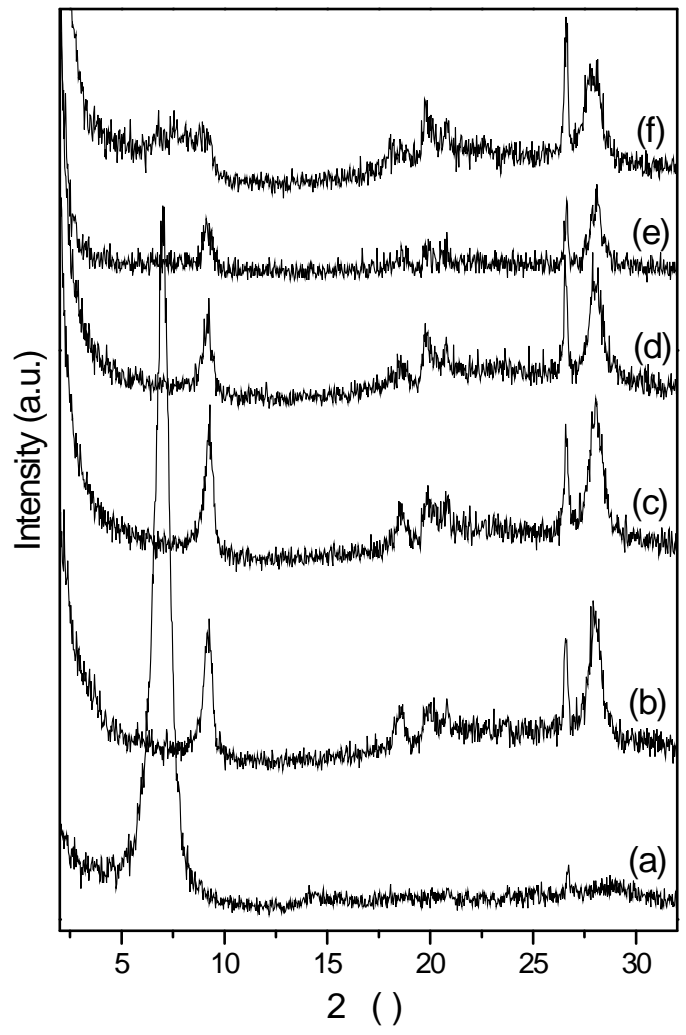
μ

Clay-CNTs μ μ μ μ μ μ

μμ XRD μ μ μ μ

i, μ Clay-CNTs μ CCVD, μ μ

2.6.1.1.



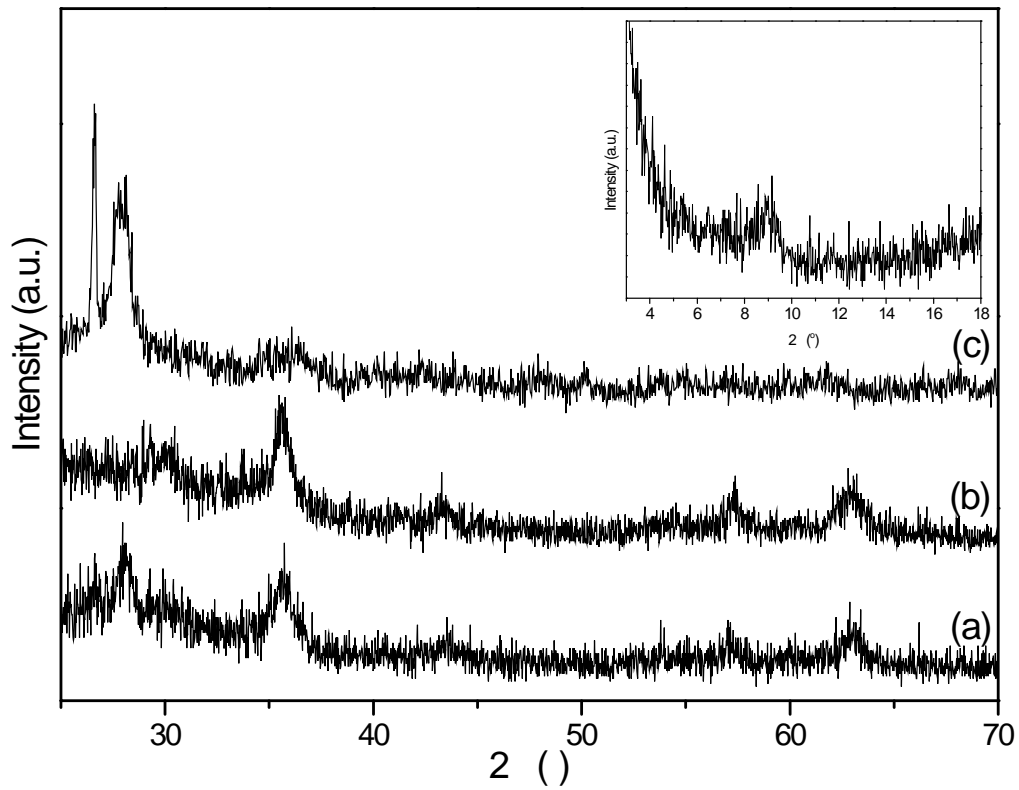
μ 2.6.1.1: μ μ Clay-CNTs μ - μ μ μ μ i  
 (a), μ μ μ (d), μ μ S Cl<sub>2</sub> (e) μ μ μ μ  
 μ μ μ (f) μ μ μ μ

(001) μ μ μ μ  
 μ μ Ni ( μ 2.6.1.1a) μ 2 7 ,  
 μ = 12.8-9.6 = 3.2Å μ 9.6  
 . μ μ μ μ μ  
 0.3Å μ μ μ μ  
 (2.9Å) μ μ





$\mu$   $-\text{Fe}_2\text{O}_3$   $\mu$   $\mu$   $\mu$   $-\text{Fe}_2\text{O}_3$   
 $\mu$   $\mu$  Scherrer<sup>232</sup>  $\mu$   
 $\sim 11$  nm.  
 H  $\mu$   $-\text{Fe}_2\text{O}_3$   
 $\mu\mu$  XRD,  $\mu\mu$  XRD  
 ( $\mu$  2.6.1.3a),  
 2 28  
 $\mu$   $\mu$   $\mu$   $\mu$   $\mu$  Clay-CNTs ( $\mu$   
 2.6.1.3c).  $\mu\mu$   
 $\mu$  311, 400, 511  
 440  $\sim 36$ ,  $\sim 43$ ,  $\sim 57$   $\sim 63$   
 $\mu\mu$   
 $\mu$  ( $\mu$  2.6.1.3b).



$\mu$  2.6.1.3:  $\mu\mu$   $\mu$   $\mu$   $\mu$   $\mu$  Clay-CNTs-  
 $\text{Fe}_2\text{O}_3$  (a)  $\mu$   $\mu$   $\mu$   $\mu$   $\mu$   $-\text{Fe}_2\text{O}_3$  (b)  
 Clay-CNTs  $\mu$   $\mu$   $\mu$   $\mu$   $\mu$   $\mu$  (c)  
 $\mu\mu$   $\mu$  2.6.1.3  $\mu$  RD,  
 $\mu$  001

8.9

d-

$\mu$  9.6Å.

$\mu$

$\mu$

$\mu$

$\mu$

$\mu$

$\mu$

## 2.6.2 $\mu$ Raman

$\mu$  Raman

Clay-CNTs  $\mu$

CCVD,  $\mu$

$\mu$   $\mu$

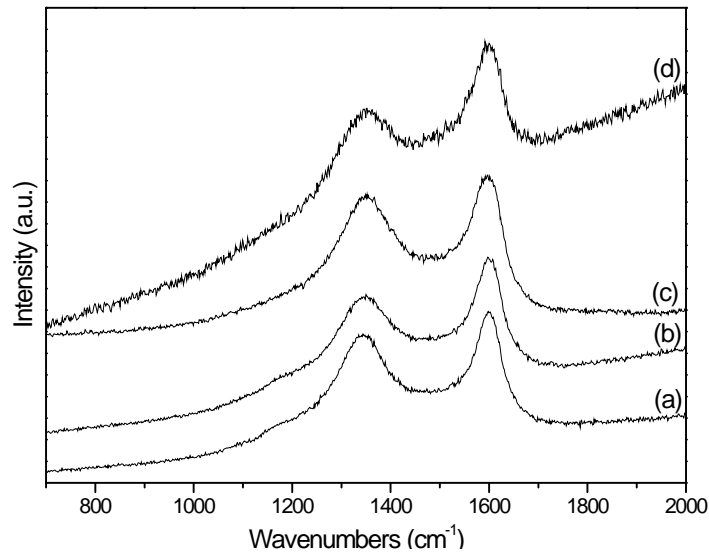
$\mu$

$\mu$  2.6.2.1.

$\mu$

$\mu$

195, 233



$\mu$  2.6.2.1:  $\mu$  Raman  $\mu$  Clay-CNTs  $\mu$  CCVD (a),  $\mu$

$\mu$  (b),  $\mu$

$\mu$   $\mu$   $\mu$

$\mu$   $\mu$  (c)

$\mu$   $\mu$   $\mu$

$\mu$

$\mu$   $\mu$  (d)

$\mu$  1580  $\text{cm}^{-1}$  (G-Band)

$E_{2g}$

$\text{sp}^2$

$\mu$

$\mu$

$\mu$

1342  $\text{cm}^{-1}$  (D band)

$\mu$   $\mu$   $\text{sp}^3$

$\mu$

$\mu$

$\mu$

$\text{sp}^2$

$\mu$

$\mu$

234-236

$\mu$

194-196

D

G

$(I_D/I_G)$ ,

$\mu$

$\mu$

197

$\mu$

$I_D/I_G$

Clay-CNTs

$\mu$

CCVD

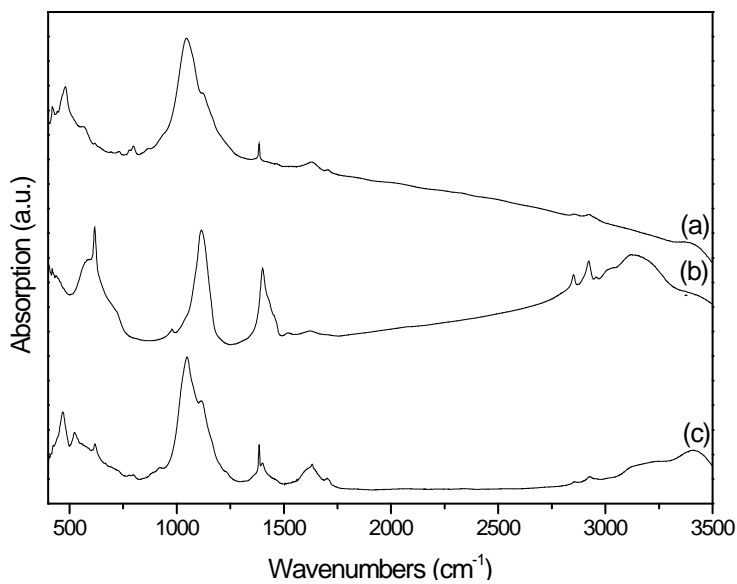
$\mu$

$\mu$



**2.6.3**

Clay-CNTs  
 (2.6.3a),  
 478 1049 cm<sup>-1</sup> Si-O Si-O-Si  
 -H C-H 1400 cm<sup>-1</sup> 2900  
 cm<sup>-1</sup>  
 Fe<sub>2</sub>O<sub>3</sub> (2.6.3b)  
 615 cm<sup>-1</sup> Fe<sub>2</sub>O<sub>3</sub><sup>252</sup>.  
 ~1400 cm<sup>-1</sup>  
 -COO<sup>-</sup> Fe<sub>2</sub>O<sub>3</sub><sup>259</sup>.  
 2850 cm<sup>-1</sup> 2920 cm<sup>-1</sup>  
 -CH<sub>2</sub> -CH<sub>3</sub><sup>252</sup>  
 1100 cm<sup>-1</sup>  
 261



**2.6.3:** (a) Clay-CNTs (b) Clay-CNTs-Fe<sub>2</sub>O<sub>3</sub> (c) Clay-CNTs-Fe<sub>2</sub>O<sub>3</sub>

Clay-CNTs-Fe<sub>2</sub>O<sub>3</sub> (2.6.3c),

Clays-CNTs  
Fe<sub>2</sub>O<sub>3</sub> - 615 cm<sup>-1</sup>,

### 2.6.4

2.6.4a  
-Fe<sub>2</sub>O<sub>3</sub>.

TG

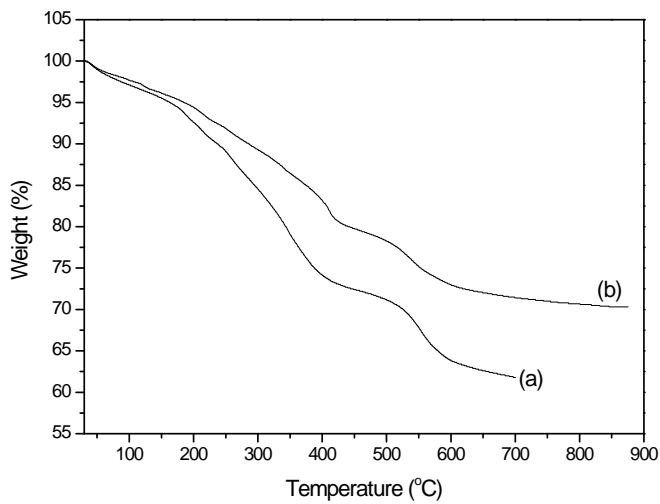
TGA  
258,

40%.

Clay-CNTs-Fe<sub>2</sub>O<sub>3</sub> (2.6.4b)

216.

Clay-CNTs-Fe<sub>2</sub>O<sub>3</sub> 30%.



2.6.4: TGA -Fe<sub>2</sub>O<sub>3</sub> (a) Clay-CNTs-Fe<sub>2</sub>O<sub>3</sub> (b)

2.6.5  $\mu$   $\mu$  -

-  $\mu$   $\mu$

$\mu$   $\mu$   $\mu$

-Fe<sub>2</sub>O<sub>3</sub>.  $\mu$   $\mu$   $\mu$

$\mu$   $\mu$  (CCVD)  $\mu$

$\mu$  (  $\mu$   $\mu$   $\mu$  )  $\mu$

,  $\mu$   $\mu$

. -  $\mu$  (Clay-CNTs)

$\mu$  CCVD, CCVD

$\mu$   $\mu$   $\mu$  350 C,

$\mu$   $\mu$   $\mu$

$\mu$   $\mu$   $\mu$   $\mu$

$\mu$   $\mu$   $\mu$   $\mu$   $\mu$   $\mu$

$\mu$   $\mu$   $\mu$   $\mu$   $\mu$   $\mu$

$\mu$   $\mu$   $\mu$   $\mu$   $\mu$   $\mu$

$\mu$   $\mu$   $\mu$  -Fe<sub>2</sub>O<sub>3</sub>  $\mu$

$\mu$   $\mu$   $\mu$  -  $\mu$   $\mu$

$\mu$   $\mu$   $\mu$   $\mu$   $\mu$

Mössbauer  $\mu$   $\mu$   $\mu$

$\mu$  -  $\mu$   $\mu$  (  $\mu$   $\mu$  )

$\mu$  )  $\mu$   $\mu$

.  $\mu$  ,  $\mu$

-  $\mu$   $\mu$   $\mu$   $\mu$

$\mu$   $\mu$   $\mu$  /

$\mu$   $\mu$   $\mu$  ,

$\mu$   $\mu$   $\mu$   $\mu$

$\mu$   $\mu$  ,

$\mu$  .







Figure 3.1.2: Pressure vs. Volume for CNTs and Sn@CNTs.

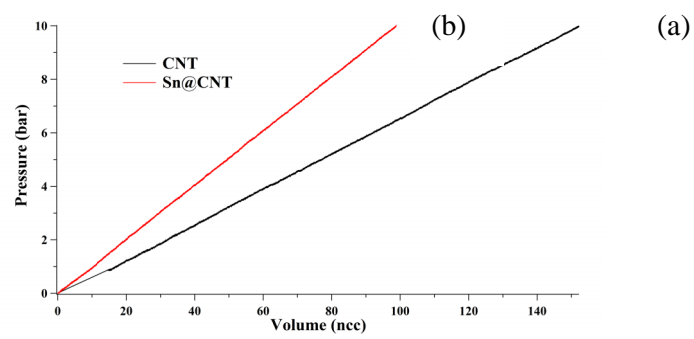


Figure 3.1.2: Pressure vs. Volume for CNTs (a) and Sn@CNTs (b).

Figure 3.1.3: Pressure vs. Volume for metal hydrides.

Figure 3.1.3: Pressure vs. Volume for metal hydrides. The graph shows a curve for 'mishmetal' that starts at the origin and increases with a concave-up shape, reaching approximately 9 bar at 160 ncc.

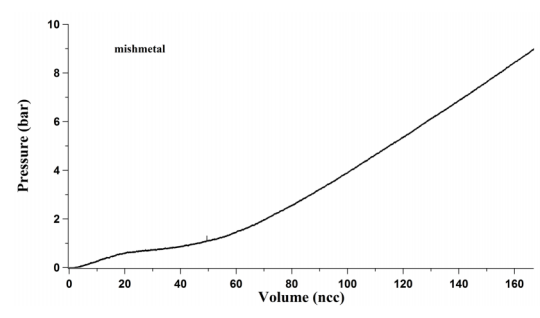


Figure 3.1.3: Pressure vs. Volume for metal hydrides.

Figure 3.1.3: Pressure vs. Volume for metal hydrides. The graph shows a curve for 'mishmetal' that starts at the origin and increases with a concave-up shape, reaching approximately 9 bar at 160 ncc.



(iii)

$$\mu - \mu$$

$$\mu$$

(

$$\mu$$

$$\dots 2 - \mu -$$

)

$$\mu$$

- .

$$\mu$$

$$\mu - \mu$$

$$\mu$$

$$\mu$$

$$\mu$$

,

$$\mu$$

$$\mu$$

$$- \mu$$

..

.

$$\mu$$

$$\mu$$

$$\mu$$

.

$$\mu$$

:

•

$$\mu$$

$$\mu$$

*FePt.*

$$\mu$$

$$\mu$$

$$\mu$$

$$\mu$$

*FePt.*

$$\mu$$

$$\mu$$

$$\mu$$

$$\mu$$

$$\mu$$

*FePt*

$$\mu$$

$$\mu$$

$$\mu$$

$$\mu$$

$$\mu$$

$$\mu$$

$$\mu$$

$$\mu$$

$$\mu$$

$$\mu$$

$$\mu$$

μ .

,

$$700 \text{ C } \mu$$

$$\mu$$

$$\mu$$

$L1_0$  FePt

.

$$\mu$$

$$\mu$$

$$\mu$$

$\mu \mu \mu$

$$\mu$$

$$\mu$$

,

..

$$\mu$$

$$\mu$$

,

$$\mu$$

$$\mu$$

$$\mu$$

$$\mu$$

$$\mu$$

$$\mu$$

$$\mu$$

$$\mu$$

$$\mu$$

$$\mu$$

$$\mu$$

$$\mu$$

XRD

FePt

$$\mu$$

,

fcc

$$\mu$$

$$\mu$$

fcc

$L1_0$

$$\mu$$

$$\mu$$

$\mu \mu$

.

$$\mu$$

Raman

«

»

$$\mu$$

$$\mu$$

$$\mu$$

$$\mu$$

FePt

$$\mu$$

.









μ

:

,

μ

μ

.

μ μ

μ

,

μ

\_\_\_\_\_

Multi-Wall Carbon Nanotubes

μ - /  
(i)

μ (Single-  
μ

μ μ

(ii) T

(... 1,3-  
μ - μ

(... 2- μ -  
μ

(iii) μ - μ

μ

μ μ

μ

μ μ

( μ - μ μ )

μ

,

μ

μ

μ

/

μ μ , μ

μ

μ

μ

μ

μ

FePt

μ

μ

μ

μ

μ

μ μ

μ

μ

μ

μ

μ

FePt

μ

μ

μ

μ

μ

μ

RuPt

μ

μ

μ

μ







,

# **Chemical Functionalization of Carbon Nanotubes and Derived Hybrids: Synthesis, Characterization and Study of Hydrogen Adsorption**

**T. TSOUFIS**

*PhD Thesis*

*Department of Materials Science and Engineering, University of Ioannina,  
Greece*

## **ABSTRACT**

In the first part of the present PhD thesis, novel chemical routes for the chemical functionalization of single- and/or multi-wall carbon nanotubes were developed. The strategies that were adopted toward this aim, involved (i) The covalent attachment of chemical groups or derivatives using appropriate reactions (e.g. 1,3-dipolar cycloaddition) (ii) The immobilization of radicals (e.g. tyrosinate radical) on the graphitic surface of carbon nanotubes and (iii) The non-covalent attachment of suitable molecules (polyaromatic hydrocarbons e.g. amino-anthracene, pyrene-amine etc) on the surface of carbon nanotubes by  $\pi$ - $\pi$  interactions.

In the second part of the thesis novel hybrid materials based on functionalized carbon nanotubes were developed and studied. Within this concept, various hybrid systems consisting of carbon nanotubes and bi-metallic (or monometallic) nanoparticles were synthesized since the combination of these two different categories of nanomaterials, may lead to the successful exploitation of their unique properties. In general, it was studied the capability to use the chemically modified surface of carbon nanotubes as nano-template where either nanoparticles directly grow and/or deposited or alternatively preformed nanoparticles attach by appropriate chemical interactions. In detail, there were synthesized novel hybrid materials of multiwalled carbon nanotubes and FePt nanoparticles by using the surface of nanotubes as nanotemplate for the dispersion and stabilization of the magnetic nanoparticles. The pre-formed capped FePt nanoparticles were connected to the chemical functionalized carbon nanotubes external surface via covalent binding through organic linkers. Using a similar methodology, pre-formed capped RuPt nanoparticles were immobilised for the first time on the external surface of chemical functionalized multi-wall carbon nanotubes via covalent interactions. Furthermore, the synthesis of novel hybrid materials consisting of  $\gamma$ -Fe<sub>2</sub>O<sub>3</sub> nanoparticles, metallic Sn nanowires and multi-wall carbon nanotubes was exploited. Initially, Sn nanowires were grown by a catalytic chemical vapour deposition method along the inner cavity of multi-wall carbon nanotubes. The produced Sn nanowires-carbon nanotubes system was then decorated with the pre-formed capped Fe<sub>2</sub>O<sub>3</sub> nanoparticles. Tin nanowires completely covered by carbon cells are protected from all sides against atmospheric oxidation (and hence are suitable for handling in air), while after a mild chemical functionalization on the

outer carbon wall suitable groups are imported which facilitate the immobilization of the nanoparticles.

Alternatively, it was studied the possibility of the direct development of nanoparticles on the surface of chemically functionalized carbon nanotubes. Single- and multi-wall carbon nanotubes were employed as nano-templates for the synthesis of various hybrid nanostructures consisting of carbon nanotubes and iron oxide nanoparticles ( $\gamma$ - $\text{Fe}_2\text{O}_3$ ,  $\alpha$ - $\text{Fe}_2\text{O}_3$  or  $\text{Fe}_3\text{O}_4$ ) via a simple, reproducible and versatile method. The strategy that was adopted involved the chemical functionalization of carbon nanotubes by two alternative routes, one targeting at the covalent functionalization of CNTs and the second one taking advantage of  $\pi$ - $\pi$  interactions. C-Fe nanoparticle composites were prepared by interaction of acetic acid vapors with iron cations dispersed on the surface of the derived functionalized nanotubes. Upon pyrolysis the created iron acetate species were transformed to magnetic iron oxide nanoparticles. The atmosphere which is used during the synthetic procedure affects significantly the nature of the nanoparticles which could be either  $\gamma$ - $\text{Fe}_2\text{O}_3$  or magnetite, or non-magnetic such as  $\alpha$ - $\text{Fe}_2\text{O}_3$ .

ovel hybrid systems of carbon nanotubes and layered silicates, in which the chemically functionalized carbon nanotubes interact with either exfoliated or ordered clay platelets were developed using a simple synthetic route. Toward this method, homogeneous, coherent, and transparent clay-carbon nanotube composite films or gels are achieved by simple mixing colloidal solutions of nanotubes with clay dispersions. Finally, a novel composite hybrid system consisting of carbon nanotubes routed on smectite clays and  $\gamma$ - $\text{Fe}_2\text{O}_3$  nanoparticles was also synthesized and studied. Multi-wall carbon nanotubes were developed on the surfaces of clay platelets, using the catalytical chemical vapour deposition method. After purification, the carbon nanotube-clay composite materials were covalently functionalized in order to create the suitable chemical groups on the surface of nanotubes. In the final step, immobilization of the preformed capped  $\gamma$ - $\text{Fe}_2\text{O}_3$  nanoparticles took place on the surface of carbon nanotubes.

The chemical functionalization of carbon nanotubes that was studied in the first part of the thesis, as well as the synthesis of the various hybrid systems that followed in the second part, were studied in detail with a combination of experimental methods including: spectroscopic techniques (Raman, FT-IR, Mössbauer, UV-Vis, STS and PR), thermal analysis (GA-DTA), X-Ray diffraction measurements (RD) and microscopies (TEM, AFM, STM, SEM). Finally, selected samples were evaluated for their ability to adsorb hydrogen under different conditions.

- 
- 1) "Electronic measurements on a single superconducting tin nanowire encapsulated in a multiwalled carbon nanotube"  
N. Tombros, L. Buit, I. Arfaoui, **T. Tsoufis**, D. Gournis, P.N. Trikalitis, S.J. Van der Molen, P. Rudolf and B.J. Van Wees.  
*Nano Letters*, 8 (2008) 3060-3064.
  - 2) "Multipurpose Organically Modified Carbon Nanotubes: From Functionalization to Nanotube Composites"  
V. Georgakilas, A. Bourlinos, D. Gournis, **T. Tsoufis**; C. Trapalis, A. Mateo-Alonso and M. Prato.  
*Journal of American Chemical Society*, 130 (2008) 8733-8740.
  - 3) "Novel Nanohybrids derived from the attachment of FePt Nanoparticles on Carbon Nanotubes"  
**T. Tsoufis**, A. Tomou, D. Gournis, A.P. Douvalis, I. Panagiotopoulos, B. Kooi, V. Georgakilas, I. Arfaoui and T. Bakas.  
*Journal of Nanoscience & Nanotechnology*, 8 (2008) 5942-5951.
  - 4) "Evaluation of first-row transition metal oxides supported on clay minerals for catalytic growth of carbon nanostructures"  
**T. Tsoufis**, L. Jankovic, D. Gournis, P. N. Trikalitis and T. Bakas  
*Materials Science & Engineering:B*, 152 (2008) 44-49.
  - 5) "Metallic tin-filling effects on Carbon Nanotubes revealed by atomically resolved spectro-microscopies"  
E. Maccallini, G. Kalantzopoulos, **T. Tsoufis**, R.G. Agostino, G. Chiarello, V. Formoso, T. Caruso, A. Policicchio, D. Gournis and E. Colavita.  
*Journal of Nano Research*, 3 (2008) 1-6.
  - 6) "Catalytic production of carbon nanotubes over Fe-Ni bimetallic catalysts supported on MgO"  
**T. Tsoufis**, P. Xidas, L. Jankovic, D. Gournis, A. Saranti, T. Bakas and M. A. Karakassides,  
*Diamond and Related Materials*, 16 (2007) 155-160.
  - 7) "Electronic, chemical and structural characterization of CNTs grown by acetylene decomposition over MgO supported Fe-Co bimetallic catalysts"

## H'

A. Policicchio, T. Caruso, G. Chiarello, E. Colavita, V. Formoso, R.G. Agostino, **T. Tsoufis**, D. Gournis and S. La Rosa,  
*Surface Science*, 601 (2007) 2823-2827.

- 8) "Direct observation of spin-injection in tyrosinate-functionalized fullerenes and single-walled carbon Nanotubes"

**T. Tsoufis**, A. Amboumogli, D. Gournis, V. Georgakilas, L. Jankovic, K. Christoforidis, Y. Deligiannakis, A. Mavrandonakis, G. Froudakis, E. Maccallini, P. Rudolf and M. Prato

Submitted to *Journal of American Chemical Society*.

- 9) "PtRu Nanoparticles Supported on Multi Wall Carbon Nanotubes as Electrocatalyst of H<sub>2</sub>O<sub>2</sub>"

**T. Tsoufis**, K. Kardimi, M. Prodromidis, A. Tomou, B. Kooi, I. Panagiotopoulos and D. Gournis.

*Under preparation*

---

## O

---

- 1) "Micropous (Zeolitic) and mesoporous (MCM-41) silicate supports of Fe/Co oxides as catalysts for carbon nanotube formation"

K. Triantafyllidis, S. Karakoulia, **T. Tsoufis**, D. Gournis, A. Delimitis, L. Nalbandian (2006)

*Symposium on Chemistry of Carbon Materials and Nanomaterials - 231st ACS National Meeting*, Atlanta, GA, March 26-30, 2006.

- 
- 1) “Highly Active Bimetallic (Iron/Cobalt) Supported Nanocatalysts for the Synthesis of Carbon Nanotubes”

**T. Tsoufis**, M. Karakoulia, A. Delimitis, K. Triantafyllidis, D. Gournis, T. Bakas, E. Maccalini, P. Rudolf

1<sup>st</sup> International Conference from Nanoparticles and Nanomaterials to Nanodevices and Nanosystems (1<sup>st</sup> IC4N), 15-18 June 2008, Halkidiki, Greece.

- 2) “

$\mu$   $\mu$  ”

\_\_\_\_\_ ,  $\mu$   $\mu$  , L. Jankovic, , , .

3  $\mu$  , 1-2  $\mu$  , 2007.

- 3) “*Decoration of Multi-Wall Carbon Nanotubes with FePt nanoparticles*”

**T. Tsoufis**, A. Tomou, D Gournis, I. Panagiotopoulos, B. Kooi, A. P. Douvalis and T. Bakas "Magnetic Nanoparticles: Challenges & Future Prospects" Workshop, Lorentz Center, Leiden, the Netherlands, 18-23 June 2007.

- 4) “  $\mu$   $\mu$   $\mu$  ”

\_\_\_\_\_ , , .  
XXI &  $\mu$   
, , 24-27  $\mu$  2006.

- 5) “  $\mu$   $MgO$  ,  $- \mu$   $Fe-Ni$

\_\_\_\_\_ , , L. Jankovic, , , .

2  $\mu$  , , . . . . «  $\mu$  » , ,  
29-30  $\mu$  2005.

- 
- 1) “*Structural and Magnetic Properties of  $\gamma$ - $Fe_2O_3$  Nanoparticles Dispersed on Clays*”, A. Douvalis, E. Diamadi, A. Tomou, **T. Tsoufis**, A. Enotiadis, D.



- Gournis, T. Bakas, *5<sup>th</sup> Workshop on Nanosciences & Nanotechnologies*, 14-16 July 2008, Thessaloniki, Greece.
- 2) “*Incorporation of pure C<sub>60</sub> into Organo-Clays*”, **T. Tsoufis**, V. Georgakilas, D. Gournis, *5<sup>th</sup> Workshop on Nanosciences & Nanotechnologies*, 14-16 July 2008, Thessaloniki, Greece.
  - 3) “*Anchored carbon nanotubes encapsulating crystalline -tin nanowires for Photovoltaic applications: morphological and structural investigation*”, E. Maccallini, G. Kalantzopoulos, **T. Tsoufis**, D. Gournis, A. Tomou, I. Panagiotopoulos, E. Cazzanelli, F. Ciuchi, T. Caruso, A. Policicchio, G. Chiarello, V. Formoso, E. Colavita, R. Agostino, *Chemical Nanotechnology Talks VIII: Energising a Sustainable Future*, 20-21 November 2007, Frankfurt, Germany.
  - 4) “*Synthesis and Characterization of Nanocomposites Consisting of Single Wall Nanotubes and Copolymers*”, E. Kassapis, A. Avgeropoulos, **T. Tsoufis**, D. Gournis, *International Symposium on Polymer Analysis and Characterization (ISPAC 2007)*, Crete, Greece.
  - 5) “*PtRu Nanoparticles Supported on Multi Wall Carbon Nanotubes as electrocatalyst of H<sub>2</sub>O<sub>2</sub>*”, K. Kardimi, A. Tomou, **T. Tsoufis**, B. Kooi, I. Panagiotopoulos, M. Prodromidis and D. Gournis, *4<sup>th</sup> Workshop on Nanosciences & Nanotechnologies*, 14-20 July 2007, Thessaloniki, Greece.
  - 6) “*μ μ FePt μ*”, . , . μ , . , . , B. Kooi, . , . , 3 μ , 1-2 μ , 2007.
  - 7) “*Metallic Tin-filling Effects on Carbon Nanotubes Revealed by Atomically Resolved Spectro-microscopies*”, E. Maccallini, G. Kalantzopoulos, R.G. Agostino, G. Chiarello, V. Formoso, T. Caruso, A. Policicchio, D. Gournis, **T. Tsoufis** and E. Colavita, *International Conference on Surfaces, Coatings and Nanostructured Materials ( anoSMat07)*, 9-11 July 2007, Algarve, Portugal.
  - 8) “*μ μ Fe/Co*” . , . μ , . , . , 3 μ , 1-2 μ , 2007.

- 9) “*μ* *Nylon-610 μ* *μ*”, . . . , . . . , . . . , . . . , . . . , XXI  
*& μ* , , 24-27 *μ* 2006.
- 10) “*Evaluation of first-row transition metal oxides supported on clay minerals for catalytic growth of carbon nanotubes*”, **T. Tsoufis**, L. Jankovic, D. Gournis, P.N. Trikalitis and T. Bakas, 4<sup>th</sup> *Workshop on Nanosciences & Nanotechnologies*, 14-20 July 2006, Thessaloniki, Greece
- 11) “*Evaluation of Fe-Ni, Fe-Co and Ni-Co bimetallic catalysts supported on MgO for large scale production of carbon nanotubes*”, **T. Tsoufis**, P. Xidas, D. Gournis, M. A. Karakassides, Tomaso Caruso, Enrico Maccallini, Raffaele G. Agostino, L. Jankovic and T. Bakas, 3<sup>rd</sup> *Workshop on Nanosciences & Nanotechnologies*, 16-18 July 2006, Thessaloniki, Greece.
- 12) “*Carbon Nanotubes growth by acetylene decomposition over MgO supported Fe-Co bimetallic catalysts and their electronic, chemical and structural characterization*”, A. Policicchio, T. Caruso, G. Chiarello, E. Colavita, R.G. Agostino, **T. Tsoufis**, D. Gournis, and S. La Rosa, *International Conference on NANO-Structures & Self-Assembling*, 2-6 July 2006, Aix en Provence, France.
- 13) “*μ* *Nylon-6/10 &* *μ*”, . . . , . . . , . . . .  
*μ* , VIII *&*  
*μ* , *μ* , 2002, .



## I.

1. S. Iijima, Helical Microtubules of Graphitic Carbon, *Nature* **354**, 56 (1991).
2. P.M. Ajayan, J.C. Charlier and A.G. Rinzler, Carbon nanotubes: From macromolecules to nanotechnology, *Proceedings of the National Academy of Sciences of the United States of America* **96**, 14199 (Dec 7, 1999).
3. S. Iijima and T. Ichihashi, Single-shell carbon nanotubes of 1-nm diameter, *Nature* **363**, 603 (1993).
4. D.S. Bethune, C.H. Kiang, M.S. De Vries, G. Gorman, R. Savoy, J. Vazquez and R. Beyers, Cobalt-catalysed growth of carbon nanotubes with single-atomic-layer walls, *Nature* **363**, 605 (1993).
5. M.S. Dresselhaus, G. Dresselhaus, A.M. Rao and P.C. Eklund, Optical properties of C<sub>60</sub> and related materials, *Synthetic Metals* **78**, 313 (1996).
6. J.W.G. Wildoer, L.C. Venema, A.G. Rinzler, R.E. Smalley and C. Dekker, Electronic structure of atomically resolved carbon nanotubes, *Nature* **391**, 59 (1998).
7. M. Kociak, K. Suenaga, K. Hirahara, Y. Saito, T. Nakahira and S. Iijima, Linking chiral indices and transport properties of double-walled carbon nanotubes, *Physical Review Letters* **89**, 155501/1 (2002).
8. C.Q. Ru, Effect of van der Waals forces on axial buckling of a double-walled carbon nanotube, *Journal of Applied Physics* **87**, 7227 (2000).
9. H. Kurachi, S. Uemura, J. Yotani, T. Nagasako, H. Yamada, T. Ezaki, T. Maesoba, R. Loutfy, A. Moravsky, T. Nakazawa, S. Katagiri and Y. Saito, paper presented at the SID Conference Record of the International Display Research Conference 2001.
10. R. Saito, R. Matsuo, T. Kimura, G. Dresselhaus and M.S. Dresselhaus, Anomalous potential barrier of double-wall carbon nanotube, *Chemical Physics Letters* **348**, 187 (2001).
11. W. Kratschmer, L.D. Lamb, K. Fostiropoulos and D.R. Huffman, Solid C<sub>60</sub>: A new form of carbon, *Nature* **347**, 354 (1990).

12. Y. Saito, M. Inagaki, H. Shinohara, H. Nagashima, M. Ohkohchi and Y. Ando, Yield of fullerenes generated by contact arc method under He and Ar: Dependence on gas pressure, *Chemical Physics Letters* **200**, 643 (1992).
13. W.Z. Li, S.S. Xie, L.X. Qian, B.H. Chang, B.S. Zou, W.Y. Zhou, R.A. Zhao and G. Wang, Large-scale synthesis of aligned carbon nanotubes, *Science* **274**, 1701 (1996).
14. M. Yudasaka, Y. Kasuya, F. Kokai, K. Takahashi, M. Takizawa, S. Bandow and S. Iijima, Causes of different catalytic activities of metals in formation of single-wall carbon nanotubes, *Applied Physics A: Materials Science and Processing* **74**, 377 (2002).
15. C. Liu, H.T. Cong, F. Li, P.H. Tan, H.M. Cheng, K. Lu and B.L. Zhou, Semi-continuous synthesis of single-walled carbon nanotubes by a hydrogen arc discharge method, *Carbon* **37**, 1865 (1999).
16. Z.J. Zhang, G. Ramanath, P.M. Ajayan, D. Goldberg and Y. Bando, Creation of radial patterns of carbonated silica fibers on planar silica substrates, *Advanced Materials* **13**, 197 (Feb 5, 2001).
17. J.L. Hutchison, N.A. Kiselev, E.P. Krinichnaya, A.V. Krestinin, R.O. Loutfy, A.P. Morawsky, V.E. Muradyan, E.D. Obraztsova, J. Sloan, S.V. Terekhov and D.N. Zakharov, Double-walled carbon nanotubes fabricated by a hydrogen arc discharge method, *Carbon* **39**, 761 (2001).
18. Y. Saito, T. Nakahira and S. Uemura, Growth conditions of double-walled carbon nanotubes in arc discharge, *Journal of Physical Chemistry B* **107**, 931 (2003).
19. T. Sugai, H. Yoshida, T. Shimada, T. Okazaki, H. Shinohara and S. Bandow, New synthesis of high-quality double-walled carbon nanotubes by high-temperature pulsed arc discharge, *Nano Letters* **3**, 769 (2003).
20. T. Guo, M.D. Diener, Y. Chai, M.J. Alford, R.E. Haufler, S.M. McClure, T. Ohno, J.H. Weaver, G.E. Scuseria and R.E. Smalley, *Science* **257**, 1661 (1992).
21. A. Thess, R. Lee, P. Nikolaev, H. Dai, P. Petit, J. Robert, C. Xu, Y.H. Lee, S.G. Kim, A.G. Rinzler, D.T. Colbert, G.E. Scuseria, D. Tomanek, J.E. Fischer and R.E. Smalley, Crystalline ropes of metallic carbon nanotubes, *Science* **273**, 483 (1996).

22. R. Sen, Y. Ohtsuka, T. Ishigaki, D. Kasuya, S. Suzuki, H. Kataura and Y. Achiba, Time period for the growth of single-wall carbon nanotubes in the laser ablation process: Evidence from gas dynamic studies and time resolved imaging, *Chemical Physics Letters* **332**, 467 (2000).
23. H. Kataura, Y. Kumazawa, Y. Maniwa, Y. Ohtsuka, R. Sen, S. Suzuki and Y. Achiba, Diameter control of single-walled carbon nanotubes, *Carbon* **38**, 1691 (2000).
24. S. Bandow, S. Asaka, Y. Saito, A.M. Rao, L. Grigorian, E. Richter and P.C. Eklund, Effect of the growth temperature on the diameter distribution and chirality of single-wall carbon nanotubes, *Physical Review Letters* **80**, 3779 (1998).
25. P.L. Walker Jr, J.F. Rakszawski and G.R. Imperial, Carbon formation from carbon monoxide-hydrogen mixtures over iron catalysts. I. Properties of carbon formed, *Journal of Physical Chemistry* **63**, 133 (1959).
26. M.S. Dresselhaus, G. Dresselhaus, K. Sugihara, I.L. Spain and H.A. Goldberg, *Graphite Fibers and Filaments* (1988).
27. M. Endo, Grow carbon fibers in the vapor phase, *ChemTec* **18**, 568 (1988).
28. Y. Li, X. Zhang, L. Shen, J. Luo, X. Tao, F. Liu, G. Xu, Y. Wang, H.J. Geise and G. Van Tendeloo, Controlling the diameters in large-scale synthesis of single-walled carbon nanotubes by catalytic decomposition of CH<sub>4</sub>, *Chemical Physics Letters* **398**, 276 (2004).
29. C.L. Cheung, A. Kurtz, H. Park and C.M. Lieber, Diameter-Controlled Synthesis of Carbon Nanotubes, *Journal of Physical Chemistry B* **106**, 2429 (2002).
30. H. Ago, S. Imamura, T. Okazaki, T. Saito, M. Yumura and M. Tsuji, CVD Growth of Single-Walled Carbon Nanotubes with Narrow Diameter Distribution over Fe/MgO Catalyst and Their Fluorescence Spectroscopy, *Journal of Physical Chemistry B* **109**, 10035 (2005).
31. N. Zhao, C. He, Z. Jiang, J. Li and Y. Li, Fabrication and growth mechanism of carbon nanotubes by catalytic chemical vapor deposition, *Materials Letters* **60**, 159 (2006).

32. Y. Li, W. Kim, Y. Zhang, M. Rolandi, D. Wang and H. Dai, Growth of Single-Walled Carbon Nanotubes from Discrete Catalytic Nanoparticles of Various Sizes, *Journal of Physical Chemistry B* **105**, 11424 (2001).
33. C.J. Lee and J. Park, Growth Model for Bamboolike Structured Carbon Nanotubes Synthesized Using Thermal Chemical Vapor Deposition, *Journal of Physical Chemistry B* **105**, 2365 (2001).
34. M. Endo, K. Takeuchi, S. Igarashi, K. Kobori, M. Shiraishi and H.W. Kroto, The production and structure of pyrolytic carbon nanotubes, *Journal of Physics and Chemistry of Solids* **54**, 1841 (1993).
35. M. Jose-Yacaman, M. Miki-Yoshida, L. Rendon and J.G. Santiesteban, Catalytic growth of carbon microtubules with fullerene structure, *Applied Physics Letters* **62**, 657 (1993).
36. B.C. Satishkumar, A. Govindaraj and C.N.R. Rao, Bundles of aligned carbon nanotubes obtained by the pyrolysis of ferrocene-hydrocarbon mixtures: Role of the metal nanoparticles produced in situ, *Chemical Physics Letters* **307**, 158 (1999).
37. K. Hernadi, A. Fonseca, J.B. Nagy, D. Bernaerts and A.A. Lucas, Fe-catalyzed carbon nanotube formation, *Carbon* **34**, 1249 (1996).
38. H. Dai, A.G. Rinzler, P. Nikolaev, A. Thess, D.T. Colbert and R.E. Smalley, Single-wall nanotubes produced by metal-catalyzed disproportionation of carbon monoxide, *Chemical Physics Letters* **260**, 471 (1996).
39. B.C. Satishkumar, A. Govindaraj, R. Sen and C.N.R. Rao, Single-walled nanotubes by the pyrolysis of acetylene-organometallic mixtures, *Chemical Physics Letters* **293**, 47 (1998).
40. J. Kong, A.M. Cassell and H. Dai, Chemical vapor deposition of methane for single-walled carbon nanotubes, *Chemical Physics Letters* **292**, 567 (1998).
41. R.T. Baker and P.S. Harris, *Chemistry and Physics of Carbon* **83**, 14 (1978).
42. G.G. Tibbetts, Why are carbon filaments tubular?, *Journal of Crystal Growth* **66**, 632 (1984).
43. M. Terrones, N. Grobert, J. Olivares, J.P. Zhang, H. Terrones, K. Kordatos, W.K. Hsu, J.P. Hare, P.D. Townsend, K. Prassides, A.K. Cheetham, H.W. Kroto and D.R.M. Walton, Controlled production of aligned-nanotube bundles, *Nature* **388**, 52 (1997).

44. Z.W. Pan, S.S. Xie, B.H. Chang, C.Y. Wang, L. Lu, W. Liu, W.Y. Zhou, W.Z. Li and L.X. Qian, Very long carbon nanotubes, *Nature* **394**, 631 (1998).
45. H. Ago, T. Komatsu, S. Ohshima, Y. Kuriki and M. Yumura, Dispersion of metal nanoparticles for aligned carbon nanotube arrays, *Applied Physics Letters* **77**, 79 (2000).
46. S. Fan, M.G. Chapline, N.R. Franklin, T.W. Tombler, A.M. Cassell and H. Dai, Self-oriented regular arrays of carbon nanotubes and their field emission properties, *Science* **283**, 512 (1999).
47. K. Hernadi, Catalytic synthesis of carbon nanotubes using zeolite support, *Zeolites* **17**, 416 (1996).
48. J.L. Bahr and J.M. Tour, Covalent chemistry of single-wall carbon nanotubes, *Journal of Materials Chemistry* **12**, 1952 (2002).
49. C.A. Dyke and J.M. Tour, Overcoming the Insolubility of Carbon Nanotubes Through High Degrees of Sidewall Functionalization, *Chemistry - A European Journal* **10**, 812 (2004).
50. N.F. Yudanov, A.V. Okotrub, Y.V. Shubin, L.I. Yudanov, L.G. Bulusheva, A.L. Chuvilin and J.M. Bonard, Fluorination of Arc-Produced Carbon Material Containing Multiwall Nanotubes, *Chemistry of Materials* **14**, 1472 (2002).
51. A. Hamwi, H. Alvergnat, S. Bonnamy and F. B guin, Fluorination of carbon nanotubes, *Carbon* **35**, 723 (1997).
52. E.T. Mickelson, C.B. Huffman, A.G. Rinzler, R.E. Smalley, R.H. Hauge and J.L. Margrave, Fluorination of single-wall carbon nanotubes, *Chemical Physics Letters* **296**, 188 (Oct 30, 1998).
53. S. Pekker, J.P. Salvetat, E. Jakab, J.M. Bonard and L. Forro, Hydrogenation of Carbon Nanotubes and Graphite in Liquid Ammonia, *Journal of Physical Chemistry B* **105**, 7938 (2001).
54. B. Khare, M. Meyyappan, M.H. Moore, P. Wilhite, H. Imanaka and B. Chen, Proton Irradiation of Carbon Nanotubes, *Nano Letters* **3**, 643 (2003).
55. K.S. Kim, D.J. Bae, J.R. Kim, K.A. Park, S.C. Lim, J.J. Kim, W.B. Choi, C.Y. Park, Y.H. Lee, Modification of Electronic Structures of a Carbon Nanotube by Hydrogen Functionalization, *Advanced Materials* **14**, 1818 (2002).



56. H. Hu, B. Zhao, M.A. Hamon, K. Kamaras, M.E. Itkis and R.C. Haddon, Sidewall Functionalization of Single-Walled Carbon Nanotubes by Addition of Dichlorocarbene, *Journal of the American Chemical Society* **125**, 14893 (2003).
57. J. Chen, M.A. Hamon, H. Hu, Y. Chen, A.M. Rao, P.C. Eklund and R.C. Haddon, Solution Properties of Single-Walled Carbon Nanotubes, *Science* **282**, 95 (1998).
58. M.S. Strano, Probing Chiral Selective Reactions Using a Revised Kataura Plot for the Interpretation of Single-Walled Carbon Nanotube Spectroscopy, *Journal of the American Chemical Society* **125**, 16148 (2003).
59. C.A. Dyke and J.M. Tour, Unbundled and Highly Functionalized Carbon Nanotubes from Aqueous Reactions, *Nano Letters* **3**, 1215 (2003).
60. J.L. Bahr, J. Yang, D.V. Kosynkin, M.J. Bronikowski, R.E. Smalley and J.M. Tour, Functionalization of Carbon Nanotubes by Electrochemical Reduction of Aryl Diazonium Salts: A Bucky Paper Electrode, *Journal of the American Chemical Society* **123**, 6536 (2001).
61. N. Tagmatarchis, V. Georgakilas, M. Prato and H. Shinohara, Sidewall functionalization of single-walled carbon nanotubes through electrophilic addition, *Chemical Communications*, 2010 (2002).
62. S. Banerjee and S.S. Wong, Functionalization of Carbon Nanotubes with a Metal-Containing Molecular Complex, *Nano Letters* **2**, 49 (2002).
63. X. Lu, F. Tian, Y. Feng, X. Xu, N. Wang and Q. Zhang, Sidewall Oxidation and Complexation of Carbon Nanotubes by Base-Catalyzed Cycloaddition of Transition Metal Oxide: A Theoretical Prediction, *Nano Letters* **2**, 1325 (2002).
64. S. Banerjee and S.S. Wong, Rational Sidewall Functionalization and Purification of Single-Walled Carbon Nanotubes by Solution-Phase Ozonolysis, *Journal of Physical Chemistry B* **106**, 12144 (2002).
65. S. Banerjee and S.S. Wong, Demonstration of Diameter-Selective Reactivity in the Sidewall Ozonation of SWNTs by Resonance Raman Spectroscopy, *Nano Letters* **4**, 1445 (2004).

66. S. Banerjee, T. Hemraj-Benny, M. Balasubramanian, D. Fischer, J. Misewich and S.S. Wong, Ozonized single-walled carbon nanotubes investigated using NEXAFS spectroscopy, *Chemical Communications*, 772 (2004).
67. A. Eitan, K. Jiang, D. Dukes, R. Andrews and L.S. Schadler, Surface Modification of Multiwalled Carbon Nanotubes: Toward the Tailoring of the Interface in Polymer Composites, *Chemistry of Materials* **15**, 3198 (2003).
68. E. Bekyarova, M. Davis, T. Burch, M.E. Itkis, B. Zhao, S. Sunshine and R.C. Haddon, Chemically Functionalized Single-Walled Carbon Nanotubes as Ammonia Sensors, *Journal of Physical Chemistry B* **108**, 19717 (2004).
69. Q. Chen, L. Dai, M. Gao, S. Huang and A. Mau, Plasma Activation of Carbon Nanotubes for Chemical Modification, *Journal of Physical Chemistry B* **105**, 618 (2001).
70. S. Chen, W. Shen, G. Wu, D. Chen and M. Jiang, A new approach to the functionalization of single-walled carbon nanotubes with both alkyl and carboxyl groups, *Chemical Physics Letters* **402**, 312 (2005).
71. V. Georgakilas, D. Gournis, M.A. Karakassides, A. Bakandritsos and D. Petridis, Organic derivatization of single-walled carbon nanotubes by clays and intercalated derivatives, *Carbon* **42**, 865 (2004).
72. E.V. Basiuk, M. Monroy-Pelaez, I. Puente-Lee and V.A. Basiuk, Direct Solvent-Free Amination of Closed-Cap Carbon Nanotubes: A Link to Fullerene Chemistry, *Nano Letters* **4**, 863 (2004).
73. A. Koshio, M. Yudasaka, M. Zhang and S. Iijima, A Simple Way to Chemically React Single-Wall Carbon Nanotubes with Organic Materials Using Ultrasonication, *Nano Letters* **1**, 361 (2001).
74. J.H. Sung, H.S. Kim, H.J. Jin, H.J. Choi and I.J. Chin, Nanofibrous Membranes Prepared by Multiwalled Carbon Nanotube/Poly(methyl methacrylate) Composites, *Macromolecules* **37**, 9899 (2004).
75. S. Qin, D. Qin, W.T. Ford, J.E. Herrera, D.E. Resasco, S.M. Bachilo and R.B. Weisman, Solubilization and Purification of Single-Wall Carbon Nanotubes in Water by in Situ Radical Polymerization of Sodium 4-Styrenesulfonate, *Macromolecules* **37**, 3965 (2004).

76. X. Gong, J. Liu, S. Baskaran, R.D. Voise and J.S. Young, Surfactant-Assisted Processing of Carbon Nanotube/Polymer Composites, *Chemistry of Materials* **12**, 1049 (2000).
77. S. Cui, R. Canet, A. Derre, M. Couzi and P. Delhaes, Characterization of multiwall carbon nanotubes and influence of surfactant in the nanocomposite processing, *Carbon* **41**, 797 (2003).
78. F. Du, J.E. Fischer and K.I. Winey, Coagulation method for preparing single-walled carbon nanotube/poly(methyl methacrylate) composites and their modulus, electrical conductivity, and thermal stability, *Journal of Polymer Science Part B: Polymer Physics* **41**, 3333 (2003).
79. N. R. Raravikar, A.S. Vijayaraghavan, P. Keblinski, L.S. Schadler and M. Ajayan, Embedded Carbon-Nanotube-Stiffened Polymer Surfaces, *Small* **1**, 317 (2005).
80. Y. Kang and T.A. Taton, Micelle-Encapsulated Carbon Nanotubes: A Route to Nanotube Composites, *Journal of the American Chemical Society* **125**, 5650 (2003).
81. H.J. Barraza, F. Pompeo, E.A. O'Rear and D.E. Resasco, SWNT-Filled Thermoplastic and Elastomeric Composites Prepared by Miniemulsion Polymerization, *Nano Letters* **2**, 797 (2002).
82. D.W. Steuerman, A. Star, R. Narizzano, H. Choi, R.S. Ries, C. Nicolini, J.F. Stoddart and J.R. Heath, Interactions between Conjugated Polymers and Single-Walled Carbon Nanotubes, *Journal of Physical Chemistry B* **106**, 3124 (2002).
83. C. Downs, J. Nugent, P.M. Ajayan, D.J. Duquette and K.S. Santhanam, Efficient Polymerization of Aniline at Carbon Nanotube Electrodes, *Advanced Materials* **11**, 1028 (1999).
84. A. Nogales, G. Broza, Z. Roslaniec, K. Schulte, I. Sics, B.S. Hsiao, A. Sanz, M.C. Garcia-Gutierrez, D.R. Rueda, C. Domingo and T.A. Ezquerra, Low Percolation Threshold in Nanocomposites Based on Oxidized Single Wall Carbon Nanotubes and Poly(butylene terephthalate), *Macromolecules* **37**, 7669 (2004).

85. J.C. Grunlan, A.R. Mehrabi, M.V. Bannon and J.L. Bahr, Water-Based Single-Walled-Nanotube-Filled Polymer Composite with an Exceptionally Low Percolation Threshold, *Advanced Materials* **16**, 150 (2004).
86. T.X. Liu, I.Y. Phang, L. Shen, S.Y. Chow and W.D. Zhang, Morphology and Mechanical Properties of Multiwalled Carbon Nanotubes Reinforced Nylon-6 Composites, *Macromolecules* **37**, 7214 (2004).
87. W.D. Zhang, L. Shen, I.Y. Phang and T. Liu, Carbon Nanotubes Reinforced Nylon-6 Composite Prepared by Simple Melt-Compounding, *Macromolecules* **37**, 256 (2004).
88. R. Shvartzman-Cohen, Y. Levi-Kalisman, E. Nativ-Roth and R. Yerushalmi-Rozen, Generic Approach for Dispersing Single-Walled Carbon Nanotubes: The Strength of a Weak Interaction, *Langmuir* **20**, 6085 (2004).
89. K. Otobe, H. Nakao, H. Hayashi, F. Nihey, M. Yudasaka and S. Iijima, Fluorescence Visualization of Carbon Nanotubes by Modification with Silicon-Based Polymer, *Nano Letters* **2**, 1157 (2002).
90. J. Zhang, J.K. Lee, Y. Wu and R.W. Murray, Photoluminescence and Electronic Interaction of Anthracene Derivatives Adsorbed on Sidewalls of Single-Walled Carbon Nanotubes, *Nano Letters* **3**, 403 (2003).
91. H. Paloniemi, T. Aaritalo, T. Laiho, H. Liuke, N. Kocharova, K. Haapakka, F. Terzi, R. Seeber and J. Lukkari, Water-Soluble Full-Length Single-Wall Carbon Nanotube Polyelectrolytes: Preparation and Characterization, *Journal of Physical Chemistry B* **109**, 8634 (2005).
92. F. Zheng, L. Liang, Y. Gao, J.H. Sukamto and C.L. Aardahl, Carbon Nanotube Synthesis Using Mesoporous Silica Templates, *Nano Letters* **2**, 729 (2002).
93. V.C. Moore, M.S. Strano, E.H. Haroz, R.H. Hauge, R.E. Smalley, J. Schmidt and Y. Talmon, Individually Suspended Single-Walled Carbon Nanotubes in Various Surfactants, *Nano Letters* **3**, 1379 (2003).
94. M.F. Islam, E. Rojas, D.M. Bergey, A.T. Johnson and A.G. Yodh, High Weight Fraction Surfactant Solubilization of Single-Wall Carbon Nanotubes in Water, *Nano Letters* **3**, 269 (2003).
95. J. Chen, D. Feng, Y. Huang, X. Ju and H.Z. Lian, Electrochemical Antitumor Drug Sensitivity Test for Leukemia K562 Cells at a Carbon-Nanotube-Modified Electrode, *Chemistry - A European Journal* **11**, 1467 (2005).

96. R. Bandyopadhyaya, E. Nativ-Roth, O. Regev and R. Yerushalmi-Rozen, Stabilization of Individual Carbon Nanotubes in Aqueous Solutions, *Nano Letters* **2**, 25 (2002).
97. B. Burtiaux, A. Claye, B.W. Smith, M. Monthieux, D.E. Luzzi and J.E. Fischer, Abundance of encapsulated C<sub>60</sub> in single-wall carbon nanotubes, *Chemical Physics Letters* **310**, 21 (1999).
98. B.W. Smith, M. Monthieux and D.E. Luzzi, Carbon nanotube encapsulated fullerenes: a unique class of hybrid materials, *Chemical Physics Letters* **315**, 31 (1999).
99. E. Dujardin, T.W. Ebbesen A. Krishnan and M.J. Treacy, Wetting of Single Shell Carbon Nanotubes, *Advanced Materials* **10**, 1472 (1998).
100. H. Wu, X.W. Wei, M.W. Shao, J.S. Gu, M.Z. Qu, Preparation of Fe-Ni alloy nanoparticles inside carbon nanotubes via wet chemistry, *Journal of Materials Chemistry* **12**, 1919 (2002).
101. J.J. Davis, M.L.H. Green, H. Allen O. Hill, Y.C. Leung, P.J. Sadler, J. Sloan, A.V. Xavier and S. Chi Tsang, The immobilisation of proteins in carbon nanotubes, *Inorganica Chimica Acta* **272**, 261 (1998).
102. H. Gao, Y. Kong, D. Cui and C.S. Ozkan, Spontaneous Insertion of DNA Oligonucleotides into Carbon Nanotubes, *Nano Letters* **3**, 471 (2003).
103. K. Koga, G.T. Gao, H. Tanaka and X.C. Zeng, Formation of ordered ice nanotubes inside carbon nanotubes, *Nature* **412**, 802 (2001).
104. J. Mart and M.C. Gordillo, Temperature effects on the static and dynamic properties of liquid water inside nanotubes, *Physical Review E* **64**, 021504 (2001).
105. J. Hu, T.W. Odom and C.M. Lieber, Chemistry and Physics in One Dimension: Synthesis and Properties of Nanowires and Nanotubes, *Accounts of Chemical Research* **32**, 435 (1999).
106. S. Frank, P. Poncharal, Z.L. Wang and W.A. Heer, Carbon Nanotube Quantum Resistors, *Science* **280**, 1744 (1998).
107. J. Hone, B. Batlogg, Z. Benes, A.T. Johnson and J.E. Fischer, Quantized Phonon Spectrum of Single-Wall Carbon Nanotubes, *Science* **289**, 1730 (2000).

108. B. Bourlon, J. Wong, C. Miko, L. Forro and M. Bockrath, A nanoscale probe for fluidic and ionic transport, *Nature Nanotechnology* **2**, 104 (2007).
109. A. Cusano, M. Pisco, M. Consales, A. Cutolo, M. Giordano, M. Penza, P. Aversa, L. Capodiecici and S. Campopiano, Novel optochemical sensors based on hollow fibers and single walled carbon nanotubes, *IEEE Photonics Technology Letters* **18**, 2431 (2006).
110. X. Tang, S. Bansaruntip, N. Nakayama, E. Yenilmez, Y.I. Chang and Q. Wang, Carbon nanotube DNA sensor and sensing mechanism, *Nano Letters* **6**, 1632 (2006).
111. A. Winkler, T. Muhl, S. Menzel, R. Kozhuharova-Koseva, S. Hampel, A. Leonhardt and B. Buchner, Magnetic force microscopy sensors using iron-filled carbon nanotubes, *Journal of Applied Physics* **99** (2006).
112. K. Litina, A. Miriouni, D. Gournis, M.A. Karakassides, N. Georgiou, E. Klontzas, E. Ntoukas and A. Avgeropoulos, Nanocomposites of polystyrene-b-polyisoprene copolymer with layered silicates and carbon nanotubes, *European Polymer Journal* **42**, 2098 (2006).
113. S.I. Cha, K.T. Kim, S.N. Arshad, C.B. Mo and S.H. Hong, Extraordinary strengthening effect of carbon nanotubes in metal-matrix nanocomposites processed by molecular-level mixing, *Advanced Materials* **17**, 1377 (2005).
114. K.T. Kim, S.I. Cha, S.H. Hong and S.H. Hong, Microstructures and tensile behavior of carbon nanotube reinforced Cu matrix nanocomposites, *Materials Science and Engineering A* **430**, 27 (2006).
115. G. Yamamoto, K. Yokomizo, M. Omori, Y. Sato, B. Jeyadevan, K. Motomiya, T. Hashida, T. Takahashi, A. Okubo and K. Tohji, Polycarbosilane-derived SiC/single-walled carbon nanotube nanocomposites, *Nanotechnology* **18** (2007).
116. J. Chen, Y. Liu, A.I. Minett, C. Lynam, J. Wang and G.G. Wallace, Flexible, aligned carbon nanotube/conducting polymer electrodes for a lithium-ion battery, *Chemistry of Materials* **19**, 3595 (2007).
117. M. Hirscher and M. Becher, Hydrogen storage in carbon nanotubes, *Journal of Nanoscience and Nanotechnology* **3**, 3 (2003).

118. Y. Liang, H. Zhang, B. Yi, Z. Zhang and Z. Tan, Preparation and characterization of multi-walled carbon nanotubes supported PtRu catalysts for proton exchange membrane fuel cells, *Carbon* **43**, 3144 (2005).
119. A. Bianco, K. Kostarelos and M. Prato, Applications of carbon nanotubes in drug delivery, *Current Opinion in Chemical Biology* **9**, 674 (2005).
120. A. Bianco, K. Kostarelos, C.D. Partidos and M. Prato, Biomedical applications of functionalised carbon nanotubes, *Chemical Communications*, 571 (2005).
121. G. Zhou and W. Duan, Field emission in doped nanotubes, *Journal of Nanoscience and Nanotechnology* **5**, 1421 (2005).
122. S.J. Kim, Vacuum gauges with emitters based on carbon nanotubes, *Technical Physics Letters* **31**, 597 (2005).
123. W.I. Milne, K.B.K. Teo, G.A.J. Amaratunga, P. Legagneux, L. Gangloff, J.P. Schnell, V. Semet, V. Thien Binh and O. Groening, Carbon nanotubes as field emission sources, *Journal of Materials Chemistry* **14**, 933 (2004).
124. S. Liao, G. Xu, W. Wang, F. Watari, F. Cui, S. Ramakrishna and C.K. Chan, Self-assembly of nano-hydroxyapatite on multi-walled carbon nanotubes, *Acta Biomaterialia* **3**, 669 (2007).
125. P.D. Cozzoli, T. Pellegrino and L. Manna, Synthesis, properties and perspectives of hybrid nanocrystal structures, *Chemical Society Reviews* **35**, 1195 (2006).
126. A.M. Jackson, J.W. Myerson and F. Stellacci, Spontaneous assembly of subnanometre-ordered domains in the ligand shell of monolayer-protected nanoparticles, *Nature Mater* **3**, 330 (2004).
127. P.V. Kamat, Photophysical, Photochemical and Photocatalytic Aspects of Metal Nanoparticles, *The Journal of Physical Chemistry B* **106**, 7729 (2002).
128. Y. Yin and A.P. Alivisatos, Colloidal nanocrystal synthesis and the organic-inorganic interface, *Nature* **437**, 664 (2005).
129. B.L. Cushing, V.L. Kolesnichenko and C.J. O'Connor, Recent Advances in the Liquid-Phase Syntheses of Inorganic Nanoparticles, *Chemical Reviews* **104**, 3893 (2004).
130. M. Daniel and D. Astruc, Gold Nanoparticles: Assembly, Supramolecular Chemistry, Quantum-Size-Related Properties, and Applications toward Biology, Catalysis, and Nanotechnology, *Chemical Reviews* **104**, 293 (2004).

131. X.S. Fang, C.H. Ye, L.D Zhang, Y.H Wang and Y.C Wu, Temperature-Controlled Catalytic Growth of ZnS Nanostructures by the Evaporation of ZnS Nanopowders, *Advanced Functional Materials* **15**, 63 (2005).
132. V. Georgakilas, D. Gournis, V. Tzitzios, L. Pasquato, D.M. Guldi and M. Prato, Decorating carbon nanotubes with metal or semiconductor nanoparticles, *Journal of Materials Chemistry* **17**, 2679 (2007).
133. J.M. Planeix, N. Coustel, B. Coq, V. Brotons, P.S. Kumbhar, R. Dutartre, P. Geneste, P. Bernier and P.M. Ajayan, Application of Carbon Nanotubes as Supports in Heterogeneous Catalysis, *Journal of the American Chemical Society* **116**, 7935 (1994).
134. H.S. Kim, H. Lee, K.S. Han, J.H. Kim, M.S. Song, M.S. Park, J.Y. Lee and J.K. Kang, Hydrogen Storage in Ni Nanoparticle-Dispersed Multiwalled Carbon Nanotubes, *The Journal of Physical Chemistry B* **109**, 8983 (2005).
135. L.M. Ang, T.S. Hor, G.Q. Xu, C.H. Tung, S. Zhao and J.L. Wang, Electroless Plating of Metals onto Carbon Nanotubes Activated by a Single-Step Activation Method, *Chemistry of Materials* **11**, 2115 (1999).
136. C. Wang, M. Waje, X. Wang, J.M. Tang, R.C. Haddon and Yan, Proton Exchange Membrane Fuel Cells with Carbon Nanotube Based Electrodes, *Nano Letters* **4**, 345 (2004).
137. J.S. Ye, H.F. Cui, X. L. Tit and W.D. Zhang, Preparation and Characterization of Aligned Carbon Nanotube-Ruthenium Oxide Nanocomposites for Supercapacitors, *Small* **1**, 560 (2005).
138. S. Liao, K.-A. Holmes, H. Tsapraillis and V.I. Birss, High Performance PtRuIr Catalysts Supported on Carbon Nanotubes for the Anodic Oxidation of Methanol, *Journal of the American Chemical Society* **128**, 3504 (2006).
139. R. Yu, L. Chen, Q. Liu, J. Lin, K.L. Tan, S.C. Ng, H.S. Chan, G.Q. Xu and T.S. Hor, Platinum Deposition on Carbon Nanotubes via Chemical Modification, *Chemistry of Materials* **10**, 718 (1998).
140. G.G. Wildgoose, C.E. Banks and R.G. Compton, Metal nanoparticles and related materials supported on Carbon nanotubes: Methods and applications, *Small* **2**, 182 (2006).
141. J. Kong, A.M. Cassell, and H. Dai, Functionalized Carbon Nanotubes for Molecular Hydrogen Sensors, *Advanced Materials* **13**, 1384 (2001).



142. E. Yoo, L. Gao, T. Komatsu, N. Yagai, K. Arai, T. Yamazaki, K. Matsuishi, T. Matsumoto and J. Nakamura, Atomic Hydrogen Storage in Carbon Nanotubes Promoted by Metal Catalysts, *The Journal of Physical Chemistry B* **108**, 18903 (2004).
143. B. Xue, P. Chen, Q. Hong, J. Lin and K.L. Tan, Growth of Pd, Pt, Ag and Au nanoparticles on carbon nanotubes, *Journal of Materials Chemistry* **11**, 2378 (2001).
144. P. Chen, X. Wu, J. Lin and K.L. Tan, Synthesis of Cu Nanoparticles and Microsized Fibers by Using Carbon Nanotubes as a Template, *The Journal of Physical Chemistry B* **103**, 4559 (1999).
145. V. Lordi, N. Yao and J. Wei, Method for Supporting Platinum on Single-Walled Carbon Nanotubes for a Selective Hydrogenation Catalyst, *Chemistry of Materials* **13**, 733 (2001).
146. W. Li, C. Liang, W. Zhou, J. Qiu, Zhou, G. Sun and Q. Xin, Preparation and Characterization of Multiwalled Carbon Nanotube-Supported Platinum for Cathode Catalysts of Direct Methanol Fuel Cells, *The Journal of Physical Chemistry B* **107**, 6292 (2003).
147. Y. Xing, Synthesis and Electrochemical Characterization of Uniformly-Dispersed High Loading Pt Nanoparticles on Sonochemically-Treated Carbon Nanotubes, *The Journal of Physical Chemistry B* **108**, 19255 (2004).
148. Z. Liu, X. Lin, J.Y. Lee, W. Zhang, M. Han and L.M. Gan, Preparation and Characterization of Platinum-Based Electrocatalysts on Multiwalled Carbon Nanotubes for Proton Exchange Membrane Fuel Cells, *Langmuir* **18**, 4054 (2002).
149. N.L. Rosi, D.A. Giljohann, C.S. Thaxton, A.K.R. Lytton-Jean, M.S. Han and C.A. Mirkin, Oligonucleotide-Modified Gold Nanoparticles for Intracellular Gene Regulation, *Science* **312**, 1027 (2006).
150. D.G. Georganopoulou, L. Chang, J.-M. Nam, C.S. Thaxton, E.J. Mufson, W.L. Klein and C.A. Mirkin, Nanoparticle-based detection in cerebral spinal fluid of a soluble pathogenic biomarker for Alzheimer's disease, *Proceedings of the National Academy of Sciences of the United States of America* **102**, 2273 (2005).

151. M.S. Raghuvver, S. Agrawal, N. Bishop and G. Ramanath, Microwave-Assisted Single-Step Functionalization and in Situ Derivatization of Carbon Nanotubes with Gold Nanoparticles, *Chemistry of Materials* **18**, 1390 (2006).
152. H.C. Choi, M. Shim, S. Bangsaruntip and H. Dai, Spontaneous Reduction of Metal Ions on the Sidewalls of Carbon Nanotubes, *Journal of the American Chemical Society* **124**, 9058 (2002).
153. L. Qu and L. Dai, Substrate-Enhanced Electroless Deposition of Metal Nanoparticles on Carbon Nanotubes, *Journal of the American Chemical Society* **127**, 10806 (2005).
154. V. Tzitzios, V. Georgakilas, E. Oikonomou, M. Karakassides and D. Petridis, Synthesis and characterization of carbon nanotube/metal nanoparticle composites well dispersed in organic media, *Carbon* **44**, 848 (2006).
155. T.M. Day, P.R. Unwin, N.R. Wilson and J.V. Macpherson, Electrochemical Templating of Metal Nanoparticles and Nanowires on Single-Walled Carbon Nanotube Networks, *Journal of the American Chemical Society* **127**, 10639 (2005).
156. B.M. Quinn, C. Dekker and S.G. Lemay, Electrodeposition of Noble Metal Nanoparticles on Carbon Nanotubes, *Journal of the American Chemical Society* **127**, 6146 (2005).
157. B. Yoon and C.M. Wai, Microemulsion-Templated Synthesis of Carbon Nanotube-Supported Pd and Rh Nanoparticles for Catalytic Applications, *Journal of the American Chemical Society* **127**, 17174 (2005).
158. R. Giordano, P. Serp, P. Kalck, Y. Kihn, J. Schreiber, C. Marhic and J.L. Duvail, Preparation of Rhodium Catalysts Supported on Carbon Nanotubes by a Surface Mediated Organometallic Reaction, *European Journal of Inorganic Chemistry* **203**, 610 (2003).
159. Y. Lin, X. Cui, C. Yen and C.M. Wai, Platinum/Carbon Nanotube Nanocomposite Synthesized in Supercritical Fluid as Electrocatalysts for Low-Temperature Fuel Cells, *The Journal of Physical Chemistry B* **109**, 14410 (2005).
160. T. Wang, X. Hu, X. Qu and S. Dong, Noncovalent functionalization of multiwalled carbon nanotubes: Application in hybrid nanostructures, *Journal of Physical Chemistry B* **110**, 6631 (2006).

161. H.M. Cheng, F. Li, X. Sun, S.D.M. Brown, M.A. Pimenta, A. Marucci, G. Dresselhaus and M.S. Dresselhaus, Bulk morphology and diameter distribution of single-walled carbon nanotubes synthesized by catalytic decomposition of hydrocarbons, *Chemical Physics Letters* **289**, 602 (1998).
162. B.R. Azamian, K.S. Coleman, J.J. Davis, N. Hanson and M.L.H. Green, Directly observed covalent coupling of quantum dots to single-wall carbon nanotubes, *Chemical Communications* **4**, 366 (2002).
163. R. Zanella, E.V. Basiuk, P. Santiago, V.A. Basiuk, E. Mireles, I. Puente-Lee and J.M. Saniger, Deposition of Gold Nanoparticles onto Thiol-Functionalized Multiwalled Carbon Nanotubes, *The Journal of Physical Chemistry B* **109**, 16290 (2005).
164. K.S. Coleman, S.R. Bailey, S. Fogden and M.L.H. Green, Functionalization of Single-Walled Carbon Nanotubes via the Bingel Reaction, *Journal of the American Chemical Society* **125**, 8722 (2003).
165. A.V. Ellis, K. Vijayamohanan, R. Goswami, N. Chakrapani, L.S. Ramanathan, P.M. Ajayan and G. Ramanath, Hydrophobic Anchoring of Monolayer-Protected Gold Nanoclusters to Carbon Nanotubes, *Nano Letters* **3**, 279 (2003).
166. G.M.Aminur Rahman, D.M. Guldi, E. Zambon, L. Pasquato, N. Tagmatarchis M. Prato, Dispersable Carbon Nanotube/Gold Nanohybrids: Evidence for Strong Electronic Interactions<sup>13</sup>, *Small* **1**, 527 (2005).
167. L. Han, W. Wu, F.L. Kirk, J. Luo, M.M. Maye, N.N. Kariuki, Y. Lin, C. Wang and C.-J. Zhong, A Direct Route toward Assembly of Nanoparticle-Carbon Nanotube Composite Materials, *Langmuir* **20**, 6019 (2004).
168. X. Li, Y. Liu, L. Fu, L. Cao, D. Wei, G. Yu and D. Zhu, Direct route to high-density and uniform assembly of Au nanoparticles on carbon nanotubes, *Carbon* **44**, 3139 (2006).
169. T. Sainsbury, J. Stolarczyk and D. Fitzmaurice, An Experimental and Theoretical Study of the Self-Assembly of Gold Nanoparticles at the Surface of Functionalized Multiwalled Carbon Nanotubes, *The Journal of Physical Chemistry B* **109**, 16310 (2005).

170. T. Sainsbury and D. Fitzmaurice, Carbon-Nanotube-Templated and Pseudorotaxane-Formation-Driven Gold Nanowire Self-Assembly, *Chemistry of Materials* **16**, 2174 (2004).
171. D. Fitzmaurice, S. Nagaraja, R. Jon, A. Preece, J. Fraser, S. Wenger and N. Zaccheroni, Heterosupramolecular Chemistry: Programmed Pseudorotaxane Assembly at the Surface of a Nanocrystal, *Angewandte Chemie International Edition* **38**, 1147 (1999).
172. D. M. Guldi, G. Rahman, M. Prato, N.J. Shuhui, and Q. Ford, Single-Wall Carbon Nanotubes as Integrative Building Blocks for Solar-Energy Conversion<sup>13</sup>, *Angewandte Chemie International Edition* **44**, 2015 (2005).
173. L. Liu, T. Wang, J. Li, Z.-X. Guo, L. Dai, D. Zhang and D. Zhu, Self-assembly of gold nanoparticles to carbon nanotubes using a thiol-terminated pyrene as interlinker, *Chemical Physics Letters* **367**, 747 (2003).
174. D.Q. Yang, B. Hennequin and E. Sacher, XPS Demonstration of  $\pi$ - $\pi$  Interaction between Benzyl Mercaptan and Multiwalled Carbon Nanotubes and Their Use in the Adhesion of Pt Nanoparticles, *Chemistry of Materials* **18**, 5033 (2006).
175. D.M. Guldi, G. Rahman, N. Jux, N. Tagmatarchis and Maurizio Prato, Integrating Single-Wall Carbon Nanotubes into Donor-Acceptor Nanohybrids<sup>13</sup>, *Angewandte Chemie International Edition* **43**, 5526 (2004).
176. V. Georgakilas, V. Tzitzios, D. Gournis and D. Petridis, Attachment of Magnetic Nanoparticles on Carbon Nanotubes and Their Soluble Derivatives, *Chemistry of Materials* **17**, 1613 (2005).
177. Y.Y. Ou and M.H. Huang, High-Density Assembly of Gold Nanoparticles on Multiwalled Carbon Nanotubes Using 1-Pyrenemethylamine as Interlinker, *The Journal of Physical Chemistry B* **110**, 2031 (2006).
178. Y. Mu, H. Liang, J. Hu, L. Jiang and L. Wan, Controllable Pt Nanoparticle Deposition on Carbon Nanotubes as an Anode Catalyst for Direct Methanol Fuel Cells, *The Journal of Physical Chemistry B* **109**, 22212 (2005).
179. K. Jiang, A. Eitan, L.S. Schadler, P.M. Ajayan, R.W. Siegel, N. Grobert, M. Mayne, M. Reyes-Reyes, H. Terrones and M. Terrones, Selective Attachment of Gold Nanoparticles to Nitrogen-Doped Carbon Nanotubes, *Nano Letters* **3**, 275 (2003).

180. A. Carrillo, J.A. Swartz, J.M. Gamba, R.S. Kane, N. Chakrapani, B. Wei and P.M. Ajayan, Noncovalent Functionalization of Graphite and Carbon Nanotubes with Polymer Multilayers and Gold Nanoparticles, *Nano Letters* **3**, 1437 (2003).
181. C. Gao, C.D. Vo, Y.Z. Jin, W. Li and S.P. Armes, Multihydroxy Polymer-Functionalized Carbon Nanotubes: Synthesis, Derivatization, and Metal Loading, *Macromolecules* **38**, 8634 (2005).
182. B. Kim and W.M. Sigmund, Functionalized Multiwall Carbon Nanotube/Gold Nanoparticle Composites, *Langmuir* **20**, 8239 (2004).
183. M.A. Correa-Duarte, J. Pérez-Juste, A. Sánchez and L. Martín, Aligning Au Nanorods by Using Carbon Nanotubes as Templates, *Angewandte Chemie International Edition* **44**, 4375 (2005).
184. B. Nikoobakht and M.A. El-Sayed, Preparation and Growth Mechanism of Gold Nanorods (NRs) Using Seed-Mediated Growth Method, *Chemistry of Materials* **15**, 1957 (2003).
185. X. Hu, T. Wang, X. Qu and S. Dong, In Situ Synthesis and Characterization of Multiwalled Carbon Nanotube/Au Nanoparticle Composite Materials, *The Journal of Physical Chemistry B* **110**, 853 (2006).
186. F. Stoffelbach, A. Aqil, C. Jerome, R. Jerome and C. Detrembleur, An easy and economically viable route for the decoration of carbon nanotubes by magnetite nanoparticles, and their orientation in a magnetic field, *Chemical Communications* **36**, 4532 (2005).
187. X. Lou, C. Detrembleur, C. Pagnouille, R. Jerome, V. Bocharova, A. Kiriya and M. Stamm, Surface Modification of Multiwalled Carbon Nanotubes by Poly(2-vinylpyridine): Dispersion, Selective Deposition, and Decoration of the Nanotubes, *Advanced Materials* **16**, 2123 (2004).
188. S. Hrapovic, Y. Liu, K.B. Male and J.H.T. Luong, Electrochemical Biosensing Platforms Using Platinum Nanoparticles and Carbon Nanotubes, *Analytical Chemistry* **76**, 1083 (2004).
189. J. Wang, M. Musameh and Y. Lin, Solubilization of Carbon Nanotubes by Nafion toward the Preparation of Amperometric Biosensors, *Journal of the American Chemical Society* **125**, 2408 (2003).

190. S. Fullam, D. Cottell, H. Rensmo and D. Fitzmaurice, Carbon Nanotube Templated Self-Assembly and Thermal Processing of Gold Nanowires, *Advanced Materials* **12**, 1430 (2000).
191. R.L. Pecsok, L.D. Shields, T. Cairns and I.G. McWilliam,  $\mu$ ,  $\mu$ ,  $\mu$ , 1980.
192. . . and . . . ,  $\mu$   $\mu$   $\mu$  " " ,  $\mu$  , , 2003.
193. . . .  $\mu$   $\mu$  *össbauer*,  $\mu$  , 2008.
194. W.Z. Li, H. Zhang, C.Y. Wang, Y. Zhang, L.W. Xu, K. Zhu and S.S. Xie, Raman characterization of aligned carbon nanotubes produced by thermal decomposition of hydrocarbon vapor, *Applied Physics Letters* **70**, 2684 (1997).
195. P.C. Eklund, J.M. Holden and R.A. Jishi, *Carbon* **33**, 972 (1995).
196. Y. Lian, Y. Maeda, T. Wakahara, T. Nakahodo, T. Akasaka, S. Kazaoui, N. Minami, T. Shimizu and H. Tokumoto, Spectroscopic study on the centrifugal fractionation of soluble single-walled carbon nanotubes, *Carbon* **43**, 2750 (2005).
197. L. Jankovic, D. Gournis, P.N. Trikalitis, I. Arfaoui, T. Cren, P. Rudolf, M.H. Sage, T.T.M. Palstra, B. Kooi, J. De Hosson, M.A. Karakassides, K. Dimos, A. Moukarika and T. Bakas, Carbon nanotubes encapsulating superconducting single-crystalline tin nanowires, *Nano Letters* **6**, 1131 (2006).
198. T. Tsoufis, P. Xidas, L. Jankovic, D. Gournis, A. Saranti, T. Bakas and M.A. Karakassides, Catalytic production of carbon nanotubes over Fe-Ni bimetallic catalysts supported on MgO, *Diamond and Related Materials* **16**, 155 (2007).
199. H. Ago, K. Nakamura, N. Uehara and M. Tsuji, Roles of metal-support interaction in growth of single- and double-walled carbon nanotubes studied with diameter-controlled iron particles supported on MgO, *Journal of Physical Chemistry B* **108**, 18908 (2004).
200. L. Ci, Z. Zhou, X. Yan, D. Liu, H. Yuan, L. Song, J. Wang, Y. Gao, J. Zhou, W. Zhou, G. Wang and S. Xie, Raman Characterization and Tunable Growth of Double-Wall Carbon Nanotubes, *Journal of Physical Chemistry B* **107**, 8760 (2003).

201. S.C. Lyu, B.C. Liu, C.J. Lee, H.K. Kang, C.W. Yang and C.Y. Park, High-Quality Double-Walled Carbon Nanotubes Produced by Catalytic Decomposition of Benzene, *Chemistry of Materials* **15**, 3951 (2003).
202. J.F. Colomer, C. Stephan, S. Lefrant, G. Van Tendeloo, I. Willems, Z. Konya, A. Fonseca, C. Laurent and J. B.Nagy, Large-scale synthesis of single-wall carbon nanotubes by catalytic chemical vapor deposition (CCVD) method, *Chemical Physics Letters* **317**, 83 (2000).
203. S. Arepalli, P. Nikolaev, O. Gorelik, V.G. Hadjiev, H.A. Bradlev, W. Holmes, B. Files and L. Yowell, Protocol for the characterization of single-wall carbon nanotube material quality, *Carbon* **42**, 1783 (2004).
204. A.G. Filho, A. Jorio, G.S. Ge, G. Dresselhaus, R. Saito and M.S. Dresselhaus, Raman spectroscopy for probing chemically/physically induced phenomena in carbon nanotubes, *Nanotechnology* **14**, 1130 (2003).
205. T. Belin and F. Epron, Characterization methods of carbon nanotubes: A review, *Materials Science and Engineering B: Solid-State Materials for Advanced Technology* **119**, 105 (2005).
206. A. Jorio, R. Saito, G. Dresselhaus and M.S. Dresselhaus, Determination of nanotubes properties by Raman spectroscopy, *Philosophical Transactions: Mathematical, Physical and Engineering Sciences (Series A)* **362**, 2311 (2004).
207. Z. Yao, N. Braidy, G.A. Botton and A. Adronov, Polymerization from the Surface of Single-Walled Carbon Nanotubes - Preparation and Characterization of Nanocomposites, *Journal of the American Chemical Society* **125**, 16015 (2003).
208. J.L. Bahr, J.P. Yang, D.V. Kosynkin, M.J. Bronikowski, R.E. Smalley and J.M. Tour, Functionalization of carbon nanotubes by electrochemical reduction of aryl diazonium salts: A bucky paper electrode, *Journal of the American Chemical Society* **123**, 6536 (2001).
209. C.A. Dyke and J.M. Tour, Covalent Functionalization of Single-Walled Carbon Nanotubes for Materials Applications, *J. Phys. Chem. A* **108**, 11151 (2004).

210. D.Q. Yang, J.F. Rochette and E. Sacher, Functionalization of Multiwalled Carbon Nanotubes by Mild Aqueous Sonication, *Journal of Physical Chemistry B* **109**, 7788 (2005).
211. W. Huang, Y. Lin, S. Taylor, J. Gaillard, A.M. Rao and Y.P. Sun, Sonication-Assisted Functionalization and Solubilization of Carbon Nanotubes, *Nano Letters* **2**, 231 (2002).
212. C.R.H. Bahl, M.F. Hansen, T. Pedersen, S. Saadi, K.H. Nielsen, B. Lebech and S. Morup, The magnetic moment of NiO nanoparticles determined by Mossbauer spectroscopy, *Journal of Physics Condensed Matter* **18**, 4161 (2006).
213. C.A. Furtado, U.J. Kim, H.R. Gutierrez, L. Pan, E.C. Dickey and P.C. Eklund, Debundling and Dissolution of Single-Walled Carbon Nanotubes in Amide Solvents, *Journal of the American Chemical Society* **126**, 6095 (May 19, 2004, 2004).
214. B.J. Landi, C.D. Cress, C.M. Evans and R.P. Raffaele, Thermal Oxidation Profiling of Single-Walled Carbon Nanotubes, *Chemistry of Materials* **17**, 6819 (2005).
215. S. Arepalli, P. Nikolaev, O. Gorelik, V.G. Hadjiev, W. Holmes, B. Files and L. Yowell, Protocol for the characterization of single-wall carbon nanotube material quality, *Carbon* **42**, 1783 (2004).
216. Z. Shi, Y. Lian, F. Liao, X. Zhou, Z. Gu, Y. Zhang and S. Iijima, Purification of single-wall carbon nanotubes, *Solid State Communications* **112**, 35 (1999).
217. M.E. Itkis, D.E. Perea, R. Jung, S. Niyogi and R.C. Haddon, Comparison of Analytical Techniques for Purity Evaluation of Single-Walled Carbon Nanotubes, *Journal of the American Chemical Society* **127**, 3439 (2005).
218. W. Zhou, Y.H. Ooi, R. Russo, P. Papanek, D.E. Luzzi, J.E. Fischer, M.J. Bronikowski, P.A. Willis and R.E. Smalley, Structural characterization and diameter-dependent oxidative stability of single wall carbon nanotubes synthesized by the catalytic decomposition of CO, *Chemical Physics Letters* **350**, 6 (2001).
219. A. C. Dillon, T. Gennett, K. M. Jones, J. L. Alleman, P. A. Parilla and M. J. Heben, A Simple and Complete Purification of Single-Walled Carbon Nanotube Materials, *Advanced Materials* **11**, 1354 (1999).



220. H. Sigel, *Metal Ions in Biological Systems*, Marcel Dekker, New York, 1994.
221. T.W. Odom, J.L. Huang, P. Kim and C.M. Lieber, Atomic structure and electronic properties of single-walled carbon nanotubes, *Nature* **391**, 62 (1998).
222. J.L. Bahr, J.P. Yang, D.V. Kosynkin, M.J. Bronikowski, R.E. Smalley and J.M. Tour, Functionalization of carbon nanotubes by electrochemical reduction of aryl diazonium salts: A bucky paper electrode, *Journal of the American Chemical Society* **123**, 6536 (Jul, 2001).
223. V. Georgakilas, D. Gournis, M.A. Karakassides, A. Bakandritsos and D. Petridis, Organic derivatization of single-walled carbon nanotubes by clays and intercalated derivatives, *Carbon* **42**, 865 (2004).
224. O. Chauvet, L. Forro, W. Bacsa, D. Ugarte, B. Doudin and W.A. Deheer, Magnetic Anisotropies of Aligned Carbon Nanotubes, *Physical Review B* **52**, R6963 (1995).
225. H.Y. Zhang, S.H. Liu, A.X. Wei, Y.Y. He, X.G. Tang, X.M. Xue, L.Z. Liang and C.Y. Wu, Electron spin resonance of carbon nanotubes prepared under two kinds of inert gas ambient, *Journal of Physics and Chemistry of Solids* **61**, 1123 (2000).
226. A. De Martino, R. Egger, K. Hallberg and C.A. Balseiro, Spin-orbit coupling and electron spin resonance theory for carbon nanotubes, *Physical Review Letters* **88**, 206402 (2002).
227. J.F. Zhou, Z.S. Wu, Z.J. Zhang, W.M. Liu and Q.J. Xue, Tribological behavior and lubricating mechanism of Cu nanoparticles in oil, *Tribology Letters* **8**, 213 (2000).
228. K. Balasubramanian and M. Burghard, Chemically functionalized carbon nanotubes, *Small* **1**, 180 (2005).
229. A. Tomou, I. Panagiotopoulos, D. Gournis and B. Kooi, L10 ordering and magnetic interactions in FePt nanoparticles embedded in MgO and Si O<sub>2</sub> shell matrices, *Journal of Applied Physics* **102**, 023910 (2007).
230. H. Zeng, S.H. Sun, T.S. Vedantam, J.P. Liu, Z.R. Dai and Z.L. Wang, Exchange-coupled FePt nanoparticle assembly, *Applied Physics Letters* **80**, 2583 (2002).

231. M.H. Lu, T. Song, T.J. Zhou, J.P. Wang, S.N. Piramanayagam, W.W. Ma and H. Gong, FePt and Fe nanocomposite by annealing self-assembled FePt nanoparticles, *Journal of Applied Physics* **95**, 6735 (2004).
232. H. Barhoumi, A. Maaref, A. Rammah, C. Martelet, N. Jaffrezic, C. Mousty, S. Vial and C. Forano, Urea biosensor based on Zn<sub>3</sub>Al-urease layered double hydroxides nanohybrid coated on insulated silicon structures, *Materials Science & Engineering C-Biomimetic and Supramolecular Systems* **26**, 328 (2006).
233. M.S. Dresselhaus, M.A. Pimenta, P.C. Eklund and G. Dresselhaus, *Raman Scattering in Materials Science*, Springer Series in Materials Science, Springer, Berlin, 2000, pp. 314.
234. S.Y. Chen, H.Y. Miao, J.T. Lue and M.S. Ouyang, Fabrication and field emission property studies of multiwall carbon nanotubes, *Journal of Physics D: Applied Physics* **37**, 273 (2004).
235. Y. Gogotsi, J.A. Libera and M. Yoshimura, Hydrothermal synthesis of multiwall carbon nanotubes, *Journal of Materials Research* **15**, 2591 (2000).
236. T. Tsoufis, L. Jankovic, D. Gournis, P.N. Trikalitis and T. Bakas, Evaluation of first-row transition metal oxides supported on clay minerals for catalytic growth of carbon nanostructures, *Materials Science and Engineering B* **152**, 44 (2008).
237. H. Murphy, P. Papakonstantinou and T.I. Okpalugo, Raman study of multiwalled carbon nanotubes functionalized with oxygen groups, *Journal of Vacuum Science & Technology B: Microelectronics and Nanometer Structures* **24**, 715 (2006).
238. M. Endo, B.J. Lee, Y.A. Kim, Y.J. Kim, H. Muramatsu, T. Yanagisawa, T. Hayashi, M. Terrones and M.S. Dresselhaus, Transitional behaviour in the transformation from active end planes to stable loops caused by annealing, *New Journal of Physics* **5** (2003).
239. B. Stahl, J. Ellrich, R. Theissmann, M. Ghafari, S. Bhattacharya, H. Hahn, N.S. Gajbhiye, D. Kramer, R.N. Viswanath, J. Weissmuller and H. Gleiter, Electronic properties of 4-nm FePt particles, *Physical Review B - Condensed Matter and Materials Physics* **67**, 144221 (2003).

240. N.N. Greenwood and T.C. Gibb, *Mössbauer Spectroscopy*, Chapman and Hall, London, 1971.
241. T. Goto, H. Utsugi and K. Watanabe, Mössbauer study of permanent magnets Fe-Pt, *Hyperfine Interactions* **54**, 539 (1990).
242. B.D. Cullity, *Introduction to Magnetic Materials*, Addison-Wesley, Menlo Park-California, 1972.
243. T. Goto, H. Utsugi and A. Kashiwakura, Effect of atomic environment on  $^{57}\text{Fe}$  hyperfine structure in Fe-Pt alloys, *Journal of Magnetism and Magnetic Materials* **104-7**, 2051 (1992).
244. Y. Tamada, S. Yamamoto, M. Takano, S. Nasu and T. Ono, Well-ordered L10-FePt nanoparticles synthesized by improved  $\text{SiO}_2$ -nanoreactor method, *Applied Physics Letters* **90** (2007).
245. T.G. Hedderman, S.M. Keogh, G. Chambers and H.J. Byrne, Solubilization of SWNTs with Organic Dye Molecules, *Journal of Physical Chemistry B* **108**, 18860 (2004).
246. T.G. Hedderman, S.M. Keogh, G. Chambers and H.J. Byrne, In-Depth Study into the Interaction of Single Walled carbon Nanotubes with Anthracene and p-Terphenyl, *Journal of Physical Chemistry B* **110**, 3895 (2006).
247. H. Paloniemi, T. Aaritalo, T. Laiho, H. Liuke, N. Kocharova, K. Haapakka, F. Terzi, R. Seeber and J. Lukkari, Water-Soluble Full-Length Single-Wall Carbon Nanotube Polyelectrolytes: Preparation and Characterization, *Journal of Physical Chemistry B* **109**, 8634 (2005).
248. A.C. Dillon, P.A. Parilla, J.L. Alleman, T. Gennett, K.M. Jones and M.J. Heben, Systematic inclusion of defects in pure carbon single-wall nanotubes and their effect on the Raman D-band, *Chemical Physics Letters* **401**, 522 (2005).
249. D. Abdula, K.T. Nguyen and M. Shim, Raman Spectral Evolution in Individual Metallic Single-Walled Carbon Nanotubes upon Covalent Sidewall Functionalization, *J. Phys. Chem. C* **111**, 17755 (2007).
250. A. Bourlinos, A. Simopoulos, D. Petridis, H. Okumura and G. Hadjipanayis, Silica-maghemite nanocomposites, *Advanced Materials* **13**, 289 (2001).

251. V. Georgakilas, V. Tzitzios, D. Gournis and D. Petridis, Attachment of magnetic nanoparticles on carbon nanotubes and their soluble derivatives, *Chemistry of Materials* **17**, 1613 (2005).
252. A.B. Bourlinos, A. Bakandritsos, V. Georgakilas, V. Tzitzios and D. Petridis, Facile synthesis of capped  $\gamma$ -Fe<sub>2</sub>O<sub>3</sub> and Fe<sub>3</sub>O<sub>4</sub> nanoparticles, *Journal of Materials Science* **41**, 5250 (2006).
253. H. Qian and K.Y. Xu, Curvature effects on pressure-induced buckling of empty or filled double-walled carbon nanotubes, *Acta Mechanica* **187**, 55 (2006).
254. D. Gournis, L. Jankovic, E. Maccallini, D. Benne, P. Rudolf, J.F. Colomer, C. Sooambar, V. Georgakilas, M. Prato, M. Fanti, F. Zerbetto, G.H. Sarova and D.M. Guldi, Clay-fulleropyrrolidine nanocomposites, *Journal of the American Chemical Society* **128**, 6154 (2006).
255. N. Tombros, L. Buit, I. Arfaoui, T. Tsoufis, D. Gournis, P.N. Trikalitis, S.J. van der Molen, P. Rudolf and B.J. van Wees, Charge Transport in a Single Superconducting Tin Nanowire Encapsulated in a Multiwalled Carbon Nanotube, *Nano Letters* **8**, 3060 (2008).
256. A.J. Stroschio and W.J. Kaiser, *Scanning Tunneling Microscopy*, Academic Press, San Diego, 1993.
257. D.L. Carroll, P. Redlich, P.M. Ajayan, J.C. Charlier, X. Blase, A. DeVita and R. Car, Electronic structure and localized states at carbon nanotube tips, *Physical Review Letters* **78**, 2811 (1997).
258. R. Zboril, A. Bakandritsos, M. Mashlan, V. Tzitzios, P. Dallas, C. Trapalis and D. Petridis, One-step solid state synthesis of capped  $\gamma$ -Fe<sub>2</sub>O<sub>3</sub> nanocrystallites, *Nanotechnology* **19** (2008).
259. L. Wang, J. Luo, M.M. Maye, Q. Fan, Q. Rendeng, M.H. Engelhard, C. Wang, Y. Lin and C.-J. Zhong, Iron oxide-gold core-shell nanoparticles and thin film assembly, *Journal of Materials Chemistry* **15**, 1821 (2005).
260. J. Vidal-Vidal, J. Rivas and M.A. Lopez-Quintela, Synthesis of monodisperse maghemite nanoparticles by the microemulsion method, *Colloids and Surfaces A: Physicochemical and Engineering Aspects* **288**, 44 (2006).
261. S. Music, S. Krehula and S. Popovic, Thermal decomposition of  $\alpha$ -FeOOH, *Materials Letters* **58**, 444 (2004).

262. D. Gournis, M.A. Karakassides, T. Bakas, N. Boukos and D. Petridis, Catalytic synthesis of carbon nanotubes on clay minerals, *Carbon* **40**, 2641 (2002).
263. L. Liu and J.C. Grunlan, Clay Assisted Dispersion of Carbon Nanotubes in Conductive Epoxy Nanocomposites, *Advanced Functional Materials* **17**, 2343 (2007).
264. M.C. Costache, M.J. Heidecker, E. Manias, G. Camino, A. Frache, G. Beyer, R.K. Gupta and C.A. Wilkie, The influence of carbon nanotubes, organically modified montmorillonites and layered double hydroxides on the thermal degradation and fire retardancy of polyethylene, ethylene-vinyl acetate copolymer and polystyrene, *Polymer* **48**, 6532 (2007).
265. D. Bonn, H. Kellay, H. Tanaka, G. Wegdam and J. Meunier, Laponite: What Is the Difference between a Gel and a Glass?, *Langmuir* **15**, 7534 (1999).
266. V. Tohver, A. Chan, O. Sakurada and J.A. Lewis, Nanoparticle Engineering of Complex Fluid Behavior, *Langmuir* **17**, 8414 (2001).
267. P. Garrigue, M.H. Delville, C. Labrugere, E. Cloutet, P.J. Kulesza, J.P. Morand and A. Kuhn, Top-Down Approach for the Preparation of Colloidal Carbon Nanoparticles, *Chemistry of Materials* **16**, 2984 (2004).
268. L. Jankovic, D. Gournis, K. Dimos, M.A. Karakassides and T. Bakas, Catalytic production of carbon nanotubes over first row transition metal oxides supported on montmorillonite, *Journal of Physics: Conference Series* **10**, 178 (2005).
269. W. Li, C. Gao, H. Qian, J. Ren and D. Yan, Multiamino-functionalized carbon nanotubes and their applications in loading quantum dots and magnetic nanoparticles, *Journal of Materials Chemistry* **16**, 1852 (2006).
270. Y. Wang, Z. Iqbal and S.V. Malhotra, Functionalization of carbon nanotubes with amines and enzymes, *Chemical Physics Letters* **402**, 96 (2005).
271. R.K. Saini, I.W. Chiang, H.Q. Peng, R.E. Smalley, W.E. Billups, R.H. Hauge and J.L. Margrave, Covalent sidewall functionalization of single wall carbon nanotubes, *Journal of the American Chemical Society* **125**, 3617 (2003).